CONSCIENCE

EROSION OF GRAVEL/SHINGLE BEACHES AND BARRIERS

by L.C van Rijn, www.leovanrijn-sediment.com, May 2024

CONTENT

1. Introduction

Beaches consisting of gravel or shingle (2 to 64 mm), pebbles and cobbles (64 to 256 mm) are generally known as *coarse clastic beaches* and can be found in many mid- and high-latitude parts (formerly glaciated) of the world (England, Iceland, Canada, etc.). These areas extend from beyond the limits of the last major ice zones to the present day ice caps and include much of the coasts of northwestern Europe, eastern North America and the far north Pacific coast. Generally, these coastlines are intricate and irregular, characterised by headland and cliff formations. The variety of depositional forms include: gravel/shingle barriers and beaches, barrier spits, bay-head barriers and transverse lag shoals. A typical gravel/shingle beach can be seen as a layer of gravel material sloping up against a cliff. A gravel barrier can be seen as a dike of gravel material; swash-aligned barriers (migrating landwards through rollover by overwashing) or longshore drift-aligned barriers are distinguished. Typical profiles are shown in **Figure 1.1**.

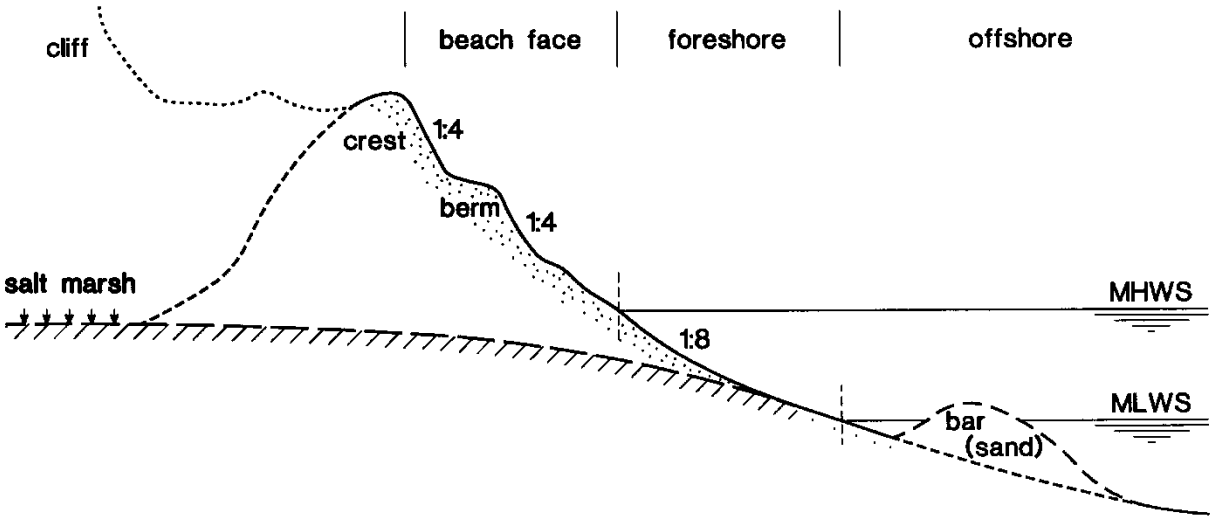

Figure 1.1 *Typical cross-shore profile of gravel beach slope*

Gravel beaches are also found along unconsolidated cliff-type coasts eroded by wave attack (like Mediterranean coasts) and along tectonic coasts where steep streams deliver coarse material to the shore. Some of these beaches have a large proportion of sand intermixed with gravel, especially in the foreshore zone just beneath the mean water line (see Figure **1.1right**). In regimes with dominating gravel populations, the sand becomes a subsidiary interstitial component. In regimes with a relatively large tidal range the back beach may consist of gravel ridges fronted by a low-tide terrace of sand (exposed at low tide). These types of beaches have less appeal for recreational activities, but they are rather efficient (high dissipation of energy through high permeability) for coastal protection.

Gravel beaches are also known as shingle beaches or coarse clastic beaches. Clasts are individual grains within coarse populations. Subgroups are pebbles and cobbles (rounded clasts between 64 and 256 mm); boulders are clasts larger than 256 mm. The term shingle is most commonly identified with the coarse beaches of southern England.

Gravel, pebbles and cobbles may consist of quartzite or flint and chert (formed by silica-bearing organisms). The quartzites tend to be more discoid, whereas the flint and chert (splintering more easily) are more flaked or fractured through impact. Pebbles of flint and chert become more ellipsoid during the transport process. Generally, the wearing of gravel is an extremely slow process. Impacts between pebbles during transport result in fractures and in removal of small surface irregularities (attrition) by grinding processes. The beach acts as a grinding machine, slowly pulvarising the coarser clasts; the finest pulvarisation products are carried offshore resulting in a loss in terms of sediment budget. A review of coarse clastic beaches is given by **Carter and Orford (1993).**

The transport pathways of gravel/shingle have been studied extensively by tracer experiments. Most studies have been qualitative rather than quantitative because of low recovery rates (5% or even less). A wide range of tracers has been used: original beach material coated with dye or paint, labelled with radio-active isotopes, pebbles of a distinctive geological composition from other sites, artificial pebbles (aluminium, plastic filled with metal, etc.). These studies give information of the movement of pebbles under wave and current-induced forces.

Gravel on beaches is moved almost exclusively by wave action (asymmetric wave motion); tidal or other currents are not effective in moving gravel/shingle material.

The coarse particles move up the beach to the run-up limit by strong bores (uprush) and move down the beach close to the line of the steepest beach slope by the backwash (less strong due to percolation) plus gravity, resulting in a saw-tooth movement. Waves of long periods on steep beaches can produce peak swash velocities up to 3 m/s. The alongshore transport path of individual clasts (20 to 40 mm) may be as large as 1,000 m per day during periods with storm waves. To prevent the longitudinal spreading of coarse materials often small-scale timber groynes are used (see **Figure 1.2**).

Generally, the upper beach consists of gravel/shingle material, while the lower beach consists of sandy material, see **Figure 1.2 (right)**. Gravel particles in shoaling and breaking waves generally move as bed load towards the beach during low wave conditions. As the near-bed peak orbital velocity in the onshore direction is greater than the offshore-directed value, the particles will experience a net onshore-directed movement during each wave cycle. The finer grains may go into suspension as a result of the turbulence produced by the breaking waves and may be transported to the lower parts of the beach zone depending on the strength of the undertow.

Figure 1.2 *Timber groynes at beach of Eastbourne, East Sussex, UK*

2. Swash zone processes

Gravel/shingle transport mainly takes place in the swash zone. The swash zone is the zone which is intermittently wet and dry showing relatively large velocities during the uprush and backwash phases of the saw-tooth swash wave cycle due to bore propagation and bore collapse, often in combination with low-frequency oscillations which generally grow in amplitude towards the shoreline. It is a particularly complex zone of the nearshore where short and long waves, tides, sediments and groundwater flow (infiltration/percolation) all play an important role. Long waves are generated by the release of bound long waves in the surf zone due to the breaking of short waves and by cross-shore variations of the short wave breakpoints (surf beat). The role of percolation is especially important on steep, coarse-grained beaches leading to beach accumulation and steepening as a result of the diminished sediment carrying capacity of the reduced backwash volume of water and velocity, following percolation into the coarse-grained bed. These effects will lead to a landward bias (asymmetry) in swash transport depending on grain size. The

swash zone is the most dynamic part of the nearshore zone of vital importance for the behaviour of gravel/shingle barriers.

Most field studies have been carried out on steep, sandy beaches with low waves (typical uprush and backwash durations of 3 to 7 s.). A key finding of these studies is that the uprush moves more sediment than the backwash under low wave conditions (offshore wave height of 1 to 2 m). Suspended sand concentrations and transport in the swash zone are an order of magnitude larger than those in the inner surf zone (concentrations up to 100 kg/m^3), (**Masselink et al., 2005**).

Reviews are given by: **Elfrink and Baldock (2002)** and **Butt and Russell (2000)**.

2.1 Run-up

When waves approach a coast, the majority of the wave energy is dissipated across the surf zone by wave breaking. However, a portion of that energy is converted into potential energy in the form of run-up on the foreshore of the beach (swash zone). Usually, the vertical wave run-up height above the still water level (SWL) is defined as the run-up level which is exceeded by 2% of the incident waves ($R_{2\%}$).

Run-up is caused by two different processes (see **Figure 2.1**):

- maximum set-up (h'), which is the maximum time-averaged water level elevation at the shoreline with respect to mean water level;
- swash oscillations (s_t), which are the time-varying vertical fluctuations about the temporal mean value (set-up water level); the run-up is approximately equal to $R = h' + 0.5H_{swash}$ with $H_{swash} = 2s_{max}$ = swash height.

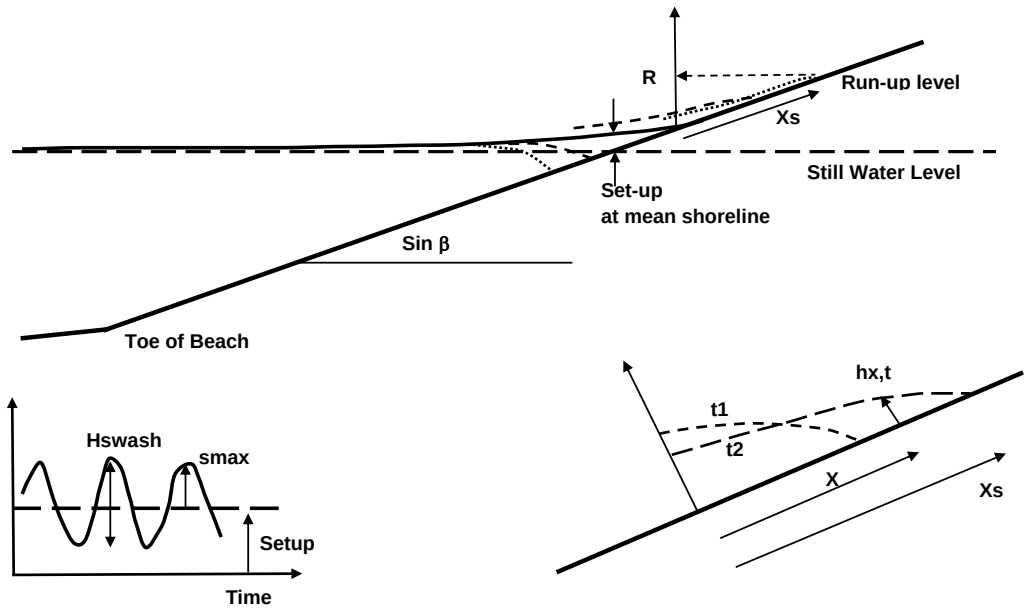

Figure 2.1 *Swash processes along beach*

Laboratory measurements with monochromatic waves on a plane beach have shown that the vertical swash height R increases with growing incident wave height until R reaches a threshold value. Any additional input of the incident wave energy is then dissipated by wave breaking in the surf zone and does not result in further growth of the vertical swash and run-up, i.e the swash is saturated, see **Figure 2.2**.

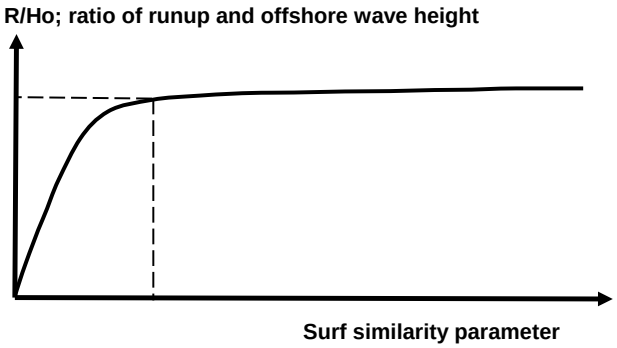

Figure 2.2 *Ratio of run-up and offshore wave height as function of surf similarity parameter*

Usually, the run-up height up to the threshold value is represented as:

$$R = \frac{\tan\beta}{(H_o/L_o)^{0.5}} \quad \gamma H_o = \gamma \tan\beta \, [H_o L_o]^{0.5} \qquad (2.1)$$

$$R = \zeta_o \gamma H_o \qquad (2.2)$$

in which: R = run-up height measured vertically from the still water level (including wave set-up height) to the run-up point, H_o = wave height seaward of the swash zone, L_o= wave length in deep water and tanβ =bottom slope, γ=proportionality coefficient. The parameter $\zeta_o = \tan\beta(H_o/L_o)^{-0.5}$ is known as the surf similarity parameter. Low ζ_o-values (<0.3) typically indicate dissipative conditions (high breaking waves on flat beaches), while higher values (>1) indicate more reflective beaches (breaking waves on steep beaches). On dissipative beaches, infragravity energy (with periods between 20 and 200 s) tends to dominate the inner surf zone, especially the swash zone.

The run-up process can be modelled by considering the collapse of a bore at the shoreline involving the rapid conversion of potential energy to kinetic energy. Excluding infiltration and percolation, the momentum equation for a water column at the head of the swash lens can be expressed as (see **Figure 2.1**):

$$\rho(\partial h \, \bar{U} / \partial t) + \rho g \, (h)(\partial h/\partial x) + \tau_{bed} - \rho g \, h \sin\beta = 0 \qquad (2.3)$$

or

$$\partial \bar{U} / \partial t + g(\partial h/\partial x) + \tau_{bed}/(\rho h) - g \sin\beta = 0 \qquad (2.4)$$

with: x= coordinate along beach slope, h=local mean water depth, τ_{bed}=bed-shear stress, $\bar{U}$ = depth-averaged velocity (long wave velocity) in swash lens. **Kobayashi and Wurjanto (1992)** have used a numerical long wave model to simulate the impact of bores on the sloping beach.
A simplified approach can be obtained by assuming that the pressure gradient term and the bed-friction term are approximately equal (but acting in opposite direction: $g(\partial h/\partial x) \cong -\tau_{bed}/(\rho h)$). The net effect of both terms can be represented by a coefficient (α_1), as follows:

$$\partial \bar{U} / \partial t - g \, (1+\alpha_1) \sin\beta = 0 \qquad (2.5)$$

with: α_1=coefficient (α_1<0 if pressure gradient is dominant; α_1>0 if bed-shear stress term is dominant). This approach only describes the uprush and backwash above the mean water level (set-up level) due the breaking of the crest of the wave.
Equation (2.5) can be integrated, yielding:

$$\bar{U} = -[g(1+\alpha_1)\sin\beta]\,t + C \qquad (2.6)$$

Using: $\bar{U} = \bar{U}_o$ at t=0, it follows that: C= $\bar{U}_o$ and thus:

$$\bar{U} = dx_s/dt = \bar{U}_o - [g(1+\alpha_1)\sin\beta]\,t \qquad (2.7)$$

At the most landward end of the swash motion it follows that: $\bar{U} = 0$ at $t=T_{end}$, yielding:

$$T_{end} = \bar{U}_o/[g(1+\alpha_1)\sin\beta] \qquad (2.8)$$

with: $\bar{U}_o \cong (gh)^{0.5}$.
The swash period from the start of the uprush to the end of the backwash is:

$$T_{swash} = 2T_{end} = 2\,\bar{U}_o/[g(1+\alpha_1)\sin\beta] \qquad (2.9)$$

Using h≅ 0.5 to 1 m, sinβ≅ 0.05 and α_1= 0, it follows that: T_{end}= 4 to 6 seconds and T_{swash}= 8 to 12 s.

Using: $H_b = \alpha_2 h$ = height of incoming bore and $\bar{U}_o = (gh)^{0.5} = [(1/\alpha_2)gH_b)]^{0.5}$, it follows that:

$$T_{swash} = 2[(1/\alpha_2)gH_b]^{0.5}/[g(1+\alpha_1)\sin\beta] \qquad (2.10)$$

The swash period increases with increasing wave height (H_b) and decreasing slope (sinβ). The swash can behave as an individual oscillating motion along the beach as long as the period of the incident bores (T) is larger or equal to that of the swash (T_{swash}). The onset of interference occurs for $T = T_{swash}$, yielding:

$$H_{b,onset} = 0.25\,\alpha_2\,(1+\alpha_1)^2\,g\,(\sin\beta)^2\,T^2 \qquad (2.11)$$

When the wave period (T) of the incident waves is smaller than that of the swash motion (T_{swash}), the new uprush interfers (overlaps) with the backwash of the previous wave resulting in two effects: (i) increased friction acting on the uprush of the new wave due to backwash of the previous one and (ii) more shoreward breaking of the new bore over the backwash of the previous one (larger water depths). The run-up level will be larger if the latter effect dominates and smaller if the former effect dominates. In the case of overlapping conditions the thickness (h) of the swash lens may grow somewhat due to increased friction and the velocity structure over the depth will show a seaward flow near the bottom due to the backwash of the previous wave and a landward flow near the surface due the uprush of the new incident wave.

Equation (2.7) can be integrated once again to find the swash excursion (x_s), yielding (x_s= 0 at t= 0):

$$x_s = [\bar{U}_o]\,t - [0.5\,g(1+\alpha_1)\sin\beta]\,t^2 \qquad (2.12)$$

The vertical swash oscillation from the start of the uprusch to the end of the backwash is:

$$s = x_s \sin\beta = [\bar{U}_o \sin\beta]\, t - [0.5\, g\, (1+\alpha_1) \sin^2\beta]\, t^2 \qquad (2.13)$$

which represents a parabolic swash oscillation in time.

Equation (2.13) can also be expressed as (see **Figure 2.3**):

$$s/s_{max} = 2t/T_{end} - t^2/(T_{end})^2 \qquad (2.14)$$

with: s_{max}= maximum swash amplitude based on Equation (2.16).
The maximum value is (at $t=T_{end}$):

$$x_{s,max} = [\bar{U}_o]^2/[2\, g\, (1+\alpha_1) \sin\beta] \qquad (2.15)$$

$$s_{max} = [\bar{U}_o]^2/[2\, g\, (1+\alpha_1)] \qquad (2.16)$$

The initial velocity at t= 0 can be approximated by the bore velocity, as follows:

$$\bar{U}_o = (gh)^{0.5} = [(1/\alpha_2) g H_b]^{0.5} \qquad (2.17)$$

with: $H_b=\alpha_2 h$= height of breaking bore at toe of beach, α_2= coefficient in range of 0.25 to 0.5.

This yields:

$$s_{max} = H_b/[2\, \alpha_2\, (1+\alpha_1)] \qquad (2.18)$$

Equation (2.18) shows that the maximum swash level of individual waves with $T > T_{swash}$ is independent of slope and equal to 1 to $2H_b$ for α_1= 0 and α_2= 0.25 to 0.5 for a smooth, impermeable beach slope. The swash level will be lower for a permeable, gravel/shingle beach slope due to infiltration processes.

Using Equation (2.11), the s_{max}-value at the onset of wave-swash interference can also be expressed as:

$$s_{max} = 0.125\, (1+\alpha_1)\, g\, T^2\, (\sin\beta)^2 \qquad (2.19)$$

and is strongly related to the incident wave period and beach slope. The parameter s_{max} increases with increasing wave period and increasing slope.

Baldock and Holmes (1999) have performed flume experiments with regular and random wave trains approaching a plane slope of 1 to 10. The bore height was measured at the intersection of the still water level and the beach slope (x= 0). The surf similarity parameter (ζ_o) based on deep water parameters is in the range of 0.4 to 1. The maximum run-up height above SWL of regular wave trains (no overlap between bores and swash) is found to be in excellent agreement with the theoretical value of Equations (2.18) and (2.19) for α_2= 0.25 and α_1= 0, suggesting that frictional effects over the beach slope are minimal. The bore height and the arrival time of the bore at x= 0 m are taken as the input values. The run-down below SWL is found to be negligble. The measured shoreline position can also be simulated quite well by using Equation (2.12). The measured shoreline velocity is very well simulated by Equation (2.7). Runs with saturated swash motion ($T < T_{swash}$) under regular wave trains (overlap between sequential incoming bores) show that the swash amplitude (variation) is reduced considerably. The maximum run-up distance and height are not so much affected. The simplified model of Equations (2.18) and (2.19) also yields reasonable results for random wave trains both with non-overlapping and overlapping conditions.
It is concluded that the shoreline motion of both non-overlapping and overlapping conditions for regular and random waves is largely driven by individual incident bores and does not exhibit a cumulative increase in additional harmonics due to swash-swash interaction. No accumulation of long wave energy has been observed.

If the surf zone is totally saturated with breaking waves, wave grouping is totally destroyed and then only free low-frequency waves will affect the swash motion.

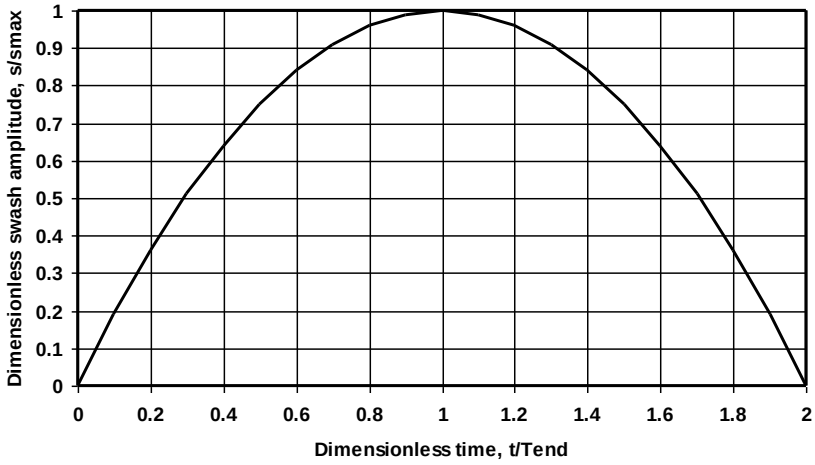

Figure 2.3 *Dimensionless swash amplitude as function of dimensionless time*

Various field studies have shown the important contributions of the incident wave periods (T < 20 s) and the infragravity wave periods (T > 20 s) to the run-up height above SWL.

Stockdon et al. (2006) have analysed wave run-up data sets (with $0.1<\zeta_o<2.5$) of ten different field experiments (west and east coasts of USA, Terschelling coast of The Netherlands) based on video techniques. The swash amplitudes ($s_{max}= 0.5H_{swash}$) related to the incident wave band were in the range of 0.1 to 1.5 m and the swash heights related to the infragravity band were in the range of 0.2 to 1 m.

Their definitions are:

$$R_{2\%} = 1.1[h' + s_{max}] \qquad (2.20)$$

h' = set-up value

$$s_{max} = 0.5[(H_{swash,hf})^2 + (H_{swash,ig})^2]^{0.5}$$

with: $R_{2\%}$= run-up height exceeded by 2% of the run-up values, $H_{swash,hf}$= vertical swash oscillation height of the high frequency incident waves and $H_{swash,ig}$= vertical swash oscillation height of the low frequency infragravity waves, s_{max}= maximum swash amplitude.

Run-up statistics were defined as the measured maximum elevations of individual water level values above SWL, see **Figure 2.4.**

The mean value of all individual values is defined to be equal to the mean set-up (h'). After subtraction of the set-up, the swash statistics can be computed. The swash oscillation height was computed from the spectrum as $H= 4(M_o)^{0.5}$, which represents the significant value similar to the calculation of significant wave height.

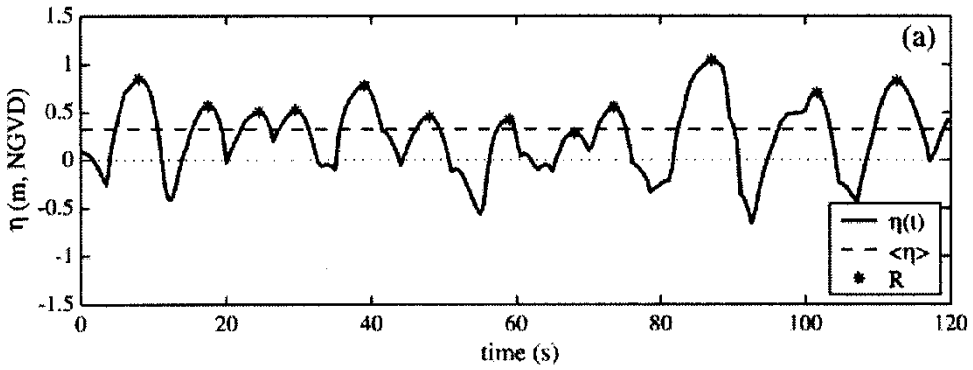

Figure 2.4 *Time series of measured water levels; <η>=set-up value (mean values of all water levels), R= run-up values (maxima of water levels); Stockdon et al. (2006)*

According to **Stockdon et al. (2006)**, the set-up values can be best parameterized by:

$$h' = 0.35\,(\sin\beta_f)\,[H_o L_o]^{0.5} \quad \text{for } \zeta_o > 0.3 \tag{2.21}$$

$$h' = 0.016\,[H_o L_o]^{0.5} \quad \text{for } \zeta_o < 0.3 \text{ (dissipative beaches)} \tag{2.22}$$

with: $\zeta_o = (\tan\beta_f)/(H_0/L_0)^{0.5}$, $\tan\beta_f$ = slope of foreshore (beach), H_o= significant wave height at deep water, L_o= significant wave length at deep water. Most set-up values are in the range of 0 to 1 m.
The inclusion of beach slope under dissipative conditions was found to result in lower correlation.

According to **Stockdon et al. (2006)**, the swash oscillation heights can be best parameterized by:

$$H_{swash,\,hf} = 0.75\,(\sin\beta_f)\,[H_o L_o]^{0.5} \quad \text{for all } \zeta_0 \tag{2.23}$$

$$H_{swash,\,ig} = 0.06\,[H_o L_o]^{0.5} \quad \text{for } \zeta_0 < 1.25 \text{ (dissipative beaches)} \tag{2.24}$$

$$H_{swash,\,ig} \cong 0 \quad \text{for } \zeta_0 > 1.25 \text{ (reflective beaches)} \tag{2.25}$$

Most swash height values are in the range of 0 to 2 m. The largest value of the parameter $(\sin\beta_f)[H_o L_o]^{0.5}$ of their data set is about 30.
On dissipative beaches ($\zeta_0 < 0.3$; beach slope larger than 1 to 20 or $\sin\beta_f < 0.05$) the swash is dominated by the infragravity band for 90% of the data. Beach slope has not much influence on the infragravity–induced swash heights at dissipative beaches. The data do not support the inclusion of beach slope for dissipative beaches. On dissipative beaches, the magnitude of the infragravity-induced swash height grows with increasing H_o.
On reflective beaches (ζ_0>1.25) the swash is dominated by the incident band for 90% of the data. The application of H_{br} in stead of H_o was not found to improve the results. The application of the surf zone slope β_s in stead of the foreshore slope (beach) β_f was not found to improve the results.
Using the data of the dissipative beaches only (**Stockdon et al., 2006**), the run-up values above SWL can be computed by:

$$R_{2\%} = 0.043\,[H_o L_o]^{0.5} \quad \text{for } \zeta_0 < 0.3 \text{ (dissipative beaches)} \tag{2.26}$$

Using the data of the reflective beaches only (**Stockdon et al., 2006**), the run-up values above SWL can be computed by:

$$R_{2\%} = 0.75\,(\sin\beta_f)[H_o L_o]^{0.5} \quad \text{for } \zeta_0 > 1.25 \text{ (reflective beaches)} \tag{2.27}$$

Since run-up and swash are dependent on beach slope, beaches with longshore variation of beach slope will show considerable variation of wave run-up in alongshore direction. The data of the Duck site on the east coast of the

USA showed that on days when the beach slope was longshore variable, the wave run-up of the incident band was also variable (up to 40% for highly three-dimensional conditions due to the presence of mega-cusps).

Van Gent (2001) has presented run-up data for steep slope structures such as dikes with shallow foreshores based on local parameters rather than on deep water parameters. Various types of foreshores were tested in a wave basin: foreshore of 1 to 100 with a dike slope of 1 to 4; foreshore of 1 to 100 with a dike slope of 1 to 2.5 and foreshore of 1 to 250 with a dike slope of 1 to 2.5. The test programme consisted of tests with single and double-peaked wave energy spectra, represented by a train of approximately 1,000 waves. The water level was varied to have different water depth values at the toe of the dike.
The experimental results for steep slope structures can be represented by (see also **Figure 2.5**):

$$R_{2\%}/H_{s,toe} = 2.3(\zeta)^{0.3} \quad \text{for } 1 < \zeta < 30 \qquad (2.28)$$

with: $\zeta = \tan\beta/[(2\pi/g)H_{s,toe}/T^2_{m-1}]^{0.5}$ = surf similarity parameter based on the T_{m-1} wave period, $H_{s,toe}$=significant wave height at toe of the structure, T_{m-1} = wave period based on zero-th and first negative spectral moment of the incident waves at the toe of the structure (=0.7 to 1 T_p), T_p = wave period of peak of spectrum, β= slope angle of structure.
The run-up level $R_{2\%}$ varies roughly from $1H_{s,toe}$ to $5H_{s,toe}$ depending on the value of the surf similarity parameter. The influence of the wave energy spectrum can be accounted for by using the spectral wave period T_{m-1} of the incident waves at the toe of the structure.
Assuming: $H_{s,toe} = 0.25$ to $0.5\ H_{s,o}$, it follows that: $R_{2\%}/H_{s,o} \cong 0.7$ to $1.6(\zeta_o)^{0.3}$.

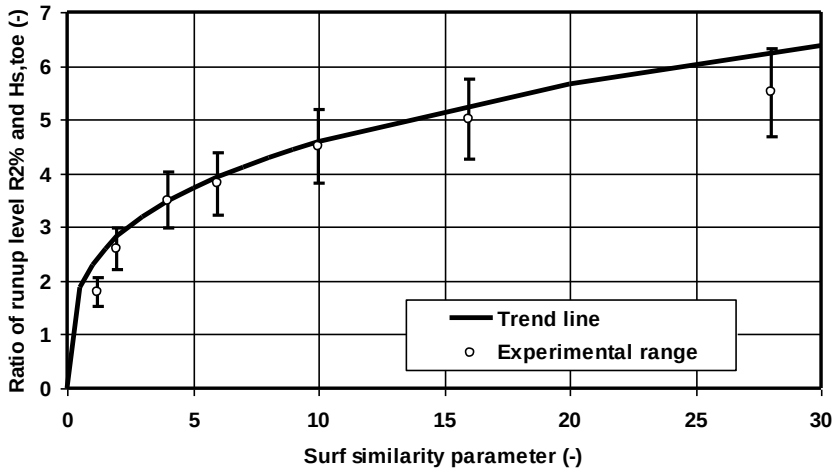

Figure 2.5 *Run-up level data as function of surf similarity parameter based on Van Gent (2001)*

During storm conditions with a significant offshore wave height of about 6 m (peak period of 11 s), the significant wave height at the toe of the gravel barrier is about 2 m (see **Figure 4.8**) resulting in a ζ_o-value of 2 to 3 and thus $R/H_{s,toe} \cong 2.5$ to 3 and $R \cong 5$ to 6 m above the mean water level. In practice, the run-up values will be significantly smaller along a coarse gravel/shingle barrier due to infiltration processes. In the large-scale wave flume tests (see **Section 3.1.2**) the maximum crest level of the swash bar generated by the swash run-up was about 1.5 to 2 m above the mean water level (about 2 $H_{s,toe}$).

2.2 Swash velocities and shear stresses

The transport of coarse sediments is most active in the swash zone of the beach face and is caused by wave uprush (decelerating flow) and backwash (accelerating flow). Both laboratory and field measurements over an impermeable bottom have shown that the swash of the incident waves on a steep beach is skewed and asymmetric (saw-tooth waves), i.e. the backwash is not simply the reverse of the uprush. Generally, onshore flow velocities during the uprush are larger but of shorter duration than the seaward velocities during the backwash. Maximum landward velocities occur at the start of the uprush, whereas maximum seaward velocities take place at the end of the backwash. The water depths that occur during the uprush are generally larger than those that occur during the backwash. These observed features are consistent with computational results of non-linear shallow water theory for swash behaviour following bore propagation and collapse over an impermeable bed (**Butt and Russell, 2000; Elfrink and Baldock, 2002**).
The dissimilarity in the hydrodynamics of the wave uprush and backwash is reflected in different modes of sediment transport. Turbulence-dominated suspended transport may be significant during the uprush phase whereas sheetflow type of bed load transport dominates during the backwash phase. During the uprush phase the sediment transport is a combination of sediments mobilised under and directly after bore collapse which are then advected landwards and of locally entrained sediments from the bed by developing boundary layer flow at the end op the uprush, whereas sediment transport during downrush mainly is related to locally entrained sediments. Measurements of sheet flow transport for half saw-tooth waves in a wave tunnel (**King, 1991**) indicate that the sediment transport under steep fronts (decelerating flow) is about twice as large as under steep rears (accelerating flow). **Nielsen (1992)** computed shear stresses under a saw-tooth wave and found that the landward peak shear stress was about twice as large as the seaward peak shear stress.

Swash motion over a steep permeable bed of coarse grains (gravel/shingle) is complicated by the presence of infiltration under wave uprush and exfiltration under wave downrush. Vertical flow through a porous bed can influence sediment motion in two ways: 1) seepage forces changing the effective weight of the surficial sediments and 2) the occurrence of boundary layer thinning (resulting in higher shear stresses) due to infiltration and thickening (smaller shear stresses) due to exfiltration. Generally, swash-related infiltration-exfiltration effects across a saturated beach face enhances the upslope transport of sediment transport (**Masselink and Hughes, 1998**) and reduces the downslope transport.

Research on swash velocities and shear stress in laboratory flumes and in the field have been done by **Cox et al. (2000), Cowen et al. (2003), Conley and Griffin (2004), Masselink et al. (2005), Pritchard and Hogg (2005), Masselink and Russell (2006)** and by **Barnes et al., (2009)**. Hereafter, the main research results are briefly summarized.

Cox et al. (2000) have performed swash zone measurements using a two-dimensional (horizontal and vertical) Laser Doppler velocitymeter in a laboratory flume with an impermeable beach slope of 1 to 10 covered by gravel particles of 6.2 mm under irregular waves with a peak period of 4 s. Bed shear stresses were determined from the logarithmic profile of the ensemble averaged velocity in the bottom boundary layer at many phases for each wave. Results of measurements in the inner surf zone (below the still water line) and in the swash zone (above the still water line) show a very asymmetric shear stress distribution (as function of time) in the surf zone and a typical saw-tooth distribution of shear stress in the swash zone. At both locations the ratio of the landward and seaward peak bed-shear stress is about 3, which is somewhat larger than the values shown in **Figure 2.6** based on the measurements **Conley and Griffin (2004)**. The landward peak bed-shear stress in the swash zone is much larger (factor 4) than the landward peak bed-shear stress in the surf zone. The peak bed-shear stress in the surf zone occurs at 0.1T and 0.85T, and at 0.05 T and 0.9T in the swash zone.

Cowen et al. (2003) have used a particle image velocimetry technique (PIV) to determine the vertically resolved two-dimensional measurements of the swash velocities and turbulence parameters in a laboratory wave flume with spilling and plunging waves. Their measurements indicate that the turbulent structure of the swash zone due to spilling waves is similar to that of plunging waves suggesting that the swash zone is driven by the turbulent bore that results from the wave breaking process and not by the mode of breaking. The uprush and downrush phases are not symmetric and are dominated by different turbulence processes. The uprush and early retreat phases are dominated by bore-advected and bore-generated turbulence that is considerably stronger than fully developed boundary layer turbulence. The temporal evolution of the post-bore uprush phases is analogous to decaying grid turbulence. During the last half of the retreat phase (downrush phase), the bore turbulence has decayed sufficiently and the wall boundary layer has grown sufficiently that boundary-generated turbulence becomes the dominant source of turbulent kinetic energy. The bed shear stress can also be estimated from the PIV-data and is found to has a strong phase dependence. The bed-shear stresses of the uprush phase are much larger than that of the downrush phase. Defining $f_{w,up}=\tau_{max,up}/(0.5\rho U_{max.up}^2)$ and $f_{w,down}=\tau_{max,down}/(0.5\rho U_{max.down}^2)$ with τ_{max}= maximum bed-shear stress and U_{max}= maximum fluid velocity, the friction factor of the uprush phase is about twice as large as that of the downrush phase in the swash zone.

Conley and Griffin (2004) have made direct measurements of bed stress under swash in the field (medium grained Barret Beach, Fire Island, New York) utilizing flush mounted hot film anemometry. Hot film sensors are thermal sensors that are maintained at a constant temperature which is higher than the ambient temperature. The energy required to maintain the temperature is related to the fluid velocity and fluid shear stress (calibration curve). In addition to the hot film package, a pressure sensor was deployed in water with a mean depth of 1.5 m approximately 10 m from the shoreline to provide information of the wave and tide conditions. A video camera was used to provide constant coverage of the hot film sensor with respect to the nearby beach face and water surface. **Figure 2.6** shows the measured dimensionless shear stress distibrution (skewed and asymmetric) based on about 100 discrete uprush events under calm wave conditions (significant wave height of 0.14 m at location of pressure sensor). This illustrates that the maximum stress exerted by the backwash flow is typically less than half of that exerted by the uprush. The duration of the backwash is, however, about 30% larger than that of the uprush. Assuming a quadratic relationship between shear stress and fluid velocity, the friction factor of the uprush phase is found to be considerably larger than that during the backwash phase in line with the findings of **Cowen et al. (2003)**.

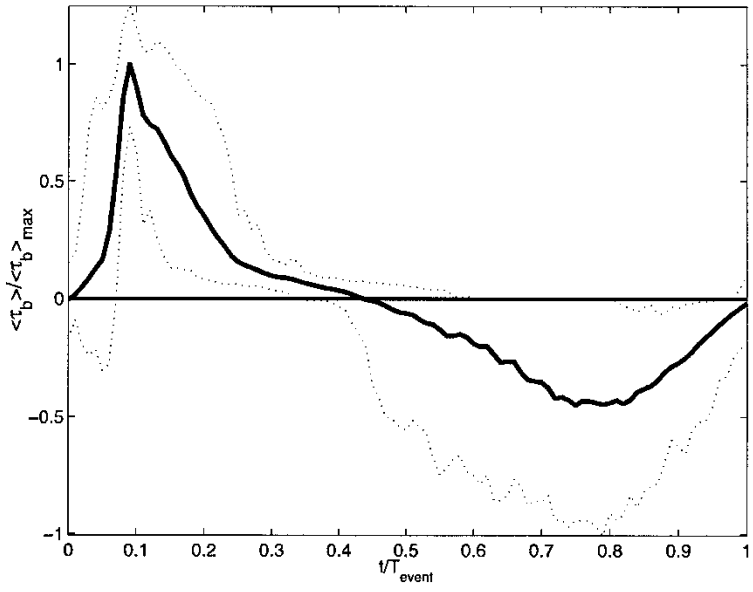

Figure 2.6 *Dimensionless bed shear stres distribution as function of time in swash zone; ensemble average of 100 individual swash events; Barret Beach, Fire Island, USA (Conley and Griffin, 2004)*

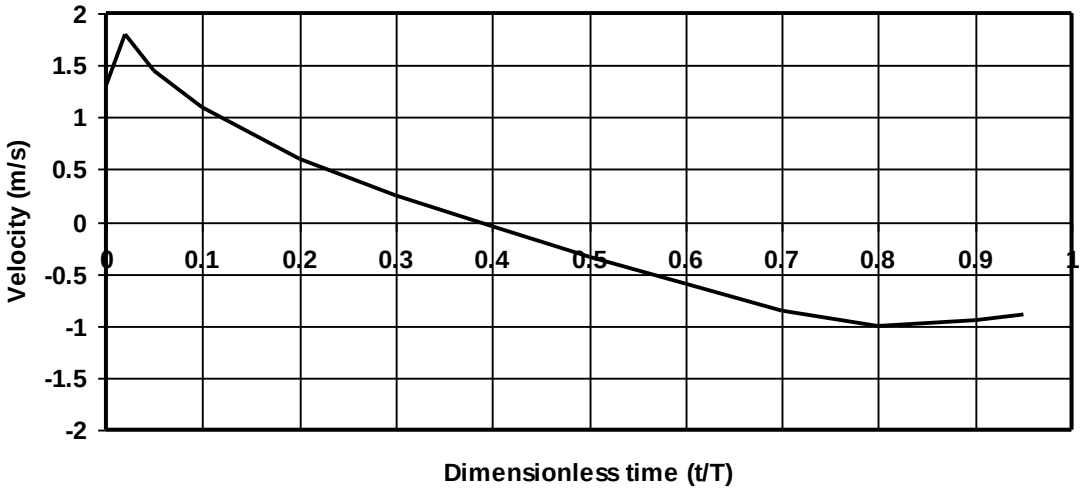

Figure 2.7 *Typical swash velocities as function of time above 0.28 mm sand bed; Perranporth Beach, Cornwall, UK (Masselink et al., 2005)*

Masselink et al. (2005) and **Masselink and Russell (2006)** have performed swash measurements in the high-tide swash zone of two macro-tidal beaches (fine sand 0.28 mm at mild sloping Perranporth Beach and coarse sand 0.55 mm at medium sloping Sennen Beach, Cornish coast, UK) using an array of mini electromagnetic current meters and optical backscatter sensors (OBS). The offshore wave height is in the range of 1 to 2 m (low wave conditions). The mean water depth at the transition between the surf zone with 100% inundation over time and the swash zone (intermittently wet and dry) is 0.25 m for Perranporth Beach and 0.4 m for Sennen Beach. The ratio of H_s/h at both transition points is of the order of 2. Their main findings show the presence of very energetic uprush and downrush velocities with values up to 2 m/s. **Figure 2.7** shows a typical (asymmetric and skewed) swash velocity distribution as a function of time. The vertical velocity gradient near the bed and the resulting bed-shear stress at the start of the uprush phase is significantly larger (factor 2) than that at the end of the backwash, see **Figure 2.6**. The time-averaged velocities are negative (offshore-directed) at both beaches and are of the order of -0.1 to -0.3 m/s during low wave conditions (offshore wave heights between 1 and 2 m). The near-bed suspended sand concentrations in the swash zone generally exceed 100 kg/m^3 at the start and the end of the backwash. During low wave conditions, the uprush induces a larger transport rate than the backwash indicating that the uprush is a more competent transporter of sediment than the backwash maintaining the beach (during low wave conditions).

Barnes et al. (2009) present direct measurements of bed-shear stress in the swash zone. The data were obtained using a shear plate with various types of roughness values (smooth to very rough). Numerical modelling was applied to calculate velocities and bed-shear stresses for the same tests. The measured bed-shear stresses and calculated velocities were used to back-calculate instantaneous local skin friction coefficients using the quadratic drag law. The data show rapid temporal variation of the bed-shear stress through the leading edge of the uprush, which is typically 2 to 4 times greater than the backwash shear stresses at corresponding low velocity. The data also indicate strong temporal variation in the skin friction coefficient, particularly in the backwash. Skin friction coefficients during the uprush are approximately twice those in the backwash at corresponding Reynolds number and cross-shore location.

According to **Ruessink and Van Rijn (2010)**, the skewness and asymmetry of the near-bed velocity in the inner surf and swash zone can to certain extent be represented by:

$$\tilde{U} = \hat{U}_1 \cos(\omega t) + \hat{U}_2 \cos(2\omega t - \beta) \qquad (2.29)$$

with: $\hat{U}_1$= amplitude of first harmonic, $\hat{U}_2$= amplitude of second harmonic, β= phase difference.
The skewness of this wave signal (velocity as a function of time) represents the wave asymmetry with respect to the onshore and offshore velocities (high and narrow peaks; wide and shallow troughs) and is defined as $S_k = \langle U^3 \rangle / (\sigma_U)^3$ with $(\sigma_U)^2 = \langle U^2 \rangle = 0.5[(\hat{U}_1)^2 + (\hat{U}_2)^2)]$ and $\langle .. \rangle$ = time-averaging.
The asymmetry with respect to time within the wave cycle (forward leaning waves) is defined as the Hilbert transform of the velocity signal which can also be defined as the skewness of the derivative of the velocity signal: $A_s = -\langle (\omega \, d\tilde{U}/dt)^3 \rangle / (\sigma_U)^3$. Symmetric waves (in time) yield a value of $A_s = 0$.
Using these definitions, it follows that:

$$S_k = \frac{0.75\,(\hat{U}_1)^2\,(\hat{U}_2)\cos(\beta)}{(\sigma_U)^3} \quad \text{and} \quad A_s = -\frac{0.75\,(\hat{U}_1)^2\,(\hat{U}_2)\sin(\beta)}{(\sigma_U)^3} \qquad (2.30)$$

$$\tan(\beta) = -A_s/S_k \;\text{ or }\; \beta = -\operatorname{atan}(A_s/S_k) \qquad (2.31)$$

$$(\hat{U}_2)^3 - 2(\sigma_U)^2 \hat{U}_2 + (4/3)(\sigma_U)^3 S_k/\cos(\beta) = 0 \qquad (2.32)$$

$$(\hat{U}_1)^2 + (\hat{U}_2)^2 = 2(\sigma_U)^2 \qquad (2.33)$$

Equation (2.32) can be solved analytically using a complex function approach, yielding:

$$\hat{U}_2 = 2(P)^{0.5}\cos(\varphi) \qquad (2.34)$$

with: $P = 2(\sigma_U)^2/3$, $Q = (4/3)(\sigma_U)^3 S_k/\cos(\beta)$ and $\varphi = 1/3[\arccos(-0.5Q\,P^{-1.5}) + n(2\pi)]$; n= 0, 1, 2 yields three roots; the smallest positive root is the solution. $\hat{U}_1$ follows from Equation (2.33).

Using linear wave theory, the standard deviation of the velocity is defined as: $\sigma_U = \pi H_{rms}/(1.41\,T\sinh(kh))$.

Based on the analysis of a large field data set of measured velocity time series, the parameters S_k, A_s and β are found to be:

S_k = $B\cos(\beta)$,
A_s = $B\sin(\beta)$,
β = $-90 + 90\tanh(0.6373/Ur^{0.5995})$,
B = $0.7939\,[1+\exp(K)]^{-1}$,
K = $2.8256[-0.6065 - {}^{10}\log(U_r)]$,
U_r = $0.75(0.5H_{Mo})\,k\,(kh)^{-3}$,
k = $(2\pi/L)$= wave number, h = water depth, $H_{Mo} = 1.41\,H_{rms}$.

Almost perfect sinusoidal waves are present for Ursell numbers smaller than $U_r < 0.01$. Skewed waves are present for $0.01 < U_r < 0.1$. Skewed and asymmetric waves (bore type waves) are present for $U_r > 0.1$. The phase angle β (in degrees) increases to -90 degrees

Figure 2.8 shows the saw-tooth near-bed velocity time signal for h= 0.3 m, H_{rms}= 0.3 m, T= 7 s. The peak landward and seaward velocities are almost the same. The duration of the forward phase is about 3 s and that of the backward phase is 4 s. The peak landward velocity occurs at about 1.3 s after t= 0 and the peak seaward velocity at about 1.3 s before t_{end}.

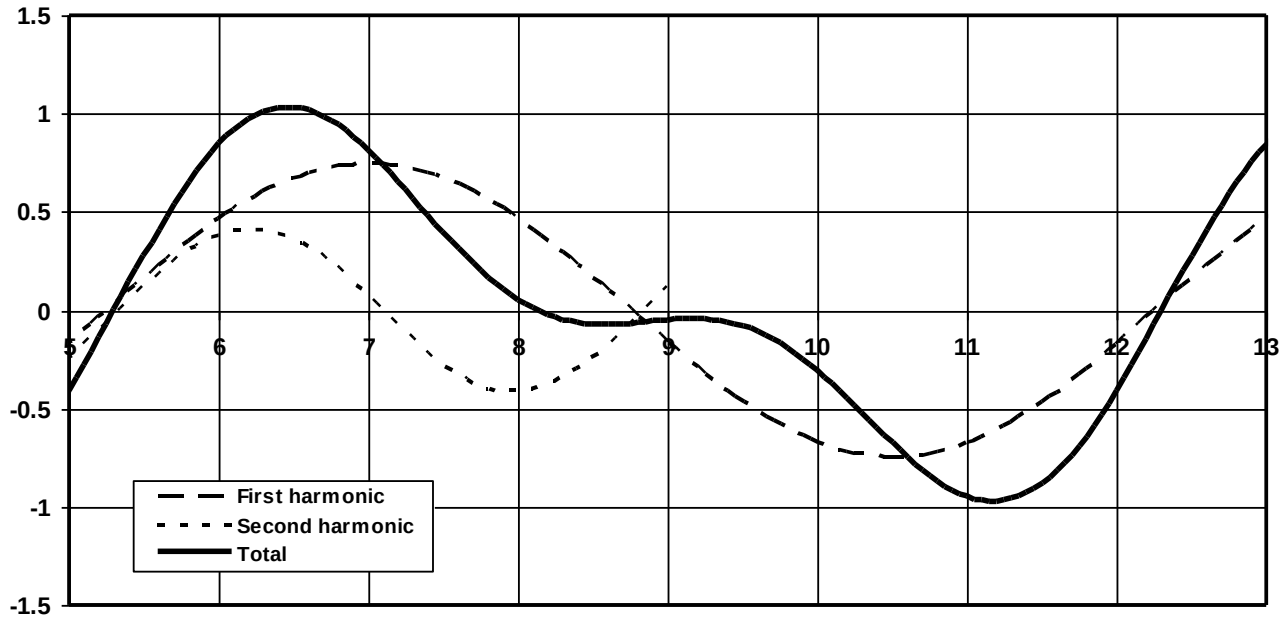

Figure 2.8 *Velocity time series for H_{rms}= 0.3 m, T= 7 s, h= 0.3 m, L= 11.9 m*

3. Laboratory and field data of gravel/shingle transport and beach profile changes

3.1 Laboratory data

3.1.1 Small-scale laboratory tests

A detailed physical model programme has been conducted in a random wave flume at HR Wallingford (**Powell, 1990**). A total of 181 detailed flume tests were undertaken at a scale of 1:17. A range of particle sizes and gradings from typical UK shingle beaches were represented by four distinct mixes of crushed anthracite, which provide the most satisfactory reproduction of natural beach permeability, sediment mobility threshold and onshore-offshore transport characteristics. Test conditions included 29 different wave conditions (based on JONSWAP spectra), four representative sediment mixes and several variations of effective beach thickness and core permeability values. All tests commenced with a standard beach face slope of 1:7 and a toe level in "deep water" seaward of the wave breaking point. Tests of "unlimited" beach thickness were run for a duration of 3000 waves, following a 3 hour profile compaction period using the largest waves calibrated for the study. Tests of restricted beach thickness (low permeability core at varying depths beneath the initial surface) were run for a duration of 1000 waves with no compaction period. Measurements were recorded of beach profile changes (at 500 wave intervals), wave run up exceedance and wave energy dissipation.
The factors tested by the flume study were: wave height (H_s), wave period (T_m), wave duration (N), beach material size (d_{50}), beach material grading (d_{85}/d_{15}) and effective thickness of beach material (D_B). Other factors of interest such as: foreshore level (D_w), water level (SWL), initial beach profile, wave spectrum shape and angle of wave attack were derived from other test results.

The test results show the following main features:

(a) The influence of wave height is most significant in the upper beach zone where an increase in height causes an increase in surf zone width (i.e. a flattening of the upper beach profile).
(b) The effect of wave period variations is apparent in the vertical dimensions of the profile; thus an increase in wave period will increase the crest elevation and lower the profile toe.
(c) Beach profiles react rapidly to changes in wave conditions. Tests show that 80% of the volumetric change occurred during the initial 500 waves of each test.
(d) The effective beach thickness appears to have greatest influence on horizontal regression of the beach above SWL. Exposure of the impermeable core and subsequent beach de-stabilisation generally occurs when the ratio D_B/d_{50} ratio is less than 30 (where D_B is the thickness of the mobile shingle layer measured normal to the initial beach slope and d_{50} is the median particle size).
(e) Beach particle size and grading appear to have some effect on beach profiles; however as only four sizes and two gradings were tested the observations cannot be considered conclusive. Smaller grain sizes appear to show more marked response to increases in wave steepness while broader grading ranges appear to result in higher crest levels.
(f) The foreshore level determines the location of the wave breaking zone. Waves breaking directly on a shingle beach will result in some form of step (swell waves) or bar and trough (storm waves) lower beach profile. Waves breaking seaward of the shingle will not develop either variation and will have reduced upper beach dimensions (crest elevation and run up distance).
(g) Variations in the steep initial beach slopes typical of shingle beaches are considered to have little effect on the ultimate beach profile, though they may affect the mode and duration of formation.
(h) Gradually varying water levels do not affect the shape of the slope of the beach profiles, but will determine the location of the crest profile on the beach face.
(i) The effect of varying the angle of wave attack on profile development data indicates that oblique wave action restricts the full development of at least part of the profile.

3.1.2 Large-scale laboratory tests

Various experiments on the behaviour of gravel and shingle slopes under wave attack have been performed by **Deltares/Delft Hydraulics (1989)** in the large-scale Deltaflume (length of 200 m, width of 5 m and depth of 7 m). Two gravel sizes have been used (d_{50}= 0.0048 m and d_{50}= 0.021 m, see **Table 3.1**). The initial beach slope was 1 to 5 (plane sloping beach) in all (nine) experiments. Irregular waves were generated (Pierson-Moskowitz spectrum). The basic data are given in **Table 3.1**.
The dynamic behaviour of beaches can be described by the parameter $H_{s,o}/((s-1)d_{50})$, as follows:
sand range (breaker bar formation): $H_{,o}/[(s-1)d_{50}] > 200$
gravel range (swash bar formation): $10 < H_{,o}/[(s-1)d_{50}] < 200$
cobble and stone range without slope deformation: $H_{,o}/[(s-1)d_{50}] < 10$

The parameter $H_{s,o}/[(s-1)d_{50}]$ of the experiments in the Deltaflume is in the range of 50 to 80.
($H_{s,o}$= offshore significant wave height, T_p= peak wave period, s= relative density, d_{50}= sediment size).

Test	Beach slope	d_{10} (m)	d_{50} (m)	d_{90} (m)	SWL above flume bottom (m)	$H_{s,o}$ (m)	T_p (s)
1	1 to 5	0.014	0.021	0.029	3	0.77	5.0
2	1 to 5	0.014	0.021	0.029	3	1.0	5.0
3	1 to 5	0.014	0.021	0.029	4.5	1.5	5.5
4	1 to 5	0.0031	0.0048	0.0065	4.5	0.62	2.9
5	1 to 5	0.0031	0.0048	0.0065	4.5	1.24	4.5
6	1 to 5	0.0031	0.0048	0.0065	4.5	1.68	5.7
7	1 to 5	0.0031	0.0048	0.0065	4.5	1.28	4.5
8	1 to 5	0.0031	0.0048	0.0065	4.5	1.08	5.1
9	1 to 5	0.0031	0.0048	0.0065	4.5	1.14	7.6

Table 3.1 *Basic data of Delta flume experiments on gravel beaches (Deltares, 1989)*

The measured bed surface profiles of Tests 1, 2, 3, 4, 5, 6 and 9 are shown in **Figures 3.1** and **3.2**.
The most characteristic features are:

- formation of swash bar above SWL (up to 2.5 m) due to onshore transport; the swash bar extends vertically to about $2H_{s,o}$ above SWL indicating the effect of wave run-up; the swash bar size increases with increasing wave height and with increasing wave period (Test 9 with T_p= 7.6 s);
- formation of a small breaker bar extending to about $1H_{s,o}$ below SWL when relative fine gravel (d_{50}= 0.0048 m) is present for $H_{,o}/((s-1)d_{50})$> 100 (Tests 4, 5 and 6);
- generation of scour pit below SWL; the scour depth extends vertically to $3H_{s,o}$ below SWL;
- small zone (with height equal to $H_{s,o}$) direct above and beneath SWL showing almost no deformation;
- ripples with length scales of 1 to 3 m and height scales of 0.1 to 0.4 m at the lower part of the fine gravel slope (d_{50}= 0.0048 m) for $\psi > 10$ ($\psi = \hat{U}^2/[(s-1)gd_{50}]$, $\hat{U}$ = peak orbital velocity based on linear wave theory); the ripples are largest in Test 9 with relatively long waves (T_p= 7.6 s); the ripple lengths are roughly equal to $2\hat{A}$ to $2.5\hat{A}$ ($\hat{A}$ = peak orbital excursion).

The formation of the swash bar is strongly related to the wave uprush and downrush near the water line. The uprush is much stronger than the downrush due to the percolation of water through the porous gravel bed surface resulting in a relatively strong velocity asymmetry in the swash zone and hence net onshore transport of gravel particles. The maximum uprush velocity can be estimated by the bore velocity near the water line: $u_b = (gh)^{0.5}$ with h in the range of 0.1 to 0.2 m yielding u_b in the range of 1 to 3 m/s.

The vertical runup can be estimated by using $R_{2\%}= 2.3(\zeta)^{0.3}$ with $R_{2\%}$ =vertical runup above SWL exceeded by 2% of the values, $\zeta= \tan(\beta)/(2\pi H_{s,toe}/(gT_p^2))$ = surf similarity parameter, $\tan(\beta)$= gradient of gravel slope, T_p= wave period (**Van Gent, 2001**). The ζ-parameter is about 1 for the Deltaflume experiments resulting in runup values of about $2H_{s,toe}$ ($\cong 2H_{s,o}$), which is in reasonable agreement with observed values (vertical swash bar level of 2 to 2.5 $H_{s,o}$).

The swash bar area (A_s) is in the range of 2 to 5 m^2 after about 4 hours (duration of storm event). The swash bar area (A_s) can be made dimensionless by using the significant wave heigth ($H_{s,toe}$) at the toe of the gravel slope, which is about equal to the offshore wave height ($H_{s,o}$) in the Deltaflume experiments. The parameter $A_s/(H_{s,toe})^2$ is in the range of 2 to 4 after about 4 hours (duration of storm event).

The dimensionless breaker bar area $A_b/(H_{s,toe})^2$ also is in the range of 1 to 2 after about 4 hours.

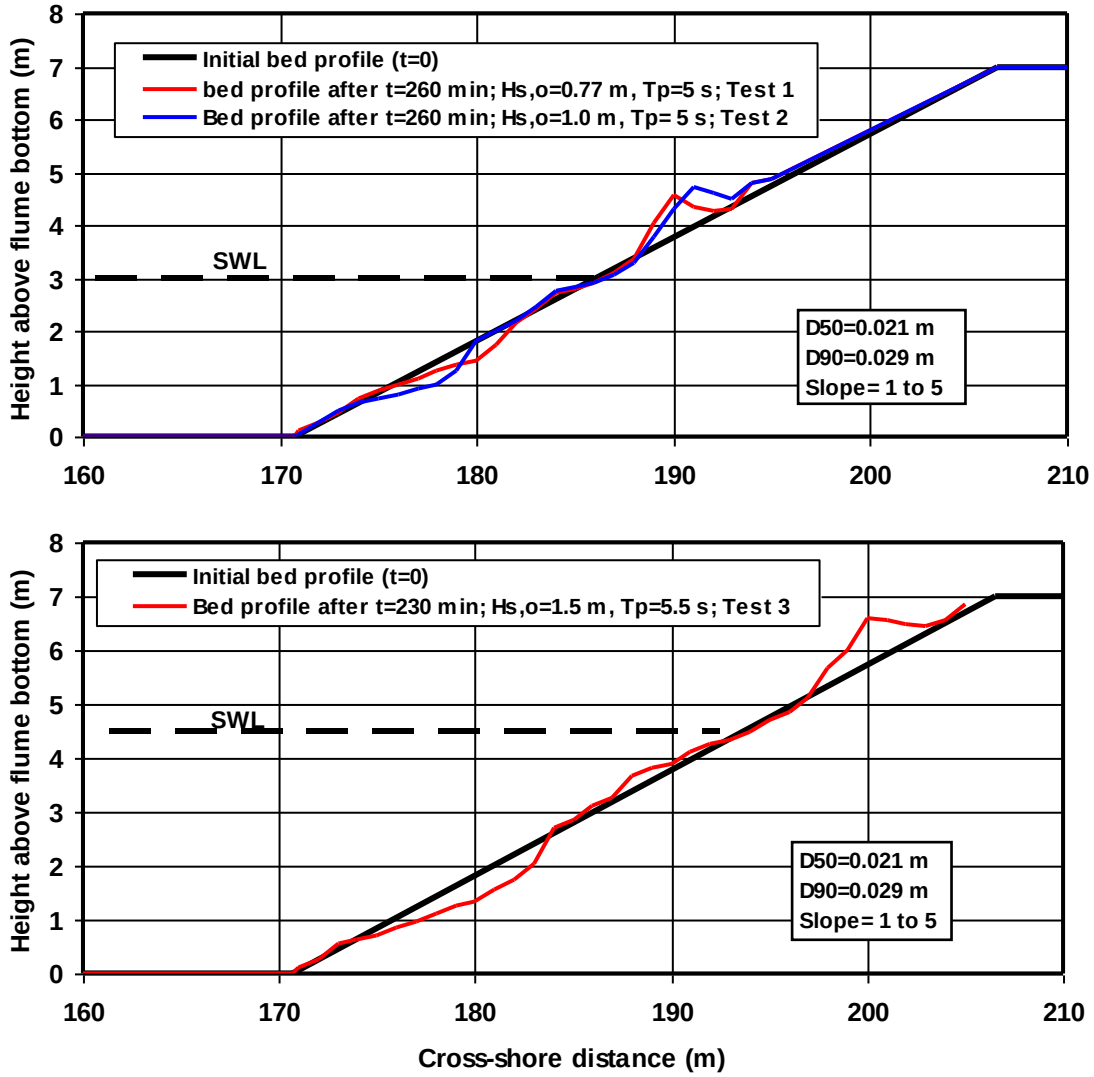

Figure 3.1

Top: *Tests 1 and 2 (d_{50}= 0.021 m; SWL=3 m)*

Bottom *Test 3 (d_{50}= 0.021 m; SWL= 4.5 m)*

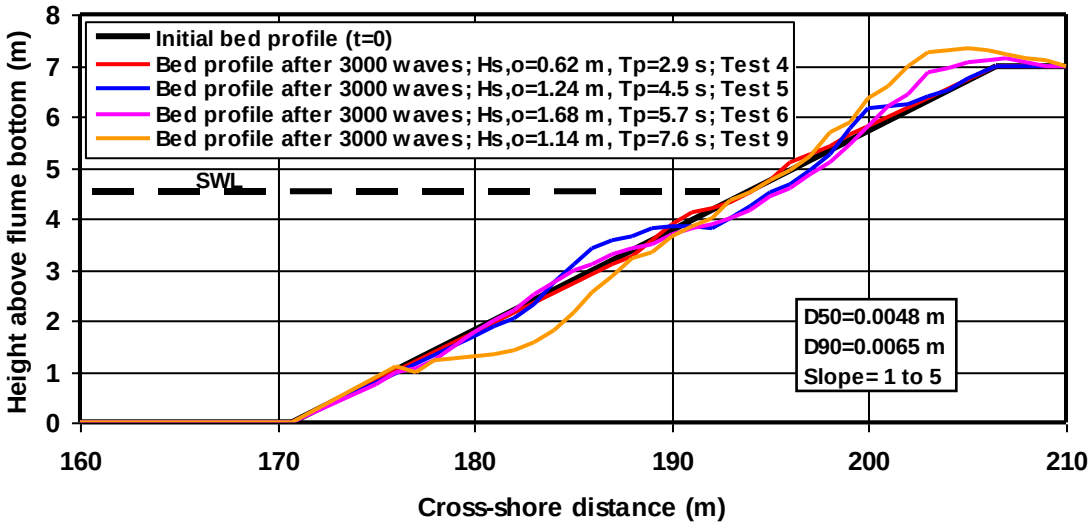

Figure 3.2 *Tests 4, 5, 6 and 9 (d_{50}= 0.0048 m; SWL= 4.5 m), Deltaflume, The Netherlands*

Various experiments on the behaviour of shingle slopes under irregular wave attack have been performed in the large-scale GWK flume in Hannover, Germany (**López et al., 2006**). The shingle material has d_{50} of approximately 0.02 m. The initial slope of the beach is about 1 to 8. The basic data are given in **Table 3.2**.
The measured bed surface profiles of Tests 1 to 5 are shown in **Figure 3.3**. As can be observed, there is a gradual development of a triangular bar with a maximum height of about 2 m (about $2H_{s,toe}$) just beyond the still water line after 12000 waves (or 57100 s). The total accretion area is about 10 m^3/m. The transport of shingle passing the water line is about 10/57100= 0.0000175 m^2/s or about 15 m^3/m/day at an offshore wave height of about $H_{m,o}$= 1 m. This value fits well in the transport plot of **Figure 4.16**.

Test	Beach slope	d_{50} (m)	SWL above flume bottom (m)	$H_{m,o}$ (m)	T_p (s)	Number of waves
1	1 to 8	0.021	4.7	0.52	3.2	3000
2	1 to 8	0.021	4.7	0.91	4.1	2000
3	1 to 8	0.021	4.7	1.07	4.3	2000
4	1 to 8	0.021	4.7	0.95	5.1	3000
5	1 to 8	0.021	4.7	1.02	7.7	2000

Table 3.2 *Basic data of GWK flume experiments on shingle beaches*

In June and July 2008 large-scale experiments on gravel barriers (d_{50}= 0.011 m) have been performed in the Deltaflume of Deltares (**Buscombe, Williams and Masselink, 2008**) by a consortium of researchers led by the University of Plymouth, UK. The aim of these (BARDEX) experiments was to study the hydrodynamic and morphodynamic characteristics of a gravel barrier backed by a lagoon with a lower water level. The sea water level was varied as a function of time to simulate tidal variations. The lagoon water level was also varied. High sea water levels were used to study the occurrence of wave overtopping and overwashing. The water level was gradually increased until barrier destruction occurred.
The test results with a constant sea level show the formation of a typical swash bar landward of the still water level with a maximum crest level of about $2H_{s,toe}$ above the still water level (SWL). The test results with a time-

varying sea level show the vertical build-up of the crest to a level equal to about $1.5H_{s,toe}$ above HWL (with HWL= maximum tidal water level).
The results of Test B3 with a constant water level on both sides of the barrier (no overtopping) are used in **Section 4.2.3** for comparison with computed results.

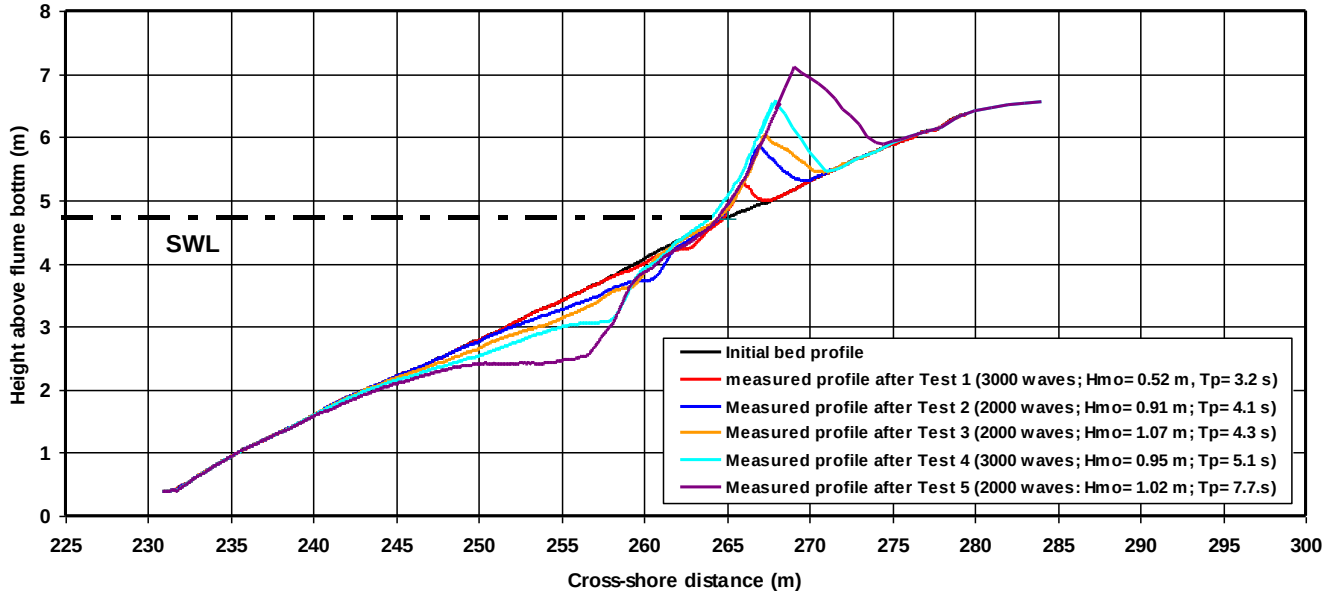

Figure 3.3 *Tests 1 to 5 (d_{50}= 0.02 m), GWK, Hannover, Germany*

3.2 Field data

Gravel transport

Chadwick (1989) used surface mounted traps to measure the alongshore gravel/shingle transport at the beach of Shoreham (West Sussex, England) during low and moderate wave conditions (wave heights between 0.3 and 0.8 m, periods between 2 and 4 s, wave angle between 20° and 40°). The beach consisted of shingle with a sand foot at about the low water mark (beach slope, tanβ= 0.10 to 0.12). Alongshore transport was measured on 18 occasions, together with concurrent measurement of wave height, angle and speed. The traps were positioned approximately on the waterline two hours before high water and the volumes of gravel/shingle collected were measured as the tide receded. Gravel/shingle transport occured mainly in the swash zone. The transports rates measured by the trap were converted to swash-zone integrated transport rates (Q_t), based on an assumed cross-shore transport distribution (maximum at break point, dropping linearly to zero at both the lower and upper limit of the swash zone). The results roughly are ($H_{s,b}$= significant wave height at break point, α_b= 13° to 20°):

Q_t= 3 m^3/day for $H_{s,b}$= 0.3 m,
Q_t= 10 m^3/day for $H_{s,b}$= 0.35 m,
Q_t= 20 m^3/day for $H_{s,b}$= 0.4 m,
Q_t= 30 m^3/day for $H_{s,b}$= 0.7 m.

Nicholls and Wright (1991) performed tracer studies to determine longshore transport rates. Three experimental studies using aluminium tracers have been analysed. All three experiments were performed on shingle beaches (with nearshore zone of sand) at Hurst Castle spit, England. The beaches are exposed to wave action from the English channel and from the Atlantic Ocean. The tidal range is about 2 m. The beach and tracer characteristics (length of shortest and longest axis) are given in **Table 3.3**. The tracers were injected at low tide as a slug at one pebble depth.

Exp.	Tracer size (mm)	Size orig. mat. (mm)	Duration of exp. (hrs)	Displace-ment of centroid (m)	Width of mobile layer (m)	Thickness of layer (m)	Longsh. transport (m^3/day)	Wave energy at br. line $(H_b)^{2.5}\sin 2\alpha$ ($m^{2.5}$)
1) 9/5-25/5 1977	33-48	32	74	32	17-27	0.09-0.19	15-50	0.25
2) 20/2-11/3 1978	31-59	32	50	50	27-37	0.05-0.15	30-135	0.52
3) 8/3-27/4 1982	26-52	16	122	165	15-25	0.09-0.19	45-160	0.11-0.16

Table 3.3 *Data of gravel tracer study at Hurst Castle spit, England (Nicholls and Wright, 1991)*

In experiments 1 and 2 the tracer particles were placed on the upper foreshore, where the original material was of similar size. In experiment 3 the tracer material was split into three identical slugs injected at three sites across the foreshore from low water to high water. Cross-shore mixing of the tracer material with the original material was observed to occur rapidly (in hours) due to high wave energy in all three cases. About 60% to 70% of the tracer material was recovered. All three experiments were characterized by high energy conditions. During experiment 3 the wave height at the breakerline varied between 0.3 and 1.3 m (time-averaged value of about 0.6 m). The longshore transport rate was calculated as the product of the longshore displacement of the tracer centroid, the mean width of the mobile layer and the mean layer thickness per unit time. The wave energy was computed neglecting wave heights smaller than 0.5 m (threshold value for initiation of motion). The estimates of the longshore transport rates in experiment 3 may be relatively large, because the tracer size was relatively large resulting in a relatively large exposure to wave-induced forces.

Barrier erosion and migration

Barrier recession rates up to 4 m per year have been observed (**Nicholls and Webber, 1988**) at Hurst beach, Christchurch Bay, England (**Figure 3.4**). Most of the recession did occur during autumn and winter months. The barrier behaviour was influenced by saltmarsh deposits (peat, mud) exposed on the foreshore and rapidly eroded. This subsoil material leads to relatively rapid settlement beneath the weight of the gravel barrier reducing the crest level of the barrier. Differential settlement of the subsoil can lead to local depressions and increased overwashing.
Bradbury and Powell (1990) give an example of barrier rollover and lowering at Hurst Spit, England (**Figure 3.4**). The beach is characterised by coarse grain sizes of about 16 mm. The crest is generally between 2 and 4 m above HW, with a crest width of 3 to 10 m. Large-scale overwashing of the spit occurred in December 1989, resulting in crest lowering (about 1.5 m) along a beach length of 800 m. The beach was moved back by about 30 to 40 m in a single storm event, see **Figure 3.4**.

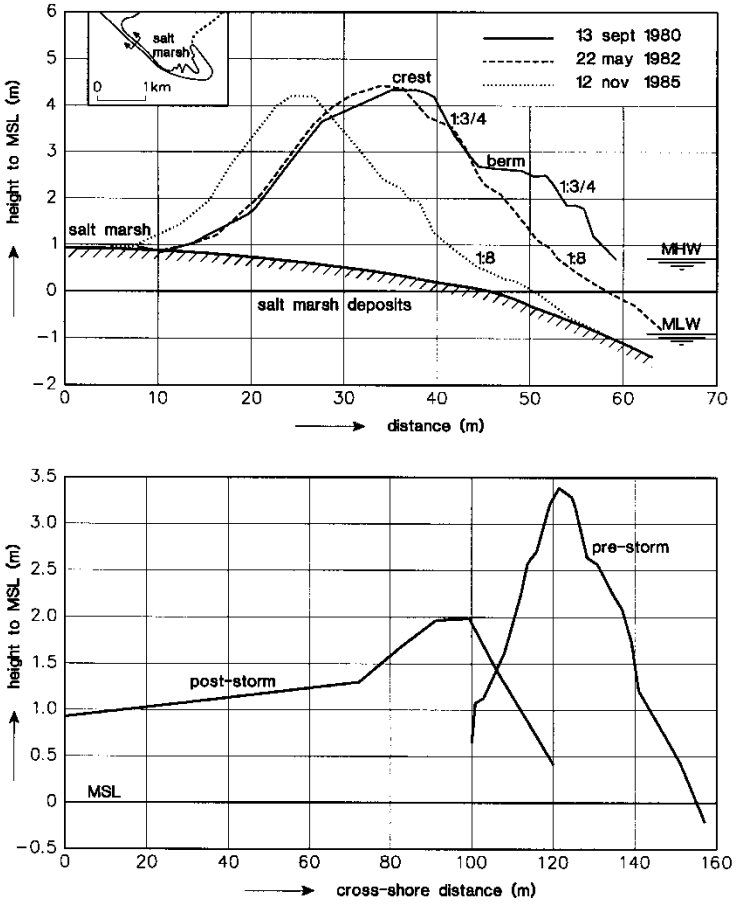

Figure 3.4
Top: Hurst beach, Christchurch Bay, England (Nicholls and Webber, 1998)
Bottom: Barrier response to storm event, Hurst Spit, South-England (Bradbury and Powell, 1990)

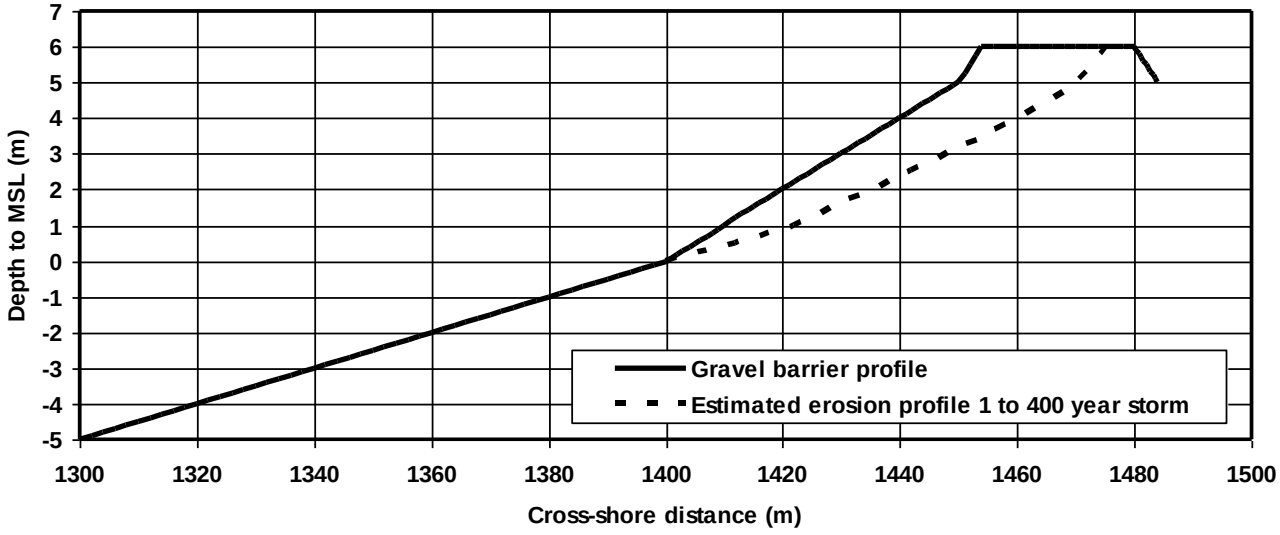

Figure 3.5 *Erosion profile of shingle barrier at Pevensey Bay, East Sussex, UK (www.pevensey-bay.co.uk)*

The **Pevensey Coastal Defence** (**Sutherland and Thomas, 2009**) uses a schematized erosion profile (as shown in **Figure 3.5**) due to a storm with a return interval of 400 years to evaluate the strength of the 9 km long shingle barrier along the coast of Pevensey Bay (East Sussex, English Channel coast of southern England) under storm conditions. The estimated erosion area based on extrapolation of observed erosion volumes is approximately 100 m^3/m. The highest waves arrive predominantly from the south-west with significant offshore wave heights up to 6 m. High water levels during major storms vary in the range of 3.5 to 4.5 m above MSL. The shingle barrier along the Pevensey Bay coast consists of a mixture of sand (smaller than 2 mm), gravel (2 to 60 mm) and cobbles (greater than 60 mm). This barrier can be overtopped by large waves, may leak or roll-back landward and ultimately may breach. Temporary flooding events did occur at Pevensey in 1926, 1935, 1965 and 1999.

Minimum barrier dimensions

A novel approach to determining the minimum required cross-sectional area to withstand gravel barrier breaching based on laboratory and field data has been developed by **Sutherland and Obhrai (2009)**. This approach uses the concept of barrier inertia (**Bradbury, 2000**) as a means of identifying the threshold of breaching of gravel barrier beaches. This is a non-dimensional measure of a barrier's ability to withstand breaching given by (see definition sketch in **Figure 3.6**):

$$B_i = R_c\, A_c/(H_{s,toe})^3 \qquad (3.1)$$

where: B_i = barrier inertia; R_c = barrier freeboard above mean water level (including tide and storm surge); A_c = cross-sectional area of barrier above mean water level; and $H_{s,toe}$ = significant wave height at the toe of the barrier.

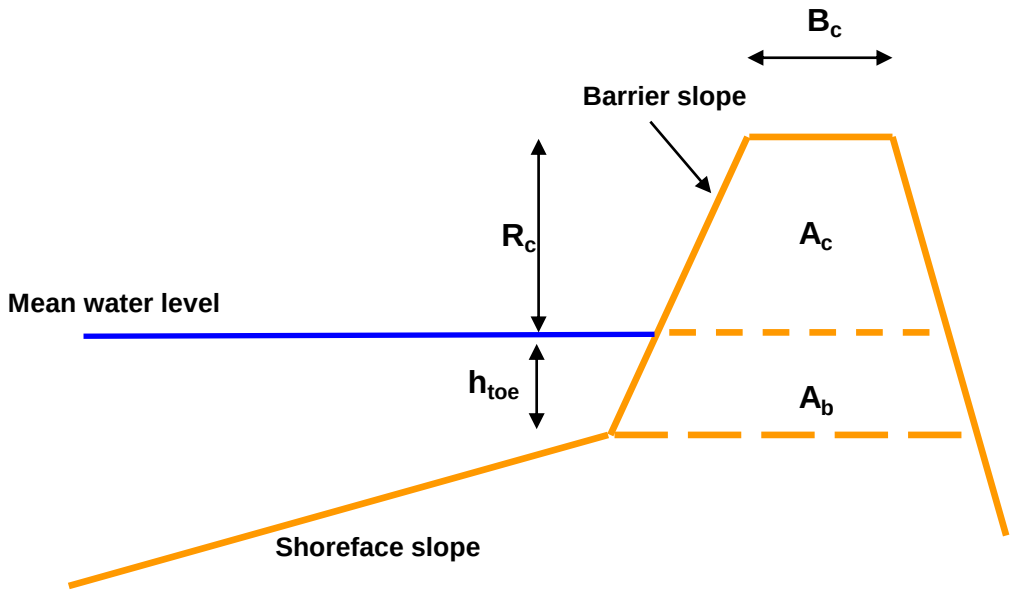

Figure 3.6 *Definition sketch of gravel barrier*

Bradbury (2000) developed an empirical framework to predict the threshold for breaching of shingle barrier beaches, based on extensive fieldwork (at Hurst Spit) and physical model data. **Obhrai et al. (2008)** extended the range of validity of this approach to lower and higher steepness waves. The **Obhrai et al. 2008** formula for the minimum required cross-sectional area (A_c) is:

$$A_c \geq (1/R_C)[-153.1\ (H_{s,toe}/L) + 10.9]\ (H_{s,toe})^3 \qquad (3.2)$$

Equation (3.2) can be roughly represented by: $A_c \geq (8/R_C)(H_{s,toe})^3$ (3.3)

Assuming: $H_{s,toe} \cong 0.5\ H_{s,o}$, it follows that: $A_c \geq (1/R_C)(H_{s,o})^3$ (3.4)

Equation (3.4) is shown in **Figure 3.5** for various values of R_c and $H_{s,o}$. The A_c-values are in the range of 15 to 250 m^2 for $H_{s,o}$ in the range of 4 to 8 m.

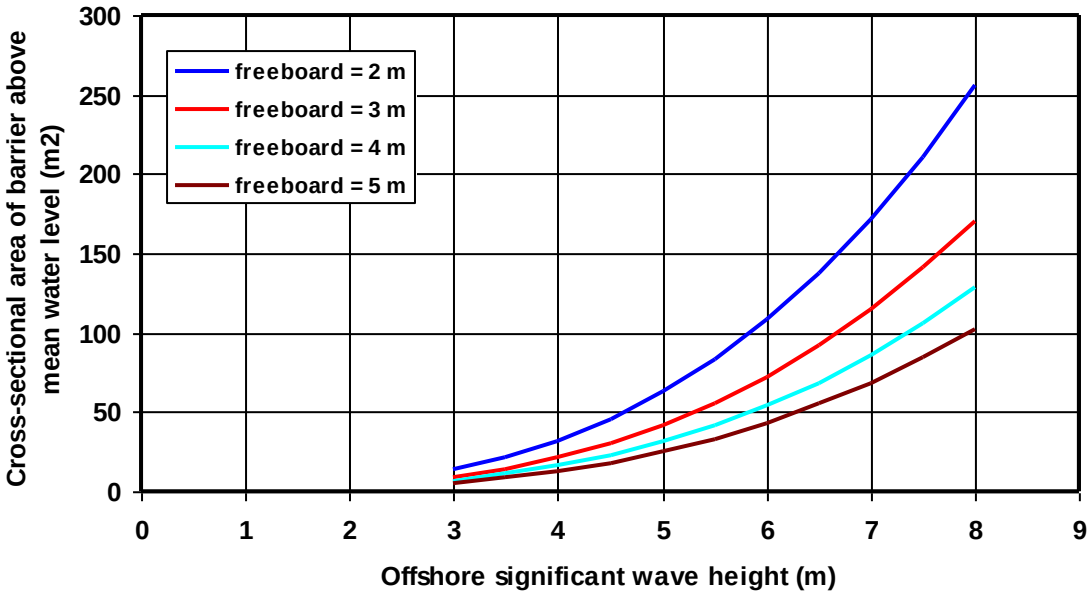

Figure 3.7 *Minimum cross-sectional area (A_c) of barrier above mean water level as funtion of freeboard and offshore significant wave height.*

4. Longshore transport of gravel/shingle

4.1 General approach

This Chapter is focused on the computation of the net longshore sediment transport (LST) along the coast of Pevensey Bay based on available wave data statistics. The LST is computed by an empirical equation which computes the LST in a zone landward of the wave breaker line. The most important input parameters are the sediment size, the beach slope, the significant wave height and the wave incidence angle at the breaker line.
The empirical LST equation including validation is explained in Section 4.2. The validation work in Section 4.4 includes a comparison to the LST-values computed by a more detailed cross-shore model (CROSMOR-model) for a steep gravel beach. The CROSMOR-model is a detailed process-based model which computes both the cross-shore and longshore wave parameters and the sediment transport components along the steep beach profile.
The computed longshore transport components integrated over the beach zone (landward of the -3 m depth line) have been used to improve the more simple empirical LST-equation.
Results of sensitivity LST-computations are given to study the effects of various key input parameters in Section 4.5. The LST-equation is also used to determine the contribution of storms to the total annual LST.

4.2. Longshore transport processes and modelling

The transport of coarse sediments is most active in the swash zone of the beach face and is caused by wave uprush (decelerating flow) and backwash (accelerating flow). Both laboratory and field measurements over an impermeable bottom have shown that the swash of the incident waves on a steep beach is skewed and asymmetric (saw-tooth waves), i.e. the backwash is not simply the reverse of the uprush. Generally, onshore flow velocities during the uprush are larger but of shorter duration than the seaward velocities during the backwash. Maximum landward velocities occur at the start of the uprush, whereas maximum seaward velocities take place at the end of the backwash. The water depths that occur during the uprush are generally larger than those that occur during the backwash (Butt and Russell, 2000; Elfrink and Baldock, 2002).
The swash zone is the zone which is intermittently wet and dry showing relatively large velocities during the uprush and backwash phases of the saw-tooth swash wave cycle due to bore propagation and bore collapse, often in combination with low-frequency oscillations which generally grow in amplitude towards the shoreline.
The swash zone is a particularly complex nearshore zone where short and long waves, tides, sediments and groundwater flow (infiltration/percolation) all play an important role. Long waves are generated by the release of bound long waves in the surf zone due to the breaking of short waves and by cross-shore variations of the short wave breakpoints (surf beat). The role of percolation is especially important on steep, coarse-grained beaches leading to beach accumulation and steepening as a result of the diminished sediment carrying capacity of the reduced backwash volume of water and velocity, following percolation into the coarse-grained bed. These effects will lead to a landward bias (asymmetry) in swash transport depending on grain size.
Measurements of sheet flow transport for half saw-tooth waves in a wave tunnel (King, 1991) indicate that the sediment transport under steep fronts (decelerating flow) is about twice as large as under steep rears (accelerating flow). Swash-related infiltration-exfiltration effects across a saturated beach face enhances the upslope transport of sediment transport and reduces the downslope transport (Masselink and Hughes, 1998).
Masselink et al. (2005) and Masselink and Russell (2006) have performed swash measurements in the high-tide swash zone of two macro-tidal beaches (fine sand 0.28 mm at mild sloping Perranporth Beach and coarse sand 0.55 mm at medium sloping Sennen Beach, Cornish coast, UK) using an array of mini electromagnetic current meters and optical backscatter sensors (OBS). The offshore wave height is in the range of 1 to 2 m (low wave conditions). The mean water depth at the transition between the surf zone with 100% inundation over time and the swash zone (intermittently wet and dry) is 0.25 m for Perranporth Beach and 0.4 m for Sennen Beach. The ratio of H_s/h at both transition points is of the order of 2. Their main findings show the presence of very energetic uprush and downrush velocities with values up to 2 m/s. During low wave conditions, the uprush induces a larger transport rate than the

backwash indicating that the uprush is a more competent transporter of sediment than the backwash maintaining the beach (during low wave conditions).

Very relevant for coastal gravel transport are the flume experiments of Meyer-Peter and Muller (1948) with relatively large water depths in the range of 0.5 to 1 m. Some of their data are shown in **Table 2.1**. The transport of gravel with d_{50}=28.7 mm is relatively low (<0.03 kg/m/s) for a current velocity of about 2 m/s. Initiation of motion starts at a velocity of about 1.8 m/s. The transport rate of gravel increases to about 10 kg/m/s for a current velocity of 3 m/s. These results show that peak velocities in the range of 2 to 3 m/s are required to produce intensive transport of gravel in the coastal zone. Most likely, the gravel transport in field conditions is somewhat smaller than that in ideal flume conditions. Limiting factors in field conditions are wider size ranges and local armouring effects.

Water depth (m)		**Median gravel size (mm)**	**Depth-averaged current velocity (m/s)**	**Gravel transport (kg/m/s)**
Range	**Values**			
0.6-0.75	0.6	28.7	2.73	8.46
	0.65	28.7	2.52	3.84
	0.7	28.7	2.34	1.91
	0.72	28.7	2.26	0.97
0.8-1.1	1.09	28.7	2.11	0.0294
	0.97	28.7	2.37	0.956
	0.96	28.7	2.40	0.952
	0.93	28.7	2.47	1.91
	0.91	28.7	2.52	1.93
	0.86	28.7	2.66	3.82
	0.85	28.7	2.68	3.79
	0.82	28.7	2.05	0.032
	0.8	28.7	2.88	8.43
	0.78	28.7	2.87	8.49
0.15-0.25	0.213	5.2	1.09	0.038
	0.182	5.2	1.26	0.154

Table 4.1 *Gravel transport in flume experiments; d_{50}=28.7; 5.2 mm (Meyer-Peter and Mueller, 1948)*

4.3 Model description

A relatively simple empirical equation is used to compute the longshore transport of gravel/shingle (LST) at Pevensey Beach as function of the wave conditions, the sediment and beach properties. The LST-equation which is implemented in the LONGMOR-model has been developed by Van Rijn (2014) and is valid for fine sand to shingle.

The LST is defined as the transport of shingle in the surf zone with breaking waves landward of the wave breaking point. This latter point varies in relation the water level and the offshore wave height. Wave breaking is more landward at high water levels and low waves and more seaward at low water levels and high waves.

Figure 4.3.1 shows the bed level at the breaker line as function of the water level (to OD) and the significant offshore wave height (data of Pevensey beach, UK).

The bed level at the breaker line is at -6.7 m OD for a water level of -2 m OD and $H_{s,o}$=4 m.

The bed level at the breaker line is at +1.9 m OD for a water level of +4 m OD and $H_{s,o}$=1.5 m.

A complicating factor is the transition of bed material size in cross-shore direction. Herein, it is assumed that the bed consists of sand seaward of the -3 m depth line and of shingle landward of the -3 m depth line (to OD≅MSL). The LST-model is based on the assumption of uniform bed material (shingle) in cross-shore direction. Thus, the model bed between the breaker line and the beach consists of shingle everywhere. In conditions with low water levels and high waves, the breaker line is far seaward of the -3 m depth contour. The model bed in this zone consists of shingle. In reality, the bed seaward of the -3 m line consists of sand. This means that the predicted LST-values of shingle are too high for conditions with low water levels and high waves. This over-prediction effect can be taken into account by a reduction factor (estimated to be about 0.7; reduction of 30%).

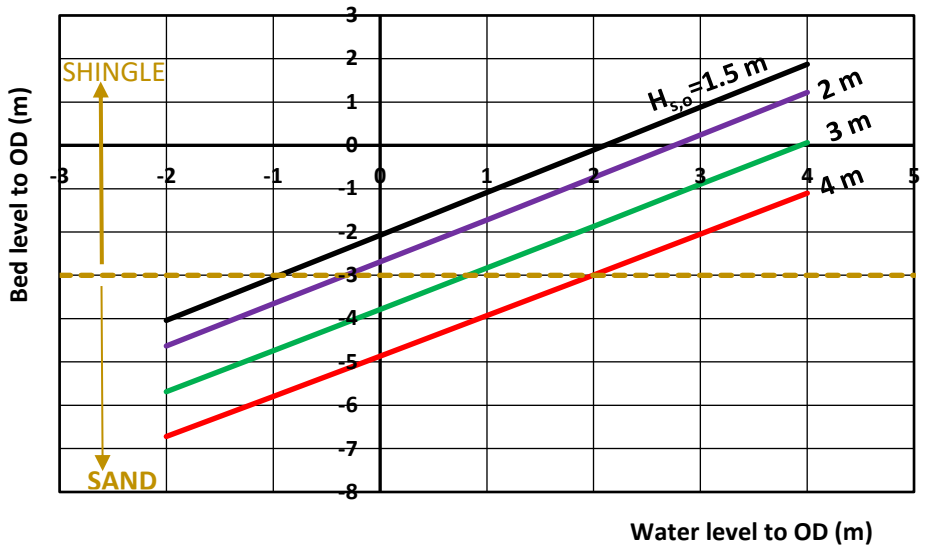

Figure 4.3.1 *Bed level at breaker line as function of water level and offshore wave height*

Detailed description empirical LST equation

The longshore sand transport of Van Rijn (2014) is described by:

$$Q_{LS}= 0.00018\ K\ K_{swell}\ (1-\varepsilon)^{-1}\ g^{0.5}\ (\tan\beta)^{0.4}\ (d_{50})^{-0.6}\ (H_{s,br})^{3.1}\ \sin(2\alpha_{br}) \qquad (4.1)$$

Q_{LS} = total longshore sediment transport (in m^3/s, including pores),

ε = porosity (≅0.4), ρ_s =sediment density (kg/m^3), d_{50}= median grain size (m),

$H_{s,br}$= significant wave height at breaker line (m), θ_{br} = wave angle at breaker line,

g = acceleration of gravity (m/s^2), tanβ = slope of beach/surf zone,

K_{swell} = swell factor, K= calibration factor (default=1).

Equation (4.1) can also be expressed, as:

$$Q_{LS}= 0.0006\ K\ K_{swell}\ (1-\varepsilon)^{-1}\ (\tan\beta)^{0.4}\ (d_{50})^{-0.6}\ (H_{s,br})^{2.6}\ V_{eff,L} \qquad (4.2)$$

$$V_{wave}= 0.3\ (gH_{s,br})^{0.5}\ \sin(2\alpha_{br}) \qquad (4.3)$$

with:

$V_{eff,L}$ = $[(V_{wave,L})^2+(V_{tide,L})^2]^{0.5}$= effective longshore velocity at mid surf zone (m/s) for tidal velocity and wave induced velocity in same direction (minus sign for opposing conditions);

$V_{wave,L}$ = wave-induced longshore current velocity (m/s) averaged over the cross-section of the surf zone.

$V_{tide,L}$ = longshore velocity in mid surf zone due to tidal forcing (=0 m/s for non-tidal cases; 0.1 m/s for micro-tidal, 0.3 m/s for meso-tidal and 0.5 m/s for macro-tidal cases).

Equation (4.1) does not account for the effect of the wave period on the longshore transport rate. However, low-period swell waves in the range of 1 to 2 m produce significantly larger transport rates compared to wind waves of the same height (H_{rms}=H). This effect can to some extent be taken into account by using a correction factor to the longshore transport rate, if the percentage of swell waves (in terms of wave height) of the total wave height record is known. Herein, it is proposed to use a swell factor, as follows:

$$K_{swell}=1.5(p_{swell}/100) + 1\ (1-p_{swell}/100) = 0.015p_{swell} + (1-0.01p_{swell}) \quad (4.4)$$

with: p_{swell}= percentage of low-period swell wave heights of the total wave height record (about 10% to 20% for sea coasts and 20% to 30% for ocean coasts).

Some values are: K_{swell}=1.05 for p_{swell}=10%; K_{swell}=1.1 for p_{swell}=20% and K_{swell}=1.5 for p_{swell}=100%.
If swell is absent (or unknown), then K_{swell}= 1.
Using this approach, the longshore transport rate increases slightly for increasing percentage of swell.

The Kamphuis (1991) method is given by:

$$Q_{LS}=2.33\ K\ [\rho_s/(\rho_s-\rho)]\ [(1-\varepsilon)\rho_s]^{-1}\ (T_p)^{1.5}\ (\tan\beta)^{0.75}\ (d_{50})^{-0.25}\ (H_{s,br})^{2}\ [\sin(2\alpha_{br})]^{0.6} \quad (4.5a)$$

$$Q_{LS}=3.8\ K\ [(1-\varepsilon)\rho_s]^{-1}\ (T_p)^{1.5}\ (\tan\beta)^{0.75}\ (d_{50})^{-0.25}\ (H_{s,br})^{2}\ [\sin(2\alpha_{br})]^{0.6} \quad (4.5b)$$

with: Q_{LS}= longshore sediment (m^3/s, including pores); $H_{s,br}$=significant wave height at breaker line (m); α_{br} =wave angle at breaker line (°); d_{50}=median particle size in surf zone (m); tan β= beach slope; T_p = peak wave period; K = calibration factor (default=1).

The Kamphuis-equation was modified by Mil-Homens et al. (2013) in:

$$Q_{LS}=0.15\ K\ [\rho_s/(\rho_s-\rho)]\ [(1-\varepsilon)\rho_s]^{-1}\ (T_p)^{0.89}\ (\tan\beta)^{0.86}\ (d_{50})^{-0.69}\ (H_{s,br})^{2.75}\ [\sin(2\alpha_{br})]^{0.5} \quad (4.6a)$$

$$Q_{LS}=0.24\ K\ [(1-\varepsilon)\rho_s]^{-1}\ (T_p)^{0.89}\ (\tan\beta)^{0.86}\ (d_{50})^{-0.69}\ (H_{s,br})^{2.75}\ [\sin(2\alpha_{br})]^{0.5} \quad (4.6b)$$

The longshore sand transport (Q_{LS}) of CERC (Shore Protection Manual 1984; Van Rijn, 1993):

$$Q_{LS}= 0.023\ K\ g^{0.5}\ \gamma^{-0.5}\ (H_{s,br})^{2.5}\ \sin(2\alpha_{br}) \quad (4.7)$$

with: γ= breaker coefficient, H_{br}= significant wave height at breaker line and α_{br}= angle between breaker line and local shoreline; K = calibration factor (default=1).

The longshore sand transport rate in the surf zone is defined in terms of parameters defined at the breaker line. Thus, the offshore wave climate has to be converted to a wave climate at the breaker line.
Waves arriving from deeper water are transformed in shallow water according to the laws of energy flux conservation and refraction (Law of Snell) for gradually varying bathymetry, yielding (Van Rijn 2011);

$$\sin\alpha_{br}= (L_{br}/L_o)\ \sin\alpha_o \quad (4.8)$$

$$H_{br}= K_{r,br}\ K_{s,br}\ H_o \quad (4.9)$$

with $K_{r,br}$= refraction coefficient at breaker line and $K_{s,br}$= shoaling coefficient at breaker line.

For gradually varying bathymetry these values are:

$$K_{r,br} = (\cos\alpha_o/\cos\alpha_{br})^{0.5} \text{ and } K_{s,br}=(n_o c_o/n_{br} c_{br})^{0.5} \quad (4.10)$$

with c = wave propagation velocity, n = coefficient, α= wave angle, index br= at breaker line and index o= at deep water.
The wave height at the breaker line $H_{br} = \gamma h_{br}$ can be computed if the breaker depth h_{br} and the breaker coefficient γ (range 0.6-0.8) are known. Generally, this procedure requires iterative computations.
An estimate of the breaker depth can be obtained by applying (Van Rijn 2011):

$$h_{br} = ((H_o^2 c_o \cos\alpha_o)/(1.8\gamma^2 g^{0.5}))^{0.4} \quad (4.11)$$

with: $c_o=L_o/T_{p,o}$. Longer (short) waves break earlier (further from the shore) resulting in higher $H_{s,br}$ and higher longshore sand transport.
Thus, wave refraction largely controls the orientation of the shoreline, when relatively smooth and regular depth contours are present (neglecting cross-shore contributions).

Definitions of directions are:

- longshore transport in positive x-direction is positive; this requires a positive wave angle to shore normal (**Figure 4.3.2**);
- longshore transport in negative x-direction is negative positive; this requires a positive wave angle to shore normal.

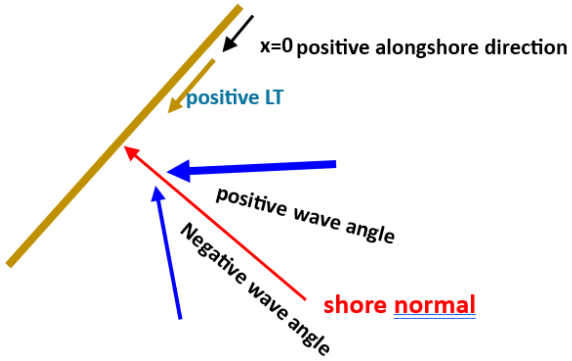

Figure 4.3.2 *Definitions of positive and negative longshore transport rate*

4.4 Model validation

Short-term and long-term field data of sand, gravel and shingle have been used earlier for verification of the LST-equation (Van Rijn, 2014). However, the quantity of gravel-shingle data was very limited.
To justify that the LST-equation of Van Rijn (2014) produces realistic results for steep gravel beaches, two approaches have been followed herein:

- the results of the LST-equation are compared to the results of the CROSMOR-model which computes the longshore sediment transport processes in more detail;
- the LST value derived from beach changes near the terminal groyne at Cooden (Pevensey beach) during storm Ciaran on 2 November 2023 is compared to the predicted LST.

Comparison of LST of LONGMOR and CROSMOR for gravel/shingle beaches

The cross-shore bed profile used in the CROSMOR-model runs consists of a relatively flat foreshore (1 to 150 and 1 to 65) and a steep gravel beach (1 to 7; between -1.5 and +6 m OD), see **Figure 4.4.1**.
Gravel(d_{50}=12 mm; d_{90}=24 mm) is assumed to be present landward of -3 m depth line.
The bed roughness is set to $k_{s,c}=k_{s,w}=2d_{50}$=0.024 m.
The offshore significant wave height is varied in the range of 1 to 4 m at offshore depth of 20 m OD.
The wave angle to the shore normal at the offshore depth is 30 degrees.
Tidal currents are not taken into account.
Two water levels have been used: low level of 0 m OD and high level of +4 m OD.
The LST-values of CROSMOR-model are almost the same for water levels of 0 and +4 m OD and low waves $H_{s,o}$ < 2 m, because the active zone of gravel transport is relatively small around the water line.
The LST-value of CROSMOR-model is relatively high for a high water level in storm conditions $H_{s,o}$ > 2 m.

Another important parameter influencing the computed LST-value of the CROSMOR-model is the wave velocity asymmetry method used. Two methods are available: Isobe-Horikawa (I-H-method; 1982) and Ruessink et al. (R-method;2012). The I-H-method produces higher peak orbital velocities than the R-method resulting in substantially higher LST-values (**Table 4.4.1**) for storm waves ($H_{s,o}$>2 m). The combination of a low water level (0 m OD) and the R-method for wave asymmetry gives a low LST-value; a high water level (+4 m OD) and I-H-method for wave asymmetry gives a high LST-value, see variation ranges of LST-values for $H_{s,o}$>2 m (**Table 4.4.1**).
The LST-values of the CROSMOR-model (mean value of variation range related to wave asymmetry methods (R or I-H) and the empirical equation are shown in **Figure 4.4.2**. The error range of the empirical LST-equation with standard coefficient is about ±50%.
The LST-values of the CROSMOR-model are somewhat lower (factor 2) than that of the empirical equation of the LONGMOR-model, which may partly be related to the poor representation of the swash zone in the CROSMOR-model. However, the empirical equation may also somewhat overestimate the LST-values. The error bars of both curves show sufficient overlap indicating that the empirical LST-equation gives very reasonable results. It may overpredict somewhat for lower wave heights.

Offshore wave height $H_{s,o}$ (m)	**Peak wave period T_p (s)**	**Offshore wave angle to s.n. (deg.)**	**Water level (m)**	**Peak orbital velocity (m/s)**	**Maximum longshore velocity (m/s)**	**LST of CROSMOR in section landward of -3 m depth (m^3/m/day)**	**LST of LONGMOR (empirical equation) (m^3/m/day)**
1	7	30	0; +4	1.1-1.3	0.4-0.5	40	120
1.5	7.5	30	0; +4	1.2-1.5	0.6-1.6	220	390
2	8	30	0; +4	1.3-1.7	0.7-1.1	440	900
2.5	8.5	30	0; +4	1.4-1.9	0.8-1.4	550-1100	1700
3	9	30	0; +4	1.6-2.0	1.0-2.2	850-4500	2900
3.5	9.5	30	0; +4	1.7-2.1	1.2-2.3	1100-6500	4600
4	10	30	0; +4	1.8-2.1	1.3-2.1	1100-8500	6700

Table 4.4.1 *Longshore gravel transport (d_{50}=12 mm) based on CROSMOR-model (file: GRAVELL.inp) and empirical equation of LONGMOR-model; s.n.=shore normal*

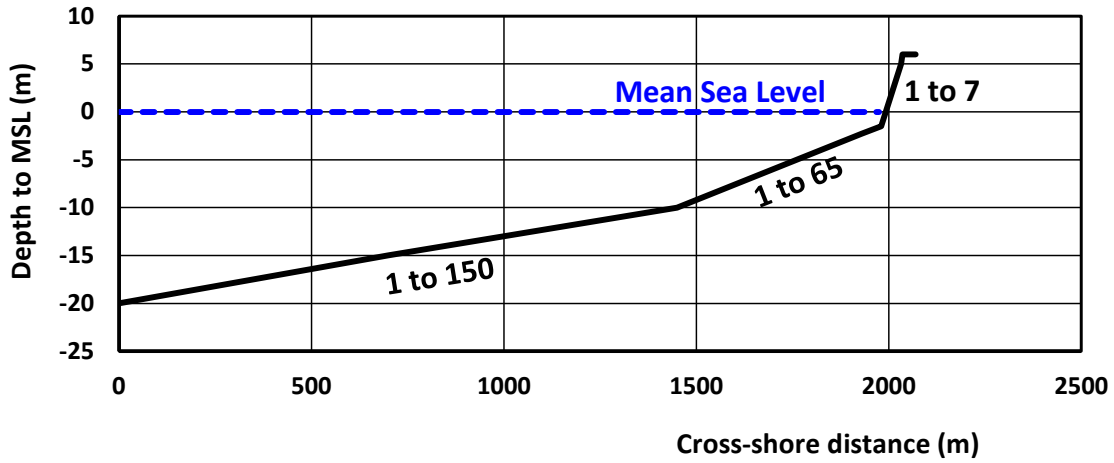

Figure 4.4.1 *Cross-shore bed profile of gravel beach*

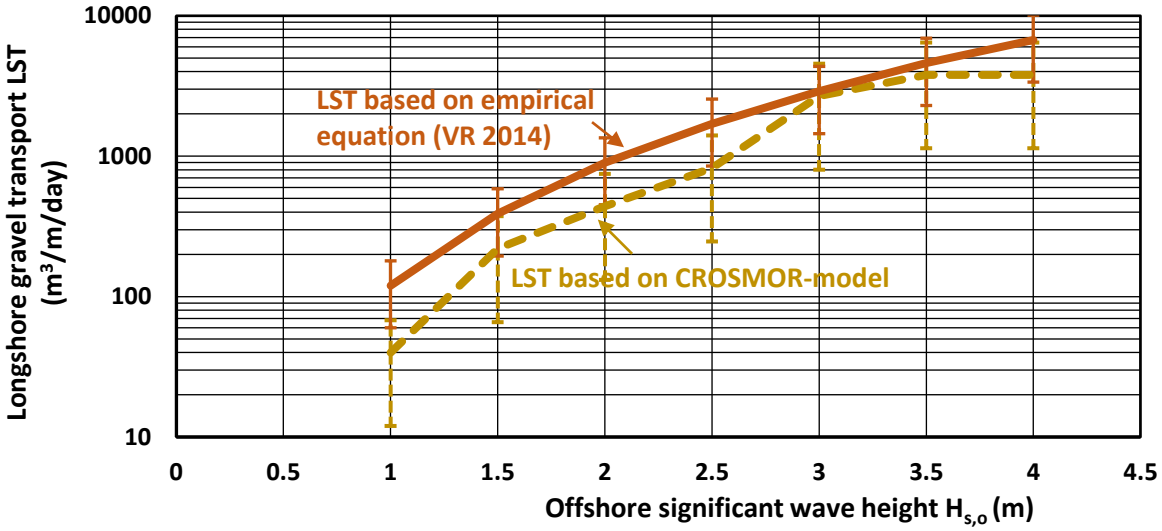

Figure 4.4.2 *Longshore gravel transport based on CROSMOR-model and empirical equation of LONGMOR-model (Van Rijn 2014); d_{50}=12 mm*

Comparison of predicted LST to measured LST during storm Ciaran on 2 November 2023

Field observations show an accumulation of sediment on the downdrift side of the terminal groyne (GC32) at Cooden of Pevensey beach, UK (surveys on 1 November and on 3 November 2023; interval=48 hours). Rather than be up against the groyne as if it had been driven east, shingle was built up against the updrift side implying material had passed over the groyne, see **Figure 4.4.3**. Surveys were extended over about 90 m east of the terminal groyne. Using these observations from east of the groyne it was possible to calculate the change in volume for this one area alone. Based on this, the net accumulation due to longshore transport of shingle is found to be about 1760 m^3 over a period of 48 hours between pre- and post surveys. Most likely, this is an under-estimation of the true LST to east, because i) the accumulation of sediment just updrift (west) of the terminal groyne is not taken into account and ii) sediment will have moved beyond the range of the survey east (> 90 m) of the groyne.

Therefore, the measured LST is herein assumed to be about 2500±500 m^3 to east over a period of 48 hours during storm Ciaran.

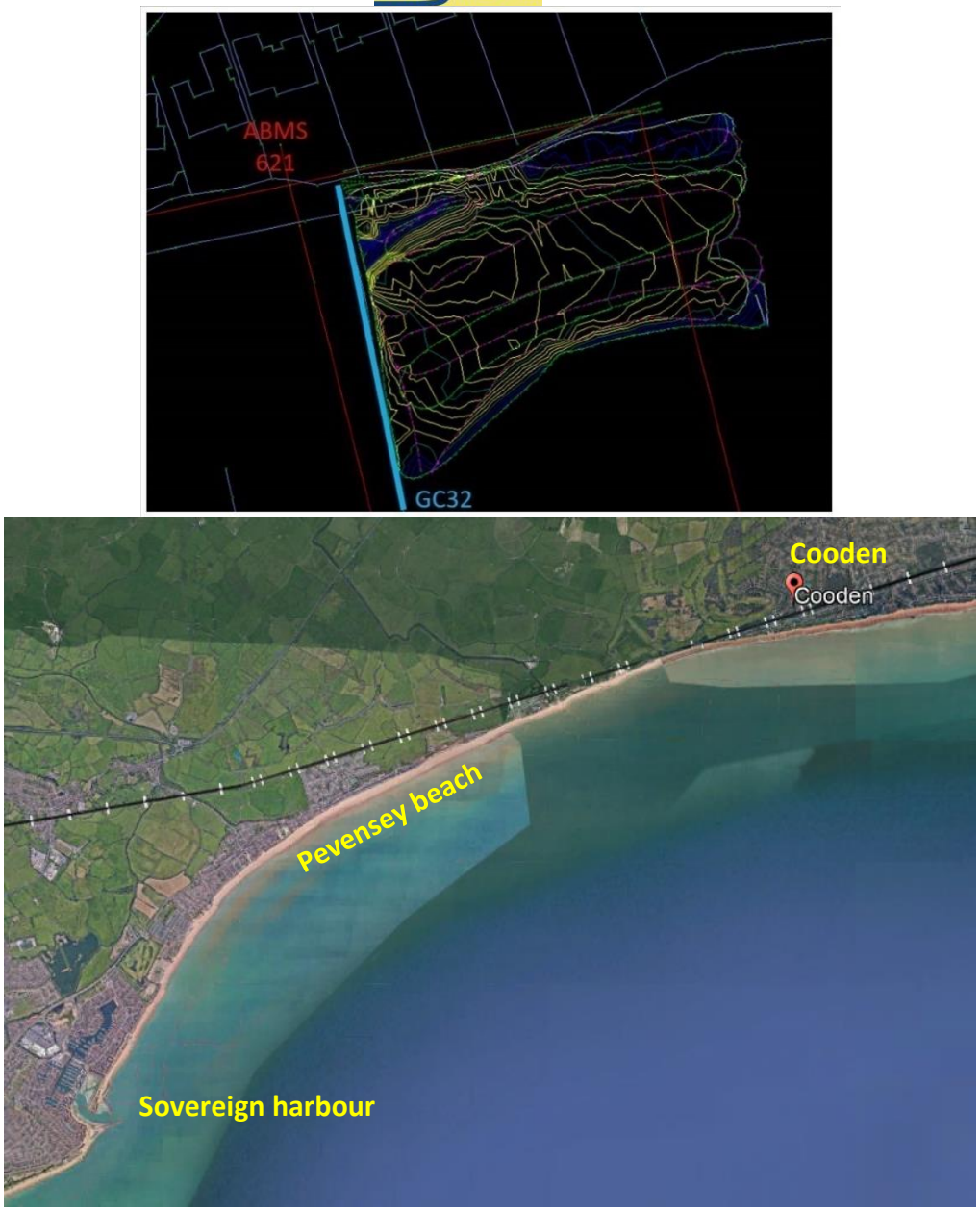

Figure 4.4.3 *Beach level changes (1-3 November 2023) east of terminal groyne GC32 at Cooden (Pevensey beach, UK) after storm Ciaran (blue=loss of sediment ≅120 m^3; Yellow=gain of sediment≅1880 m^3)*

The LST-model of Van Rijn (2014) has been used to compute the LST during storm Ciaran.
The basic data are given in **Table 4.4.2**.
The offshore water depth is 12 m to MSL (≅OD).
The surf zone slope is set to 0.1 (1 to 10).
The wave breaking coefficient is 0.6.
The friction coefficient is 0.9.
The single diameter is d_{50}=0.012 m (12 mm).
The correction factor related to shingle only landward of -2 m is set to 0.7.
The LST is computed for a period of 48 hours (interval between the pre and post beach surveys).
The actual storm duration is 24 hours.
The wave data of the pre- and post-storm periods are set to $H_{s,o}$=1.5 m, T_p=7 s, wave direction=201°.

Figure 4.4.4 shows the computed LST to east along the frontage. The LST at location Cooden is about 3100 m^3 to east over 48 hours, which is somewhat higher (25%) than the measured value of 2500±500 m^3.

Time on 2 November 2023 **(hours)**	**Water level to MSL** **(m)**	**Offshore significant wave height $H_{s,o}$** **(m)**	**Peak wave period T_p** **(s)**	**Wave direction to N** **(degrees)**
0	3	3.5	7	180
1	3.4	3.6	7.9	177
2	3.6	3.8	8.2	180
3	2.8	4.2	9.5	185
4	1.8	3.8	9.2	183
5	0.6	4.2	9.5	193
6	-0.4	3.8	9.5	190
7	-1	4.1	9.5	197
8	-1.3	4.3	10	203
9	-1.1	4.2	10	200
10	-0.3	3.3	10	206
11	1	3.5	11	210
12	2.2	3.2	10.5	208
13	3	2.9	10	217
14	3.1	2.8	10.5	214
15	2.9	3	11.8	223
16	1.8	2.9	10	219
17	0.5	2.8	10	227
18	-0.8	2.4	10.3	230
19	-1.4	2.2	10	228
20	-2	2	8.5	225
21	-1.8	1.9	9	225
22	-1	1.8	9	223
23	0.4	2.1	8.5	227
24	1.8	2.2	8.5	230

Table 4.4.2 *Basic water level and wave data of Storm Ciaran on 2 November 2023*

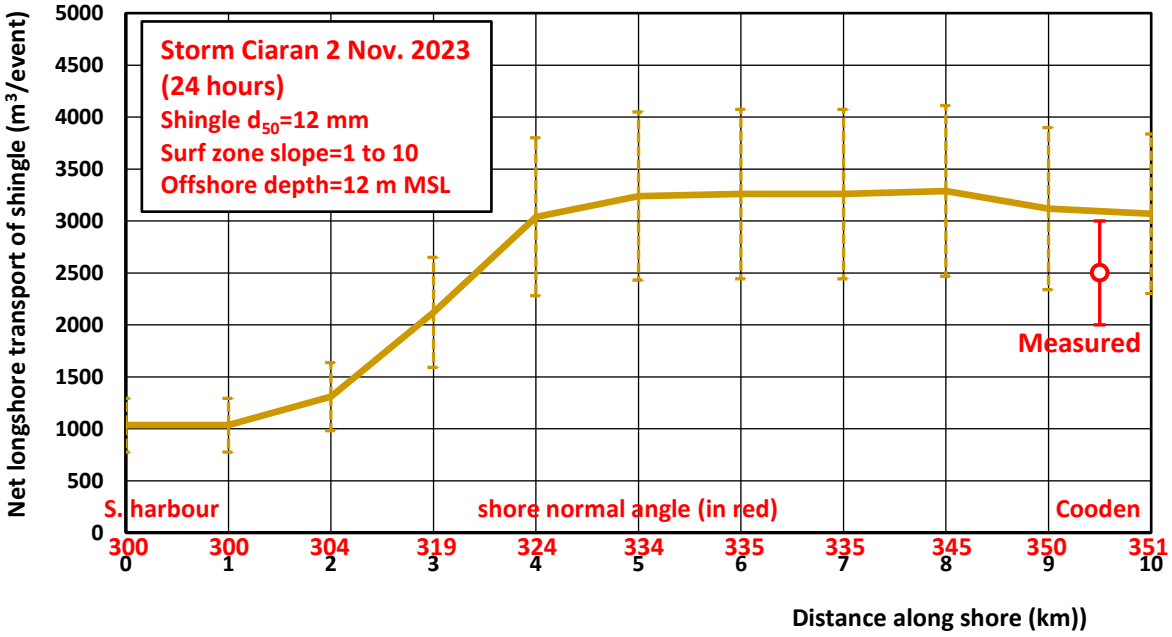

Figure 4.4.4 *Computed LST along frontage during storm Ciaran on 2 November 2023*

4.5 Longshore transport in period 2004 to 2022 at Pevensey beach, UK

The wave transformation in the nearshore zone is assumed to behave as that along a straight uniform coastline so that fairly simple wave refraction and shoaling equations are applicable.
Using this approach, the nearshore wave heights along the curved part (0 to 5 km from Sovereign-harbour) of the coastline are most likely somewhat overestimated.
The LST-model of Van Rijn including simple wave refraction and shoaling equations has been used to compute the net annual LST at various locations along the frontage using the wave data time series (half-hourly values over the year) measured at Pevensey Buoy location (water depth of about 10 m to OD) in the period 2004 to 2022. The wave data set of year 2003 is incomplete and has there not been used.
Erroneous values (wave heights > 6 m) and missing values (data values 9999) are replaced by realistic values based on the data of slightly earlier or later times.

The LST computations are based on the following:

- the tidal water level fluctuations over the tidal cycle are based on the water level data of Newhaven (20 km west of Sovereign-harbour); the water level data are multiplied by a factor 1.1, as the tidal range of Sovereign-harbour is 10% higher than that of Newhaven;
- the wave transformation from the wave buoy location to the nearshore is done by assuming a uniform shoreline with shore-parallel depth contours and the validity of the Law of Snell to represent wave refraction.

The basic input data of the LST-model are:

- median sediment diameter; d_{50}=12 mm;
- average seabed slope in surf zone; tan β=0.1 (slope 1 to 10);
- angle of the shore normal to North (see **Table 4.5.1**);
- significant wave height at breaker line (based on wave refraction and wave breaking);
- wave angle to shore normal at the breaker line (based on wave refraction);
- offshore depth to MSL (Mean Sea Level)=12 m;

- water level based on measured tidal water levels;
- coefficient wave breaking; γ_{br}=0.6;
- coefficient wave damping due to bed friction; γ_{damp}=0.9;
- transport coefficient; default K=0.7 (based on model calibration/validation)

Distance to Sovereign-harbour (km)	Shore normal angle to N (degrees)
0	300
1	300
2	304
3	319
4	329
5	334
6	335
7	335
8	345
9	350
10	351

Table 4.5.1 *Shore normal angle to North along Pevensey beach, UK*

The computed net LST and the LST-components to East and to West at end location Cooden (shore normal=350° to N) at 9 km from Sovereign harbour (Pevensey beach, UK) are shown in **Figure 4.5.1**. The wave data set of year 2003 is incomplete and has there not been used.
The net LST varies in the range of 17,000 m^3/year (in 2010) to 51,000 m^3/year (in 2020) to the East, which is the correct order of magnitude compared to the long term validation data of Pevensey beach.

Analysis of the computed results shows:

- the trendline of net LST is gradually increasing over time from 34,000 m^3/year in 2004 to 40,000 m^3/year in 2022; the average transport over the period 2004-2020 is about 36,000 m^3/year;
- the LST components to the West are quite small in the range of -1000 m^3/year to -3500 m^3/year;
- the LST-pattern follows the pattern of the longshore wave power (maximum in years 2008, 2014, 2015, 2020 and minimum in years 2005, 2010, 2018); LST is high when LWP is high and vice versa.

The wave rose plots of the years 2020 (lowest net LST) and 2020 (highest net LST) are shown in **Figure 4.5.2.**
The wave classes of 1.5-3.5 m from SW is about 5.1% for year 2010 and 14.4% for year 2020, which explains the differences in net LST. Waves > 2.5 m are rare: 0.6% (5 hours) in 2020 and 1.4% (12 hours) in 2020.

The net annual LST-value of about 35,000 to 40,000 m^3/year at Cooden for 12 mm-gravel/shingle is of the correct order of magnitude (annual sediment losses at Cooden are about 30,000 m^3/year). The computed net LST-values may be somewhat too high (10% to 20%) because the applied wave transformation from offshore to nearshore is rather simplistic resulting in overprediction of the wave heights at the breaker line.

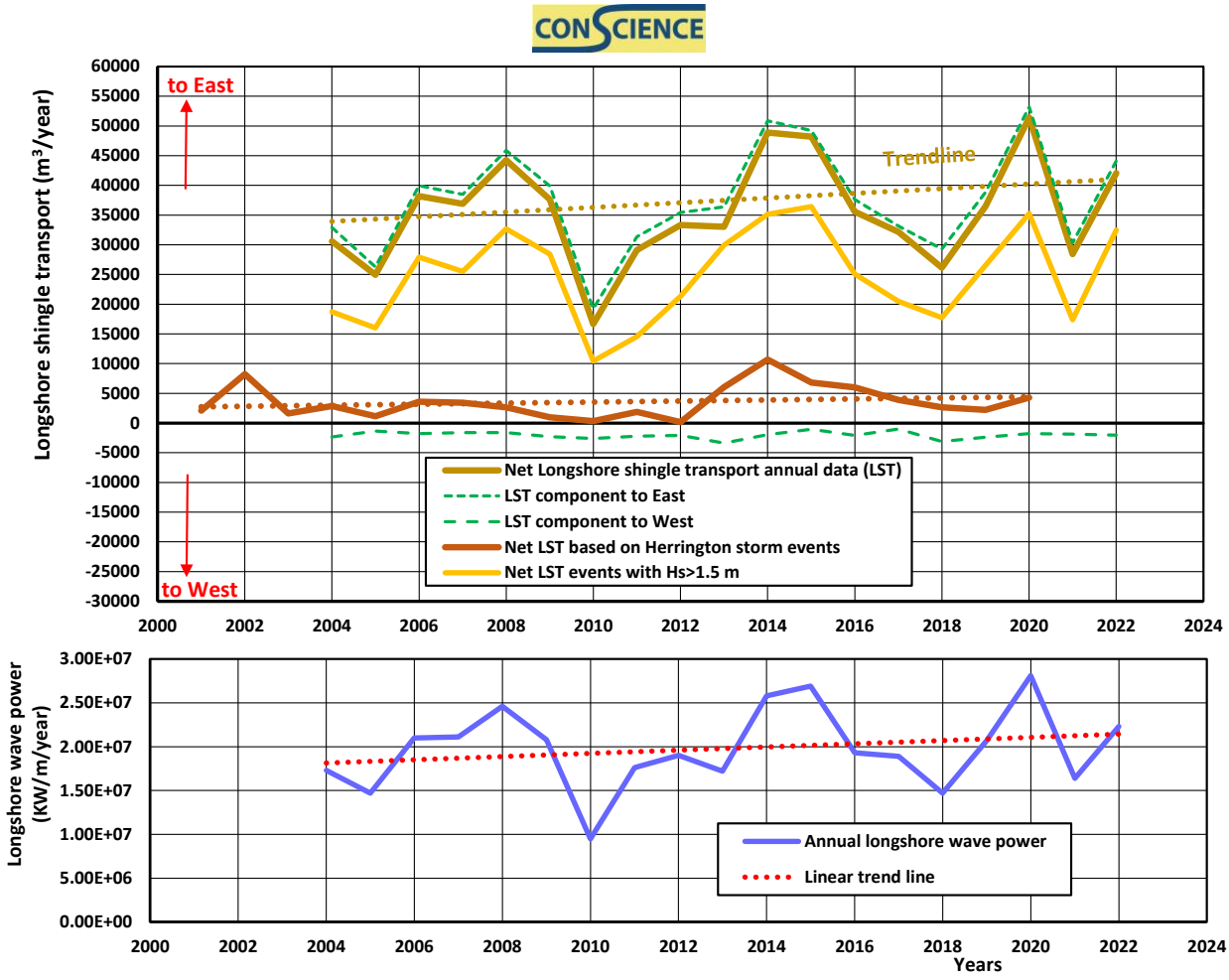

Figure 4.5.1 *LST-components (upper) and longshore wave power (lower) at location Cooden*

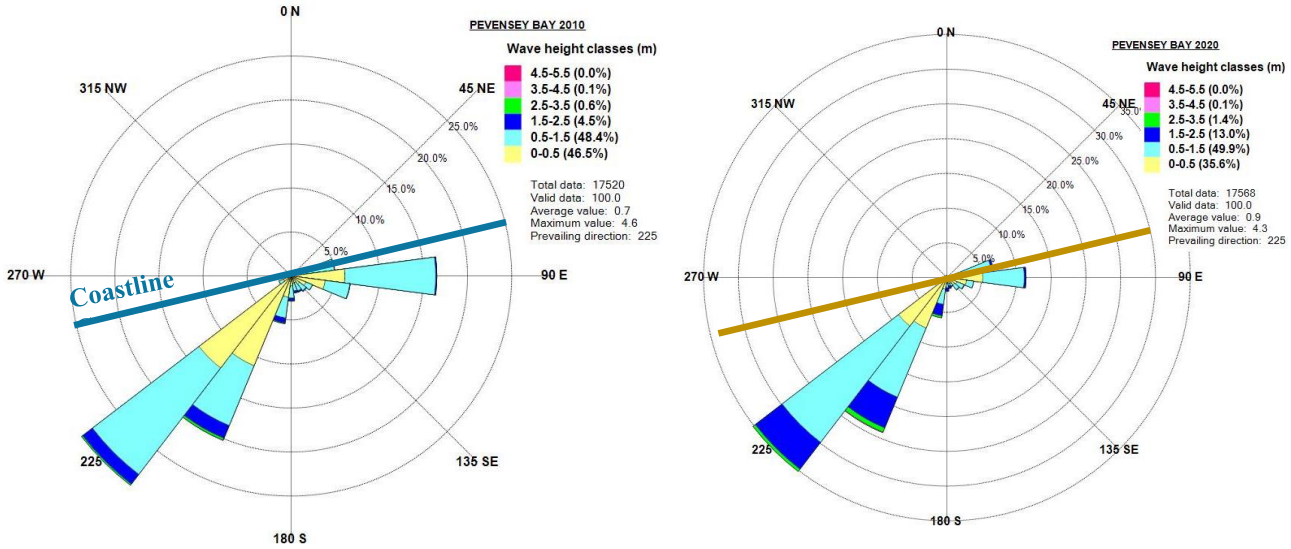

Figure 4.5.2 *Wave rose plots of 2010 and 2020*

Figure 4.5.1 also shows the LST-values of the 221 Herrington-storm events (4 boundary conditions: maximum water level, significant offshore wave height, peak wave period and wave direction to North). The offshore depth is set to the value of 46 m to OD (OD≅MSL), which is the depth at Hastings wave buoy. It is assumed that the peak of each storm event has a duration of **at least 3 hours** with approximately constant conditions. Nearly all events come from SW-directions. The LST-values during storm events of 3 hours vary in the range of 200 m^3/year (in 2010 and 2012) to 10,000 m^3/year (in 2014). The LST of the storm events also show an increasing trend. Compared to the net annual values, the contribution of the storm events to the net annual values is maximum 20%.

Net longshore transport per wave height class

The contribution of the various offshore wave height classes on the net LST at Cooden (Pevensey beach, UK) in year 2019 (as an example) is shown in **Figure 4.5.3.** Based on this plot, it follows that:

- offshore waves higher than 1 m produce about 90% of the total net annual LST and thus waves < 1 m produce only 10% of the net annual LST; thus, the modelling of small waves is not very important;
- offshore waves higher than 1.5 m (storms) produce about 75% of the total net LST;
- offshore waves higher than 2 m (storms) produce about 45% of the total net LST;
- offshore waves higher than 3 m (major storms) produce about 5% of the total net LST.

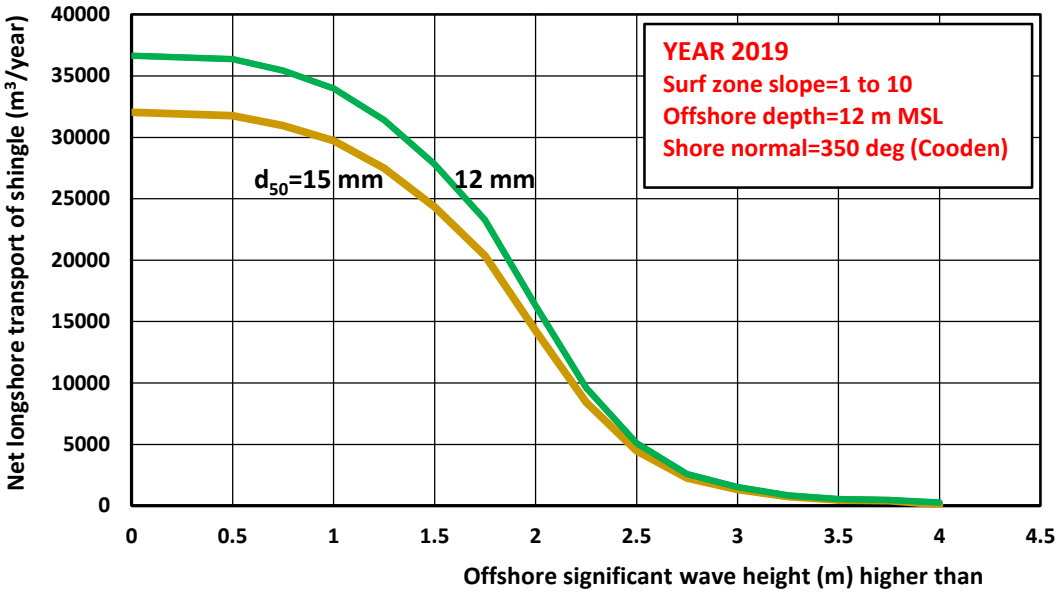

Figure 4.5.3 *Computed net annual LST at Cooden for year 2019; d_{50}=12, 15 mm; wave data from P-buoy*

Figure 4.5.4 shows the net LST per wave height class at location Cooden for all years between 2003 and 2022. Four classes are distinguished: $H_{s,o}$< 1m; 1-1.5 m, 1,5-2 and 2-4 m. Based on data:

- the contribution of wave class $H_{s,o}$< 1 m to the total LST= 8%;
- the contribution of wave class $H_{s,o}$=1-1.5 m to the total LST= 18%;
- the contribution of wave class $H_{s,o}$=1.5-2 m to the total LST= 26%;
- the contribution of wave class $H_{s,o}$>2 m to the total LST= 48%.

The wave height classes > 1.5 m (storm events) contribute most to the total longshore transport (about 75%).

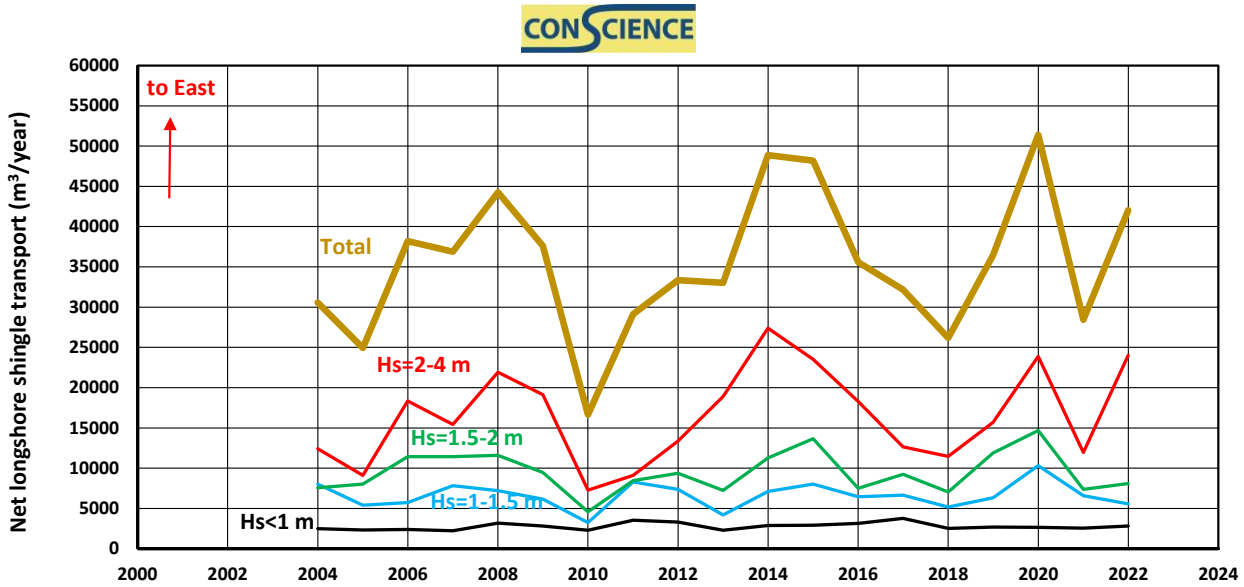

Figure 4.5.4 *Net longshore transport per wave height class at location Cooden over the period 2004-2022*

Effect of grain size

The effect of grain size on annual LST is shown in **Table 4.5.2** and in **Figure 4.5.3** for the net LST at end location Cooden in year 2019.

The net annual LST is about 36,500 m^3/year for 12 mm gravel/shingle and about 32,000 m^3/year for 15 mm-gravel/shingle. The eastward LST-component is about 10% higher than the net value; the westward LST-component is about 7% of the net value, which emphasizes the dominant wave direction from south-west.

Sediment size (mm)	Net annual LST (m^3/year)	Eastward LST (m^3/year)	Westward LST (m^3/year)
12 mm	36500	38800	-2400
15 mm	32000	34000	-2000

Table 4.5.2 *Computed LST-components at location Cooden (9 km from Sovereign-harbour)*

Effect of storms

Three storms affected the south coast of the UK within the time span of a week (13-20 February 2022).

On 18 February at 1 hour 45 minutes after high water, the Cefas (Hastings) wave buoy (only 1 km from the Pevensey wave point) recorded a significant wave height of 5.3 m (4.8 m at Pevensey buoy) when SWL is about 3.7 m OD.

The wave and water level data are, as follows:

- storm 14 February: $H_{s,o} + WL_{max}$=2.8 + 2.3 = 5.1 m;
- storm 17 February: $H_{s,o} + WL_{max}$=3.0 + 3.1 = 6.1 m;
- storm 18 February: $H_{s,o} + WL_{max}$=3.7 + 4.8 = 8.1 m.

The computed LST values are as follows:

- day 13 to 15 February (72 hours): LST=1465 m^3 (3.5%);
- day 15-18 February (72 hours): LST=1730 m^3 (4%);
- day 18-19.5 February (36 hours): LST=2310 m^3 (5.5%);
- day 13 to 19.5 February (180 hours; 1 week): LST=5500 m^3 (13%);
- all days of year 2022: LST=42,000 m^3 (100%).

Thus, the contribution of a storm period of 1 week with multiple storms to the total annual LST can be up to about 15%.

Effect of water level

The water level varies due to tidal effects and wind setup effects in the range of -2 m below MSL (Mean Sea level) to +4.5 m above MSL.

The effect of a constant water level on the net LST at Cooden has been studied for year 2010 (mildest waves) and 2020 (most severe waves), see **Figure 4.5.5**. In each computation, the water level is set to a constant value in the range of -2 m to +5 m.

Using a constant water level of -2 m gives a net LST of 50,000 m^3/year at Cooden in 2020.

Using a constant water level of +5 m gives a net LST of 55,000 m^3/year at Cooden in 2020 (increase of 10%).

A water level increase leads to a larger offshore water depth and thus to a longer offshore wave length for the same wave period. As longer (short) waves break further away from the shore, the wave height at the breaker line is higher and the surf zone is wider resulting in higher LST-values. However, the effect is modest, see **Figure 4.5.5**.

Based on this, it concluded that the LST during storm events with higher water levels is not so much influenced by the precise water level.

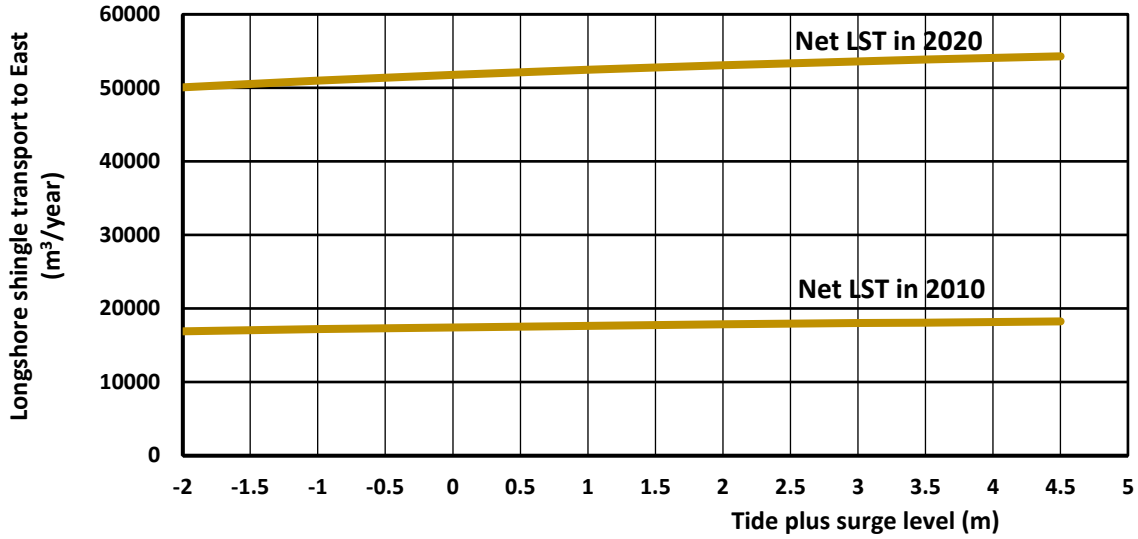

Figure 4.5.5 *Effect of water level on net LST at Cooden in 2010 and 2020 (wave data from Pevensey Buoy)*

Effect of coastline orientation

The shore normal angle between Sovereign-harbour and Cooden varies in the range of 300 to 350 degrees to North.

Figure 4.5.6 shows the net annual LST (based on uniform coast approach) along the coast of Pevensey Bay in year 2019. The wave data are taken from the wave buoy data at offshore depth of -12 m OD.

It can be seen that the net annual LST increases from about 2000 m^3/year near Sovereign-harbour to about 37,000 m^3/year at the end location Cooden of Pevensey beach (UK). The LST-gradients are highest (resulting in beach erosion) in sections KM25 and in KM7-9.

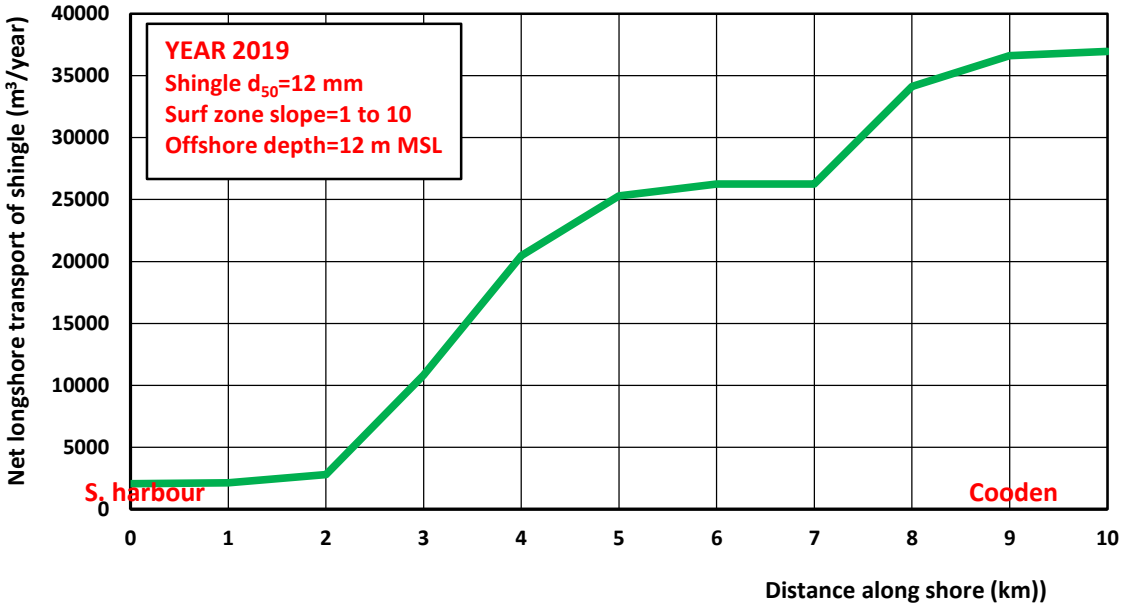

Figure 4.5.6 *Computed net annual LST along Pevensey Beach for year 2019; d_{50}=12 mm; wave data P-buoy*

5. Model simulation of gravel barrier erosion

5.1 General

The cross-shore transport processes can be broadly schematized in two categories, as follows:

- beach accretion and build up due to onshore transport process around the high tide line during daily waves;
- beach erosion at the upper beach zone due to offshore transport processes during storm events with high water levels and waves.

Available large-scale laboratory and field data are briefly studied to better understand these processes in Section 5.3.
A detailed cross-shore model (CROSMOR) is explained and validated using laboratory and field data from Pevensey bay and other gravel/shingle sites in the UK in Sections 5.4 and 5.5.
The validated CROSMOR-model is used to compute the upper beach erosion during storm events.
Computation examples are shown in Sections 5.6 to 5.8.
The computed beach erosion values are used to derive a simple beach erosion prediction mode in Section 5.9.

5.2 Available models

5.2.1 Parametric SHINGLE model (HR Wallingford)

The beach profile prediction model SHINGLE was developed at HR Wallingford (**Powell, 1990**) as a coastal management tool. It is a parametric model which allows the user to predict changes of shingle beach profiles based on input conditions of sea state, water level, existing profile, sediment size and the underlying stratum. The profile shape and its location against an initial datum can be predicted and confidence limits for the predictions determined. This capability can be used to predict potential erosion of existing shingle beaches or to predict the performance of shingle renourishment schemes.
The data used to derive the basic algorithms for the SHINGLE-model were obtained from a physical model programme conducted in a random wave flume (see **Section 3.1.1**). The results have been validated against field trials at several UK locations.
The SHINGLE-model addresses two aspects of profile prediction: the predicted profile shape and the location of the predicted profile against an initial datum. These aspects are dealt with from a probabilistic rather than deterministic approach, requiring an understanding of the confidence limits that can be placed on the profile prediction.

The prediction process breaks the profile into three curves between the following limits:

1. beach crest and SWL;
2. SWL and top edge of the profile step;
3. top edge of the profile step and the lower limit of profile deformation.

These curves are characterised by a series of profile descriptors defining the position and elevation of each transition point. These profile descriptors are linked with non-dimensional groupings of the most influencial profile development variables to give three non-dimensional equations. The actual form of these equations was determined from regression analysis of the flume test data. Confidence limits were determined from the variation of the test results at any point along the predicted profiles.

The position of the predicted end profile relative to the initial profile assumes that beach material moves only in an onshore-offshore direction and that differential longshore transport is zero. The areas under the two curves are compared relative to a common datum and the predicted curve is shifted along SWL axis until the areas

equate to provide the location of the predicted profile. If differential longshore transport is significant and a reasonable value can be assigned to the area of loss/gain, then a simple correction can be made to the predicted profile location.

The input data required are:

- initial profile, including foreshore,
- depth and slope of the underlying non-mobile stratum,
- beach particle size (d_{50}),
- effective beach thickness ratio (D_B/d_{50}),
- offshore wave height (H_s),
- offshore wave period (T_m),
- either ½ tidal cycle parameters of start and finish water levels plus stepped increment size or still water level (SWL),
- area change due to differential longshore transport if applicable,
- groyne and/or seawall cross-section.

5.2.2 Process-based CROSMOR2008 model

Hydrodynamics and sand transport

The CROSMOR2008-model is an updated version of the CROSMOR2004-model (**Van Rijn, 1997, 2006, 2007d**). The model has been extensively validated by **Van Rijn et al. (2003)**. The propagation and transformation of individual waves (wave by wave approach) along the cross-shore profile is described by a probabilistic model (**Van Rijn and Wijnberg, 1994, 1996**) solving the wave energy equation for each individual wave. The individual waves shoal until an empirical criterion for breaking is satisfied. The maximum wave height is given by $H_{max}= \gamma_{br}$ h with γ_{br}= breaking coefficient and h= local water depth. The default wave breaking coefficient is represented as a function of local wave steepness and bottom slope. The default breaking coefficient varies between 0.4 for a horizontal bottom and 0.8 for a very steep sloping bottom. The model can also be run a with a constant breaking coefficient (input value). Wave height decay after breaking is modelled by using an energy dissipation method. Wave-induced set-up and set-down and breaking-associated longshore currents are also modelled. Laboratory and field data have been used to calibrate and to verify the model. Generally, the measured $H_{1/3}$-wave heights are reasonably well represented by the model in all zones from deep water to the shallow surf zone. The fraction of breaking waves is reasonably well represented by the model in the upsloping zones of the bottom profile. Verification of the model results with respect to wave-induced longshore current velocities has shown reasonably good results for barred and non-barred profiles (**Van Rijn et al., 2003; Van Rijn and Wijnberg, 1994, 1996**).

The application of a numerical cross-shore profile model to compute the erosion of the beach and duneface poses a fundamental problem which is related to the continuous decrease of the water depth to zero at the runup point on the beach face. The numerical modelling of the (highly non-linear) wave-related processes in the swash zone with decreasing water depths is extremely complicated and is in an early stage of development. In the CROSMOR-model the numerical solution method is applied up to a point (last grid point) just seaward of the downrush point, where the mean water depth is of the order of 0.2 to 0.5 m. The complicated wave mechanics in the swash zone (wet-dry zone) is not explicitly modelled, but taken into account in a schematized way (subgrid model). The limiting water depth of the last (process) grid point is set by the user of the model (input parameter; typical values of 0.2 to 0.5 m). Based on the input value, the model determines the last grid point by interpolation after each time step (variable number of grid points).

The cross-shore wave velocity asymmetry under shoaling and breaking waves is described by the semi-empirical method of **Isobe and Horikawa (1982)** with modified coefficients (**Grasmeijer and Van Rijn, 1998**; **Grasmeijer, 2002**) or by the new method (see Section 2) proposed by **Ruessink and Van Rijn (2010)** based on input specifications. Near-bed streaming effects are modelled by semi-empirical expressions based on the work of **Davies and Villaret (1997, 1998, 1999)**. The streaming velocities at the edge of wave boundary layer may become

negative for decreasing relative roughness values (A_w/k_w with A_w= peak wave excursion near bed; k_w= wave-related bed roughness value).

The depth-averaged return current (u_r) under the wave trough of each individual wave (summation over wave classes) is derived from linear mass transport and the water depth (h_t) under the trough. The mass transport is given by 0.125 g H^2/C with C= $(g\ h)^{0.5}$ = phase velocity in shallow water. The contribution of the rollers of broken waves to the mass transport and to the generation of longshore currents (**Svendsen, 1984; Dally and Osiecki, 1994**) is taken into account. The vertical distribution of the undertow velocity is modelled by schematizing the water depth into three layers with a logarithmic distribution in the lower two layers and a power distribution in the upper layer, yielding velocities which approach to zero at the water surface.

Low-frequency waves are generated in the surf zone due to spatial and temporal variation of the wave breaking point resulting in spatial and temporal variation of the wave-induced set-up creating low-frequency waves (surf beat). This involves a transfer of energy in the frequency domain: from the high frequency to the low frequency waves. The total velocity variance (total wave energy) consists of high-frequency and low-frequency contributions ($U^2_{rms}=U^2_{hf,rms}+U^2_{lf,rms}$). The low-frequency waves are represented by a semi-empirical expression based on analysis of Deltaflume experiments (**Van Rijn, 2008, 2009**).

The detailed swash processes in the swash zone are not explicitly modelled but are represented in a schematized way by introducing an effective onshore-directed swash velocity ($U_{sw,on}$) in a small zone just seaward of the last grid point, see **Figure 4.1**. It is assumed that the peak onshore-directed component of the swash velocity is much larger than the peak offsshore-directed swash velocity close to the shore. The peak onshore swash velocity is of the order of 1.5 to 2 m/s, see **Figure 2.7**. The swash velocity is added to the other cross-shore components of the near-bed velocity (orbital velocity, streaming) and then combined with the longshore near-bed velocity. The resulting instantaneous velocity is used to determine the instantaneous bed-shear stress and then the instantaneous bed-load transport (within the wave cycle).

The sediment transport of the CROSMOR2008-model is based on the TRANSPOR2004 formulations (**Van Rijn, 2006, 2007a,b,c,d**). The effect of the local cross-shore bed slope on the transport rate is taken into account (see **Van Rijn, 1993, 2006**).

The sediment transport rate is determined for each wave (or wave class), based on the computed wave height, depth-averaged cross-shore and longshore velocities, orbital velocities, friction factors and sediment parameters. The net (averaged over the wave period) total sediment transport is obtained as the sum of the net bed load (q_b) and net suspended load (q_s) transport rates. The net bed-load transport rate is obtained by time-averaging (over the wave period) of the instantaneous transport rate using a formula-type of approach.

The net suspended load transport is obtained as the sum ($q_s= q_{s,c} + q_{s,w}$) of the current-related and the wave-related suspended transport components (**Van Rijn, 1993, 2006, 2007**). The current-related suspended load transport ($q_{s,c}$) is defined as the transport of sediment particles by the time-averaged (mean) current velocities (longshore currents, rip currents, undertow currents). The wave-related suspended sediment transport ($q_{s,w}$) is defined as the transport of suspended sediment particles by the oscillating fluid components (cross-shore orbital motion). The oscillatory or wave-related suspended load transport ($q_{s,w}$) has been implemented in the model, using the approach given by **Houwman and Ruessink (1996)**. The method is described by **Van Rijn (2006, 2007a,b,c,d)**. Computation of the wave-related and current-related suspended load transport components requires information of the time-averaged current velocity profile and sediment concentration profile. The convection-diffusion equation is applied to compute the time-averaged sediment concentration profile based on current-related and wave-related mixing. The bed-boundary condition is applied as a prescribed reference concentration based on the time-averaged bed-shear stress due to current and wave conditions.

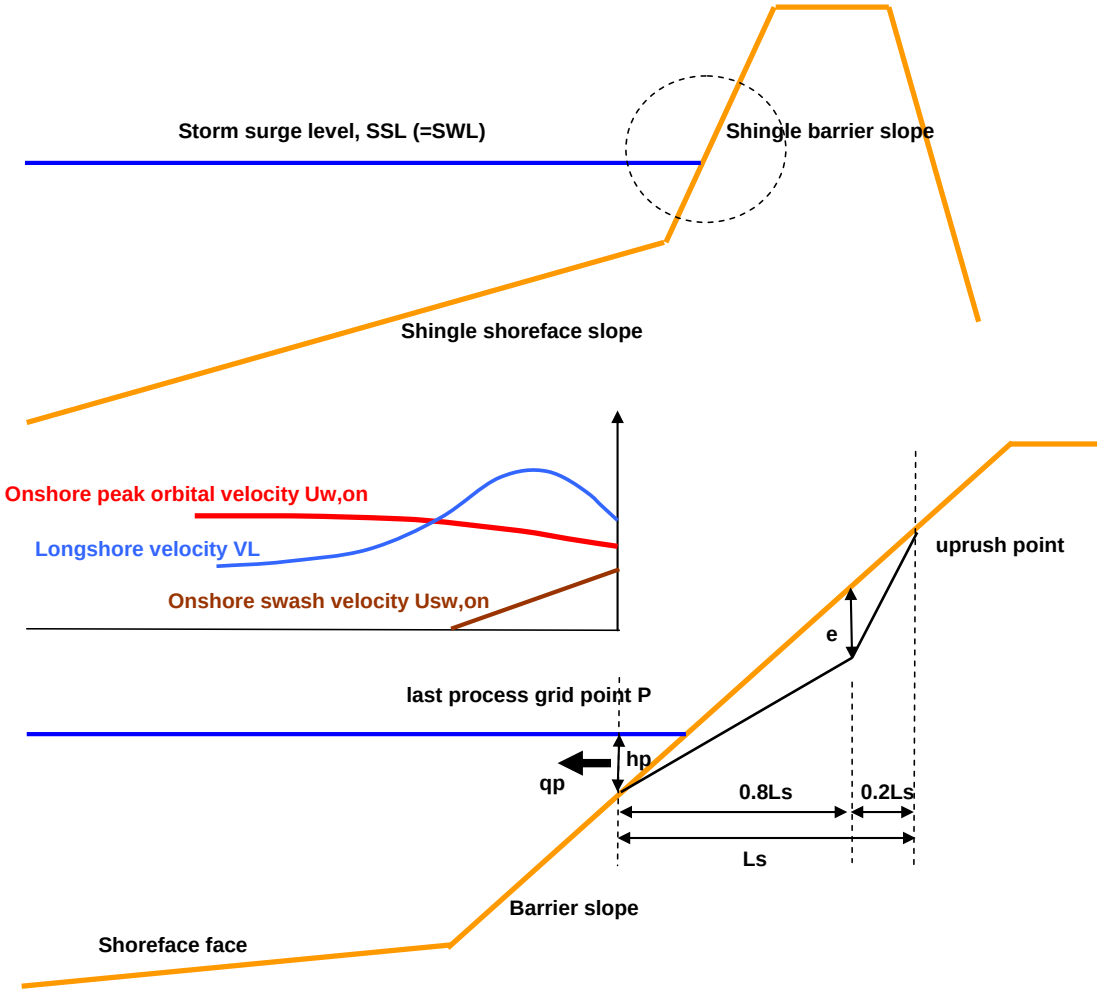

Figure 5.2.1 *Schematization of swash erosion zone for shingle barrier*

Bed level changes and deposition in swash zone

Bed level changes seaward of the last grid point are described by:

$$\rho_s(1-p)\partial z_b/\partial t + \partial(q_t)/\partial x = 0 \qquad (5.1)$$

with: z_b= bed level to datum, $q_t = q_b + q_s$= volumetric total load (bed load plus suspended load) transport, ρ_s= sediment density, p= porosity factor.

In discrete notation:

$$\Delta z_{b,x,t} = -[(q_{t,})_{x-\Delta x} - (q_t)_{x+\Delta x}]\ [\Delta t/(2\ \Delta x(1-p)\rho_s] \qquad (5.2)$$

with: Δt= time step, Δx= space step, $\Delta z_{b,i,x,t}$ = bed level change at time t (positive for decreasing transport in positive x-direction, yielding deposition). The new bed level at time t is obtained by applying an explicit Lax-Wendorf scheme.

Deposition and erosion in the swash zone between the waterline and the uprush point (landward of the last gridpoint) is a typical morphological feature of wave attack on a steep slope and is represented in a schematized way by using a subgrid model. The length of the swash zone is determined as the distance between the last grid point and the uprush point. In the case of steep shingle slopes the run-up level can be determined by an empirical expression: $R_s = (H_{s,o} L_{s,o})^{0.5}$ with a maximum value of 5 m above the mean water level. The maximum run-up is set to 5 m because the run-up along a steep, permeable shingle slope with percolation effects will be significantly smaller than along a rigid, smooth slope.
The total deposition or erosion area (A_D or A_E) over the length of the swash zone is herein defined as: $A_D = q_p \Delta t/((1-p)\rho_s)$ with: q_p= cross-shore transport computed at last grid point P at the toe of swash zone, Δt= time step, p= porosity factor of bed material, ρ_s= sediment density. The deposition (or erosion) profile in the swash zone is assumed to have a triangular shape, see **Figure 5.2.1.** The maximum deposition or erosion (e) can then be determined from the area A_D. The cross-shore transport on steep shingle slopes is onshore directed during low wave conditions due to the dominant effect of the velocity asymmetry and the percolation of fluid through the porous bed surface. The cross-shore transport is offshore-directed during storm conditions.

5.3 Simulation results of gravel/shingle slopes

5.3.1 Deltaflume experiments (Deltares)

Tests 1, 2 and 9 of the Deltaflume experiments in 1989 (**Table 3.1**) have been used to verify the CROSMOR-model for gravel slopes.
Since the CROSMOR-model is a model for individual waves; the wave height distribution is assumed to be represented by a Rayleigh-type distribution schematized into 6 wave classes. Based on the computed parameters in each grid point for each wave class, the statistical parameters are computed in each grid point. The limiting water depth is set to 0.5 m (water depth in last grid point). Based on this value (including the computed wave-induced set-up), the model determines by interpolation the number of grid points (x= 0 is offshore boundary, x= L is most landward computational grid point). The effective bed roughness is set to a fixed value of $k_s = 2d_{50}$.
In all runs the sediment transport is dominated by bed load transport processes. The instantaneous orbital velocities are based on the method of **Ruessink and Van Rijn (2010)**. Low-frequency surf beat motion is taken into account based on a semi-empirical approach.

Figures 5.3.1 and **5.3.2** show simulation results of Deltaflume Test 1 and 2 after 260 minutes for shingle with d_{50}= 0.021 m based on the process-based CROSMOR-model and the parametric SHINGLE-model. Qualitatively the results of the CROSMOR-model are in reasonable agreement with the measured values. A swash bar of the right order of size is generated above the waterline in both experiments, but the computed swash bars are too smooth whereas the measured swash bars have a distinct triangular shape. The computed erosion zone is somewhat too large. The computed swash bar of Test 1 is much too small (only 0.05 m high) if the swash velocity is neglected (c_{sw}= 0). The computed run-up level has been varied in Test 2 to evaluate the effect on the computed bed profile. A relatively high run-up level results in a lower bar with a larger length. The swash bar produced by the parametric SHINGLE-model is much too small for Test 1 and 2.

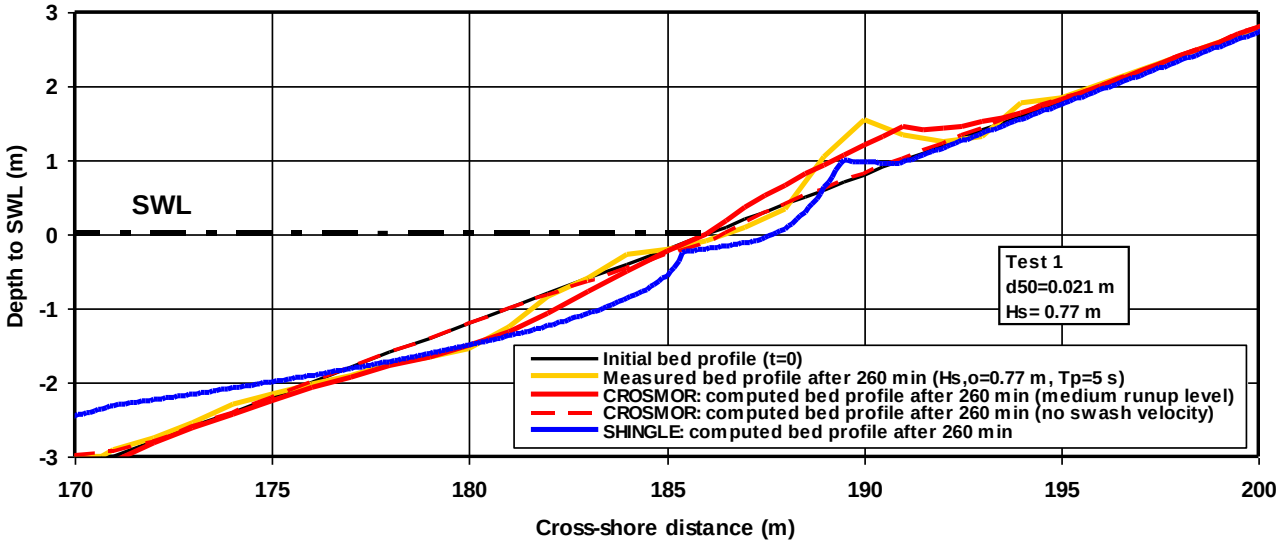

Figure 5.3.1 *Simulation of Deltaflume Test 1 ($H_{s,o}$=0.77 m; d_{50}=0.021 m)*

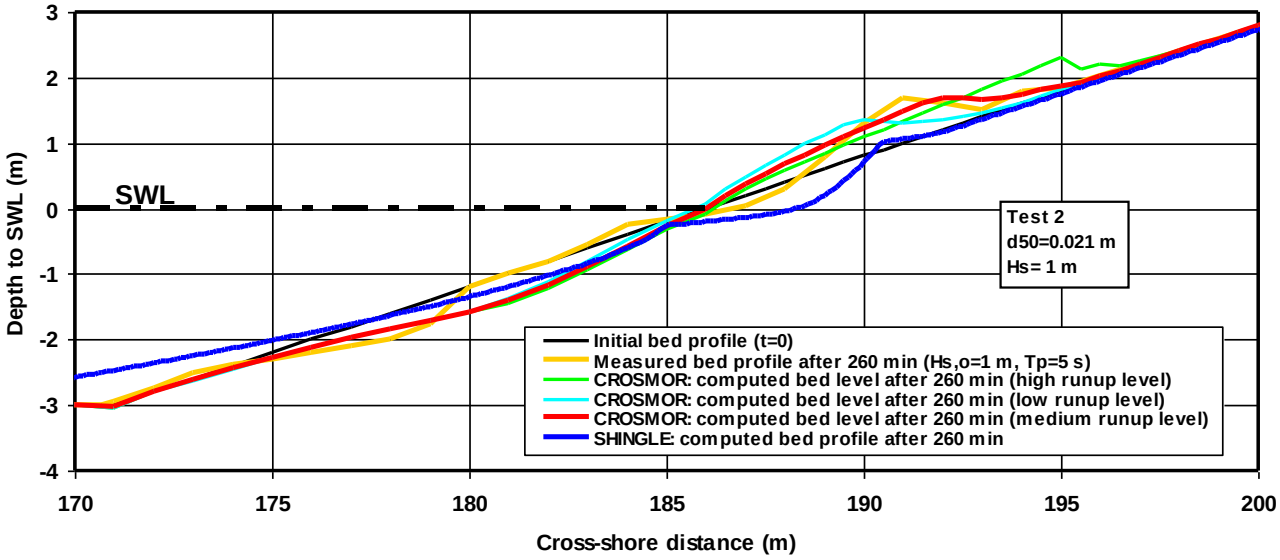

Figure 5.3.2 *Simulation of Deltaflume Test 2 ($H_{s,o}$=1 m; d_{50}=0.021 m)*

Figure 5.3.3 shows simulation results of Deltaflume Test 9 after 380 minutes for gravel with d_{50}= 0.0048 m. This test shows the presence of a relatively large swash bar further away from the water line and a relatively large erosion zone between the -3 m and -1 m depths. The simulation results of the CROSMOR-model also show a swash bar but at a much lower level on the gravel slope. The computed erosion zone is much too small. Since the swash bar area is of the right order of magnitude and the computed erosion area is much too small, the gravel is coming from the entrance section of the model, which is not correct. The swash bar produced by the SHINGLE- model is of the right order of magnitude, but the location of the computed swash bar is too low.

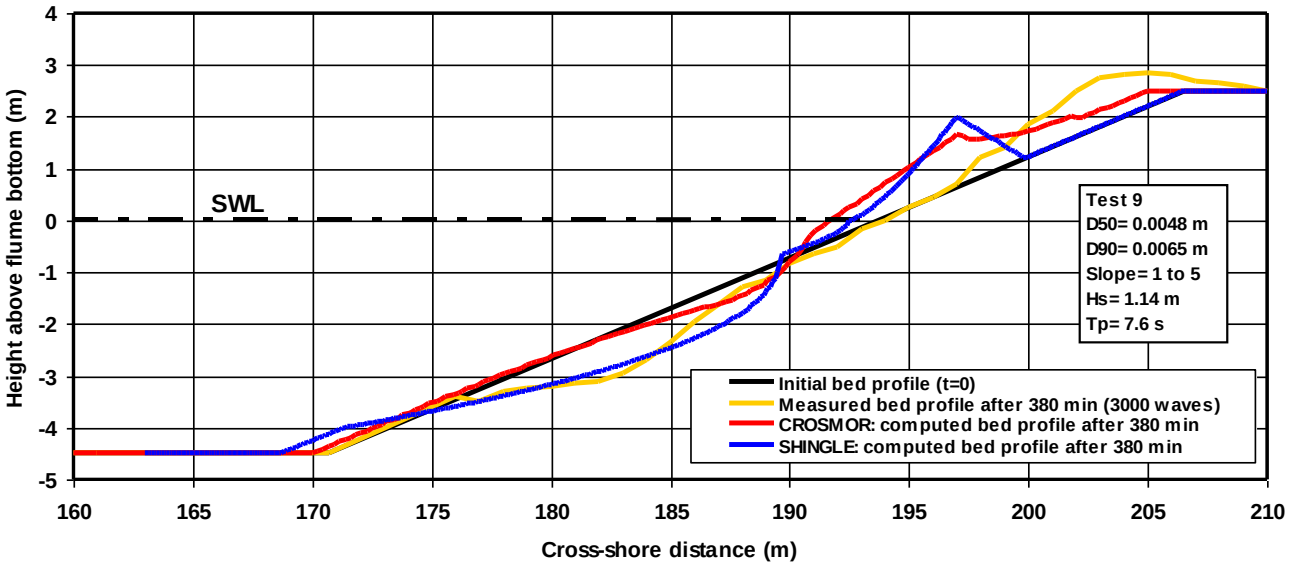

Figure 5.3.3 *Simulation of Deltaflume Test 9 ($H_{s,o}$=1.14 m; d_{50}=0.0048 m)*

5.3.2 GWK flume experiments

Tests 1 to 5 of the GWK flume experiments (see **Table 3.2**) have been used to verify the CROSMOR-model for gravel slopes.

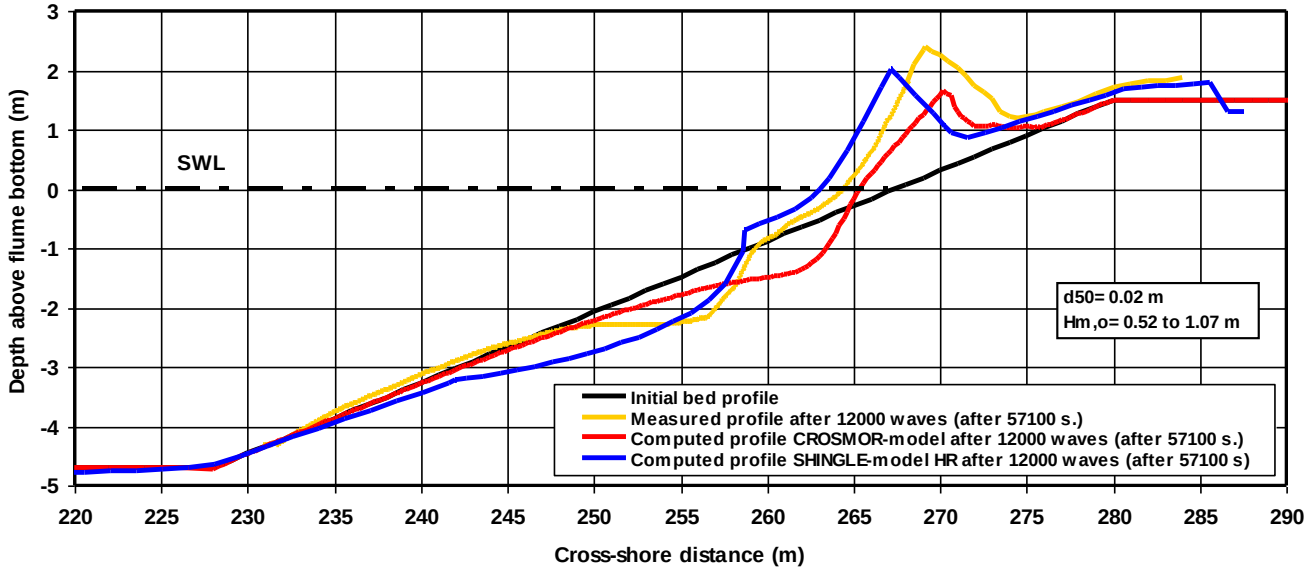

Figure 5.3.4 *Simulation of GWK Test 1 to 5 ($H_{m,o}$= 0.52 to 1.07 m; d_{50}=0.02 m)*

Figure 5.3.4 shows the simulation results of the GWK Tests 1 to 5 using both the parametric SHINGLE model of HR Wallingford and the process-based CROSMOR-model of Deltares. The computed swash bar area of the SHINGLE model is of the right order of magnitude, but its location on the profile is somewhat too low. The computed erosion volume below the still water line is much too large. The computed swash bar area of the

CROSMOR-model is somewhat too small, but its position on the profile is rather good. The computed erosion zone is of the right order of magnitude, but its position on the profile is much too high.

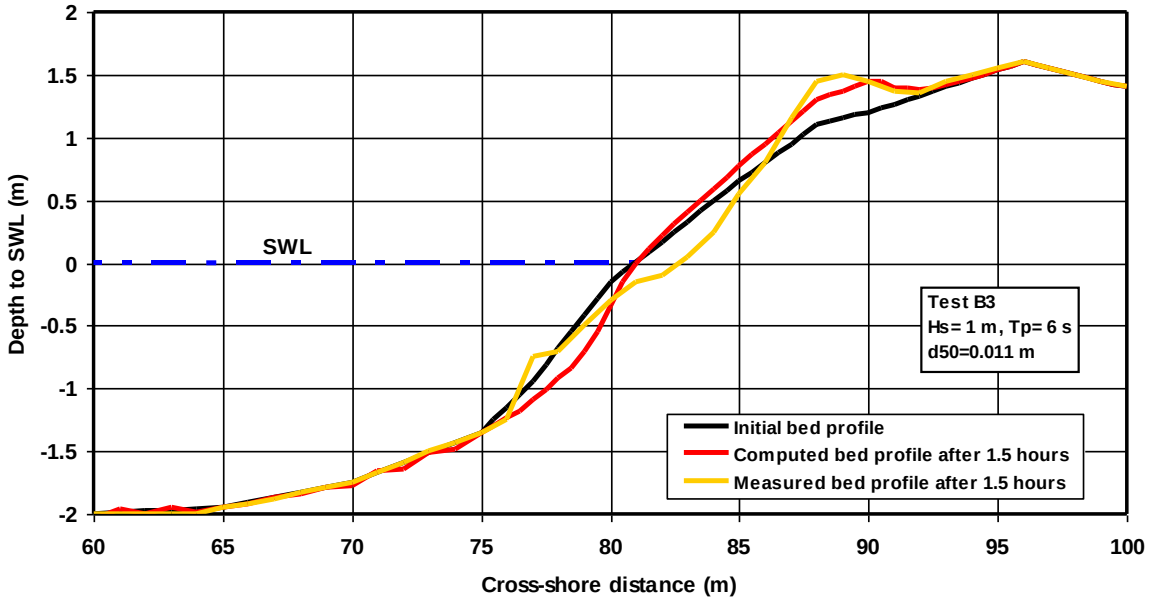

Figure 5.3.5 *Simulation of BARDEX Test B3 ($H_{m,o}$= 1.0 m; d_{50}= 0.011 m)*

5.3.3 BARDEX experiments Deltaflume

Test B3 of the BARDEX experiments (**Buscombe, Williams and Masselink, 2008**) has been used to verify the CROSMOR-model for gravel slopes.
Figure 5.3.5 shows the simulation results of the CROSMOR-model. The computed swash bar area is of the right order of magnitude (2 m^3/m). The computed erosion volume also is of the right order of magnitude, but its position on the profile (below SWL) is much too low.
The results of the SHINGLE model runs are not shown, because the model did not produce meaningful results for this case (computed beach slope everywhere seaward of the initial slope). The SHINGLE model uses an equilibrium slope concept, by which the model slope is forced away from the slope in the flume. The actual beach used in the flume tests may have been somewhat too steep for that size of shingle.

5.4 Validation and calibration of CROSMOR-model

To justify that the CROSMOR-model produces realistic results for steep gravel beaches, two approaches have been followed:

- the transport rates of gravel in unidirectional flow (river flow) computed by the CROSMOR-model are compared to the measured values of gravel flume experiments of Meyer-Peter and Mueller (1948);
- the longshore transport rates of gravel in coastal flow computed by the CROSMOR-model are compared to the measured values of longshore gravel transport at two field sites in the UK (Shoreham and Hurst Castle Spit).

Comparison with gravel transport data of Meyer-Peter Mueller (1948)

To show that sediment transport of the CROSMOR-model can also be used to simulate gravel transport as measured in the flume experiments of Meyer-Peter and Mueller (MPM, 1948), the CROSMOR-model has been used in river mode (no waves; input file GRAVELR.inp) for a channel with a gravel bed.

Gravel transport data of MPM are given in **Table 4.1**. Three values of the d_{50} of the gravel bed have been used: d_{50}=6, 12 and 18 mm; d_{90}=12, 24, 36 mm. The bed roughness is set to k_s=1 d_{90}. The water depth is set to a constant value of h=1 m. The depth-averaged current velocity is in the range of 1 to 3 m/s. The water temperature is 15 °C and the salinity is 0 promille (fresh water). The computed gravel transport rates of the CROSMOR-model are shown in **Figure 5.4.1**. The computed values of the transport equation of Meyer-Peter and Mueller MPM (1948) are also shown in **Figure 5.4.1**. The MPM-equation is especially valid for coarse grains based on a series of flume experiments with gravel material (d_{50}=5.2 and 28.7 mm), see **Figure 5.4.1**.

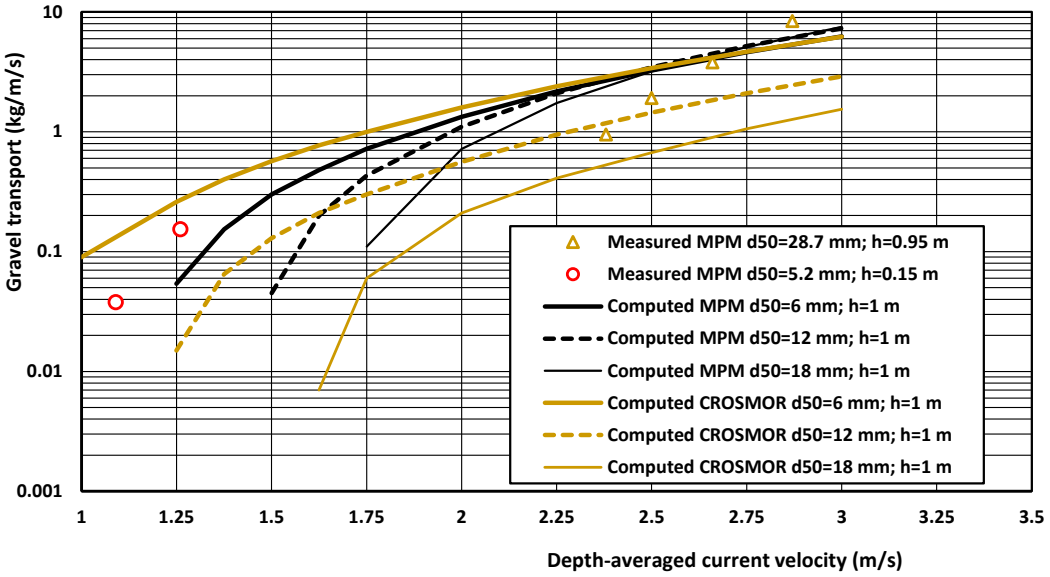

Figure 5.4.1 *Gravel transport as function of depth-averaged current velocity (GRAVELR.inp)*

The results of the MPM-equation show that the effect of grain size on the gravel transport is minor for current velocities higher than 2.25 m/s. The transport rates of the CROSMOR-model and the MPM-equation are in good agreement for d_{50}=6 mm. The CROSMOR-model underpredicts somewhat for d_{50}=12 mm (factor 2) and more severely (factor 5) for d_{50}=18 mm. The median grain size (d_{50}) at Pevensey beach is about 12 mm, which means that the CROSMOR-model may underpredict the gravel transport at Pevensey beach.

Comparison with longshore gravel transport data at Shoreham and Hurst Castle spit, UK

Measured longshore transport data of gravel/shingle are rather scarce. Herein, measured data from 2 sites in the UK are used for comparison to the computed values of the CROSMOR-model. These two sites are: Shoreham (Chadwick, 1989) and Hurst Castle Spit (Nicholls and Wright, 1991). The measured data are shown in **Table 5.4.1**. The offshore wave data are not known. It is assumed that the offshore wave height is about twice the value measured at the breaker line ($H_{s,o}$=2$H_{s,br}$).

Field sites UK	d_{50} (mm)	tanβ (-)	$H_{s,br}$ (m)	θ_{br} (°)	T_p (s)	$Q_{t,mass}$ (kg/s)	Type of load
Shoreham UK 1989	20	0.1	0.3	15	3	0.05	bed load
	20	0.1	0.35	15	3	0.167	bed load
	20	0.1	0.4	15	3	0.3	bed load
	20	0.1	0.7	15	4	0.5	bed load
Hurst Castle Spit UK 1991	32	0.1	0.75	15	6	0.5	bed load
	32	0.1	1.0	15	6	1.5	bed load

d_{50} = particle size; tanβ= beach slope, $H_{s,br}$= significant wave height at breakerline, θ_{br} = wave angle to shore normal at breakerline, T_p = peak wave period,

Table 5.4.1 *Measure longshore transport data of two field sites (shingle) in UK*

The input data of the CROSMOR-simulation runs for these two gravel/shingle sites are given in **Table 5.4.2**. A schematized cross- profile has been used, which is assumed to be valid for both sites. The beach with d_{50} of 20 mm used in the CROSMOR-model has a steep slope of 1 to 8. The crest level of the beach is at 10 m above MSL (mean sea level). The shoreface has a slope of 1 to 20. The tidal range is 4 m. The offshore significant wave height is varied in the range of 0.7 to 8 m. The bed roughness values are taken equal to the median grain sizes ($k_{s,c}=k_{s,w}=d_{50}$).

Figure 5.4.2 shows the cross-shore distribution of the computed significant wave height for superstorm conditions with an offshore wave height of $H_{s,o}$= 8 m (T_p = 15 s) and an offshore wave incidence angle of 0 (waves normal to the coast). The storm surge level is set to 4 m above mean sea level. The wave height is almost constant up to the depth contour of -7 m. Landward of this depth, the wave height gradually decreases to a value of about 6 m at the toe of the beach (at x= 740 m). At the beach slope (1 to 8) the wave height strongly decreases from 6 m to about 1 m at the landward end of the gravel beach.
Computed wave-induced longshore velocities are also shown in **Figure 5.4.2** for offshore wave incidence angles of 15° and 30°. The longshore velocity increases strongly landward of the -15 m depth contour where wave breaking becomes important (5% wave breaking at -15 m, 40% breaking at -9 m, 70% breaking at -5 m; 100% breaking at -2 m). The longshore current velocity has a maximum value of 3 m/s for an offshore wave angle of 15° and 4 m/s for an angle of 30°, just landward of the toe of the beach slope.
Figure 5.4.2 also shows the cross-shore distribution of the computed cross-shore and longshore transport of shingle (mainly bed load transport) for an offshore wave incidence angle of 15°. The offshore wave height is 8 m. The cross-shore transport shows onshore values at the shoreface up to the toe of the shingle beach (-3 m depth line) and at the most landward end of the beach (swash bar generation over length of a few meters). The cross-shore transport of shingle is seaward at the beach between x = 754 m and x = 791 m. The longshore transport increases strongly landward of -4 m line and is maximum at the location where the longshore velocity is maximum (around 0 m depth line).

Parameter	Values
Bed profile	slope of 1 to 20 between -30 m and -3 m slope of 1 to 8 between -3 m and +10 m
Sediment d_{50}; d_{90}	0.02 m; 0.04 m
Bed roughness k_s	0.04 m
Horizontal mixing	0.1 m^2/s
Peak tidal water level	2 m (flood); -2 m (ebb)
Peak tidal velocity	0.6 m/s (flood); -0.6 m/s (ebb)
Offshore significant wave height $H_{s,o}$	2, 3, 4, 5, 6, 8 m (6 wave classes using Rayleigh distribution)
Peak wave period T_p	7, 8, 9,10, 12, 15 s
Storm surge level above MSL	0, 0.5, 1, 2, 3, 4 m

Table 5.4.2 *Data of field case of schematized shingle barrier*

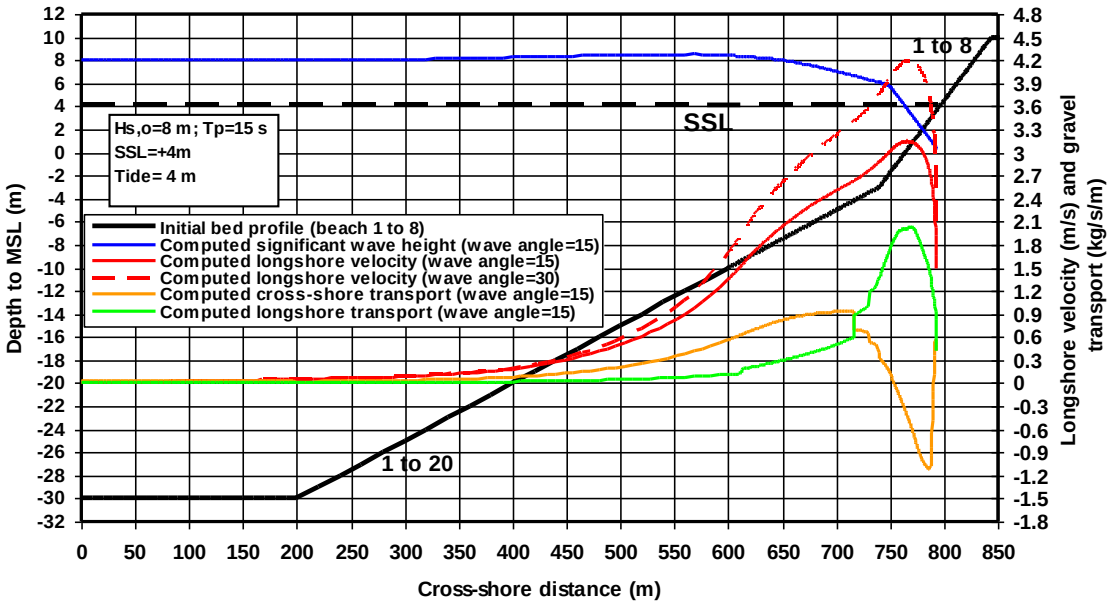

Figure 5.4.2 *Bed profile, wave height, longshore velocity and shingle transport for offshore wave height of $H_{s,o}$= 8 m and offshore wave incidence angles of 15° and 30°; schematized shingle barrier*

Figure 5.4.3 shows the computed values (in m^3/day) of the longshore transport integrated over the cross-shore profile for a range of offshore wave heights between $H_{s,o}$= 0.7 and 8 m. The computed values vary roughly between 5 m^3/day and 9000 m^3/day (including pores). About 80% of the longshore transport occurs in the surf zone landward of the -6 m depth contour and about 70% landward of the -4 m depth line.
Measured longshore transport rates based on the work of Chadwick (1989) and Nicholls and Wright (1991) are also shown in **Figure 5.4.3** assuming that the offshore significant wave height is twice the observed nearshore breaking wave height. The computed longshore transport rates (in m^3/day) for coarse gravel/shingle of 20 to 32 mm roughly are a factor of 2 to 3 too small for low wave conditions. This confirms that the CROSMOR-model may underpredict for coarse gravel conditions (d_{50}>20 mm).
It is noted that the measured values essentially represent the longshore transport of shingle/gravel in the swash zone (wave uprush and downrush zone). It should be realized that this zone is represented rather crudely using a sub-grid model approach. It emphasizes the fact that measured calibration data are required for fine tuning of the CROSMOR-model.

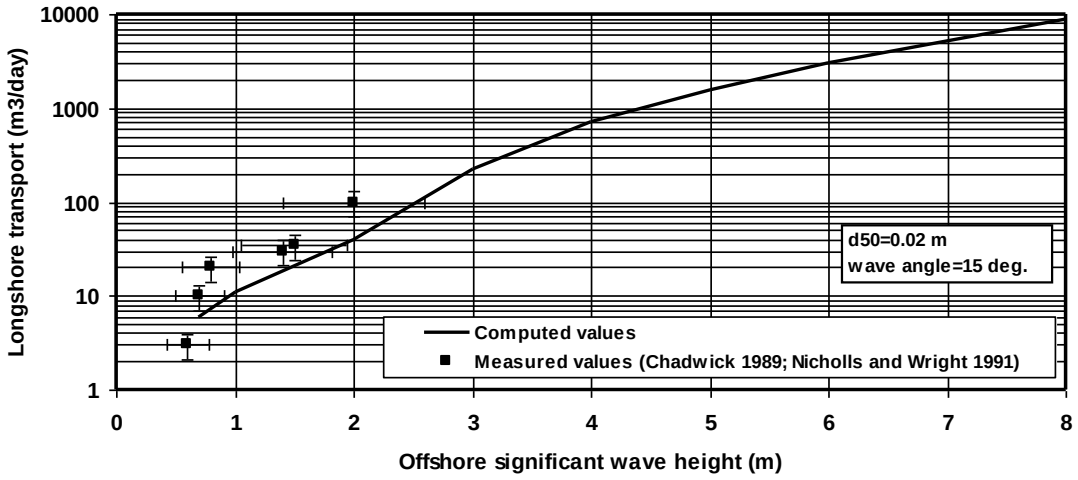

Figure 5.4.3 *Longshore transport as function of offshore wave height*

Offshore significant wave height $H_{s,o}$ (m)	Peak wave period T_p (s)	Storm surge level above Mean Sea Level (m)	Computed Longshore transport (kg/s)	(m³ incl.pores/day)
0.7	5	0	0.11	6
1	6	0	0.21	11
2	7	0	0.75	40
3	8	0.5	4.1	220
4	9	1	13	700
5	10	2	29	1565
6	12	3	56	3025
8	15	4	162	8750

Table 5.4.3 *Integrated longshore transport of gravel (d_{50}=20 mm)*

5.5 Calibration/validation of CROSMOR-model for Pevensey Beach

To demonstrate the applicability of the model for the gravel/shingle beach at Pevensey Bay, the CROSMOR-model has been applied to the 9 km long shingle barrier at Pevensey Bay, East Sussex, UK.
The ensemble-mean bed profile of Pevensey Bay location 5*73* is used as the standard bed profile in CROSMOR-runs. The maximum horizontal variation around the mean profile is about ±5 m. The maximum vertical variation around the mean profile is about ±0.75 m.
The cross-shore profile characteristics and boundary conditions as used in the CROSMOR-runs are given in **Table 5.5.1**.
The tidal data are taken from Admiralty Tide Tables 2009 for Station Eastbourne, UK.
To obtain a conservative estimate of the erosion volume along the profile for storm conditions (CROSMOR-model shows tendency for underprediction of gravel), the seaward-directed undertow velocities have been increased by 50% and the erosion rate in the swash zone has been increased (sef = 2, Van Rijn, 2009). Furthermore, the swash velocities near the water line and the streaming near the bed resulting in onshore transport of gravel have been neglected (c_{sw}= 0, c_{LH} = 0).
In all, eight conditions are considered, see **Table 5.5.2**. These cases are derived from the probability curves of joint data of maximum water levels and maximum wave heights**.**
Three cases (A,B,C,D) represent events with a return interval of at least 1 to 400 years. The offshore wave incidence angle is arbitrarily set to 30° to include wave-driven longshore velocities.

At Pevensey Bay, the highest surges would probably come from the south-west as would the largest offshore waves. However, Pevensey is sheltered by Beachy Head and the offshore bathymetry; so the largest waves in deep water are not the largest waves inshore. The most severe wave conditions are for waves from the south, which would generate a smaller surge. It is highly unlikely that the highest waves will come at the same time as the highest water levels. In fact, water levels and wave heights are almost completely uncorrelated. As regards the uncorrelated case, a 400 year return interval occurs for any combination of wave height and water level return intervals that, when multiplied, gives 400 years. An example of a joint return interval of 400 years is a 100 year return interval for the wave height and 4 year return interval for the water level.

Parameters	**Values**
Bed profile	slope of 1 to 630 between -10 and -3 m OD (flat shoreface) slope of 1 to 40 between -3 m and -0.5 m slope of 1 to 7 between –0.5 m and +4 m slope of 1 to 4.5 between +4 m and +6 m crest width of 20 m
Sediment d_{50}; d_{90}	0.012 m; 0.024 m (scaling factor gravel transport=2)
Bed roughness k_s	0.024 m ($2d_{50}$)
Horizontal mixing	0.1 m^2/s
Storm settings (H_s>3 m)	f_{rip}=1.5 (undertow =50%); sef=2; c_{LH}=0; C_{sw}=0
Daily wave settings (H_s< 2m)	f_{rip}=1.0 (undertow =standard) sef=1; c_{LH}=1; C_{sw}=0.3
Peak tidal water level	Mean tidal range = 5.0 m OD (OD is approx. MSL) Spring tidal range = 6.7 m OD; Neap tidal range = 3.7 m OD
Longshore peak tidal velocity offshore	0.5 m/s (flood); -0.5 m/s (ebb)
Offshore significant wave height $H_{s,o}$	1.5 to 5.5 m; 6 wave classes using Rayleigh distribution for each case
Peak wave period T_p	8 to 11 s
Wave angle to coast normal	10^o to 30^o
Storm surge level above MSL	0 to 2 m
File	GraPnew.inp

Table 5.5.1 *Data of shingle barrier at Pevensey Bay, UK*

Case	**Maximum water level WL_{max} (m)**	**Storm setup S (m)**	**Tidal range (m)**	**Offshore wave height $H_{s,o}$ (m)**	**Offshore wave period T_p (s)**	**Offshore wave angle to s.n. (degrees)**
A (>1 to 400 years)	4.5	2.0	5	3.0	8	30
B (>1 to 400 years)	4.0	1.5	5	5.0	10	30
C (>1 to 400 years)	3.8	1.3	5	5.5	11	30
D (>1 to 400 years)	3.8	1.3	5	4.5	9	30
E (1 to 20 years)	3.5	1.0	5	4.0	8.5	30
F (1 to 1 year)	2.5	0	5	3.0	8	30
G (minor storm)	2.5	0	5	2.5	7	30
H (non-storm)	2.5	0	5	1.5	6	10

Table 5.5.2 *Storm wave cases (s.n.=shore normal)*

Longshore transport (LST)

The LST of the CROSMOR-model has been computed for two offshore wave heights ($H_{s,o}$=1.5 m with T_P=6 s and $H_{s,o}$=3 m with T_p=8 s, offshore wave angle=30°) and varying water levels (-2 m to +4.5 m to MSL).
The basic input data are given in **Table 5.5.1**.
The water level is constant in each run. The longshore velocity at the offshore boundary is set to 0.3 m/s.
It is assumed that the gravel/shingle material is present only in the section landward of the -3 m depth contour.
Figure 5.5.1 shows the computed LST-value (CROSMOR-model) landward of the -3 m depth contour as function of the water level (tide level+surge level). The LST decreases for lower water levels, mainly because the length of the exposed bed with shingle material is shorter for low water levels.
The LST is reasonably constant for water levels higher than 0 m (Mean Sea Level). Based on this, it is concluded that the LST during storm events with high water levels is not so much influenced by the precise water level.

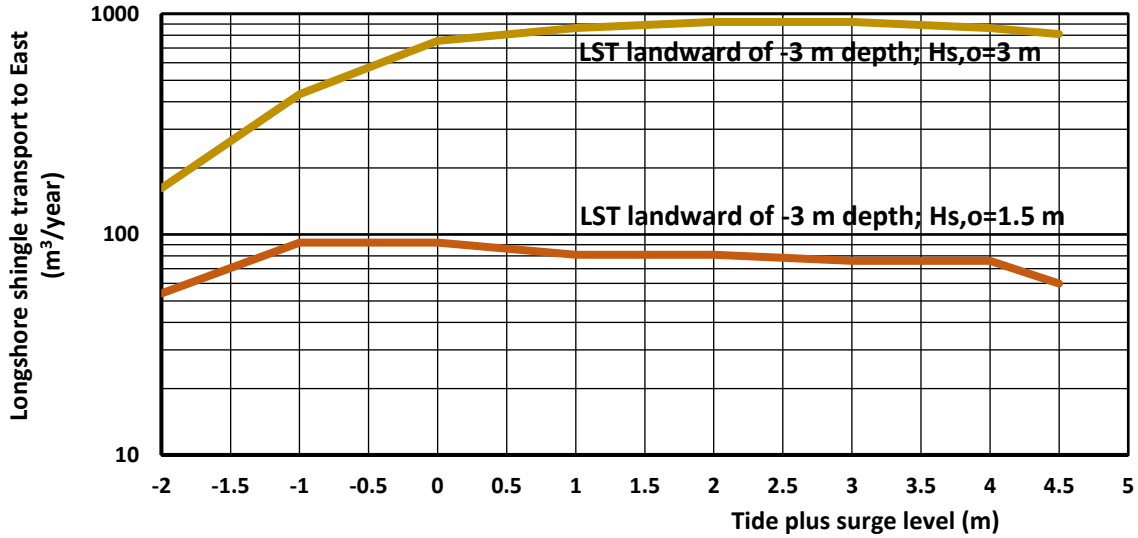

Figure 5.5.1 *Longshore shingle transport as function of water level; $H_{s,o}$=1.5 and 3 m (CROSMOR-model)*

Beach profile changes

Figures 5.5.2 to **5.5.10** show the bed profile changes after 24 hours based on the process-based CROSMOR-model for each Case. CROSMOR-runs without swash velocities and increased undertow (+50%) produce the largest erosion values at the upper beach for Cases A to F ($H_{s,o}$> 2.5 m).
The computed erosion area after 24 hours (based on standard undertow) is of the order of 2 to 20 m^3/m. The highest erosion volume is about 18 m^3/m for Case B ($H_{s,o}$=5 m; WL_{max}=4 m). The smallest erosion value is about 2 m^3/m for Case G ($H_{s,o}$=2.5 m; WL_{max}=2.5 m).
Most of the erosion occurs in the zone above and 1.5 m below the maximum water level.
The maximum computed recession at the crest is of the order of 5 m for Case A, B, C and D with high water levels.
In all cases the computed erosion profile is seaward of the envelope erosion profile (erosion area of about 100 m^3/m) as used by the Pevensey Coastal Defense for the 1 to 400 year storm case. The erosion profiles used by Pevensey Coastal Defense seem to be rather conservative.
The eroded material is deposited at the lower beach between +3 m above OD and -1 m below OD.
Case H with low waves of $H_{s,o}$=1.5 m leads to swash bar development accretion at the upper beach (up to +4 m OD).
Based on the results of Cases A to H, it is concluded that offshore waves with $H_{s,o}$> 2 m lead to erosion at the upper beach and offshore waves with $H_{s,o}$< 2 m lead to accretion at the upper beach (swash bar development).
Analysis results of large-scale flume experiments with gravel beaches shows that the onshore transport capacity

is of the order of 10 m^3/m per day for offshore waves of 1 m/s. Hence, storm erosion can be restored during daily conditions with relatively low waves.

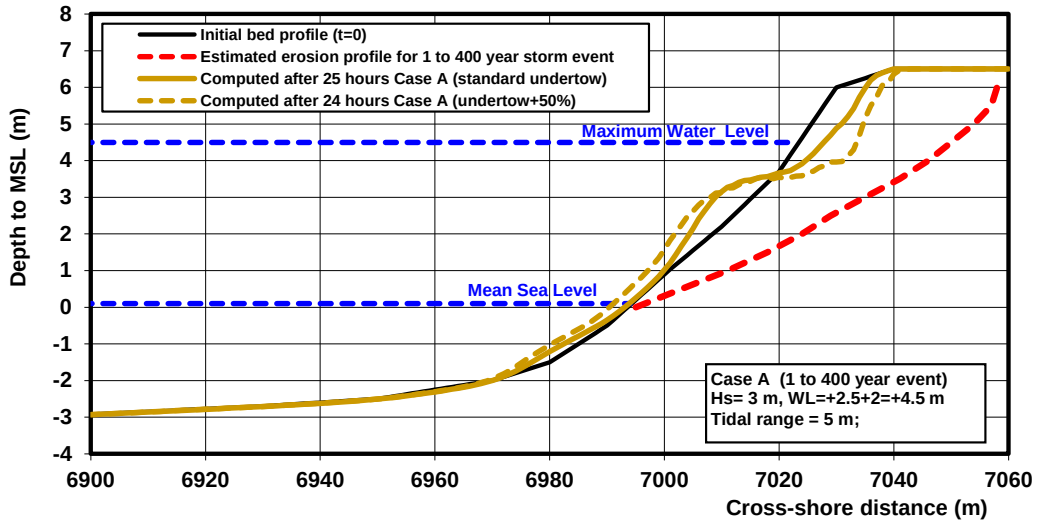

Figure 5.5.2 *Computed bed profile changes of CROSMOR for Case A, Pevensey beach (d_{50}=12 mm)*

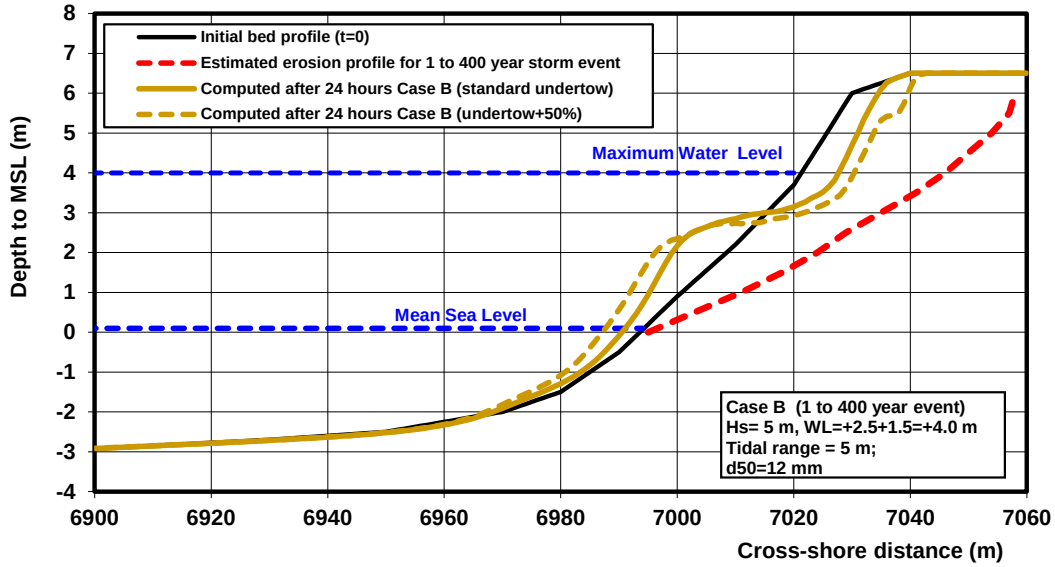

Figure 5.5.3 *Computed bed profile changes of CROSMOR for Case B, Pevensey beach (d_{50}=12 mm)*

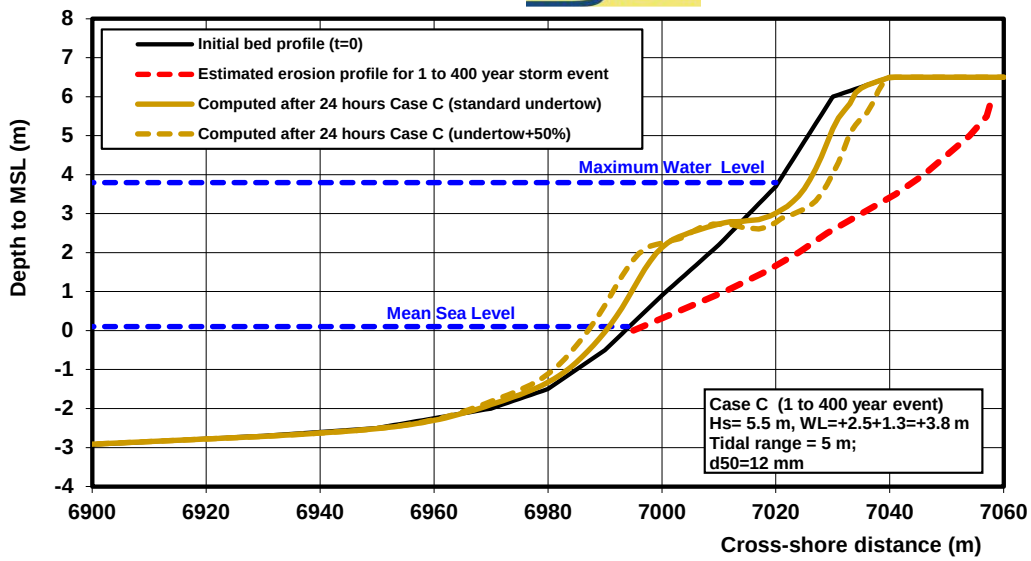

Figure 5.5.4 *Computed bed profile changes of CROSMOR for Case C, Pevensey beach (d_{50}=12 mm)*

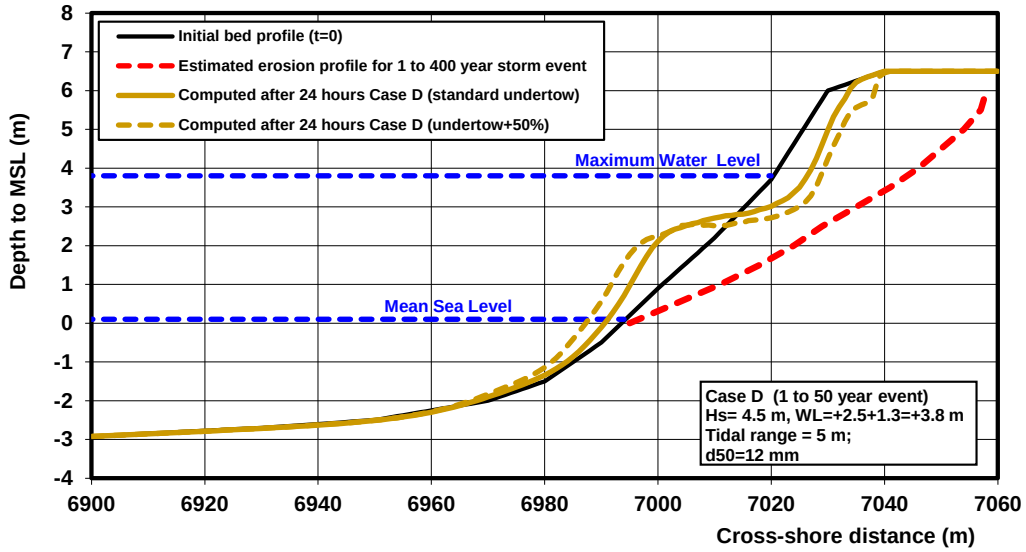

Figure 5.5.5 *Computed bed profile changes of CROSMOR for Case D, Pevensey beach (d_{50}=12 mm)*

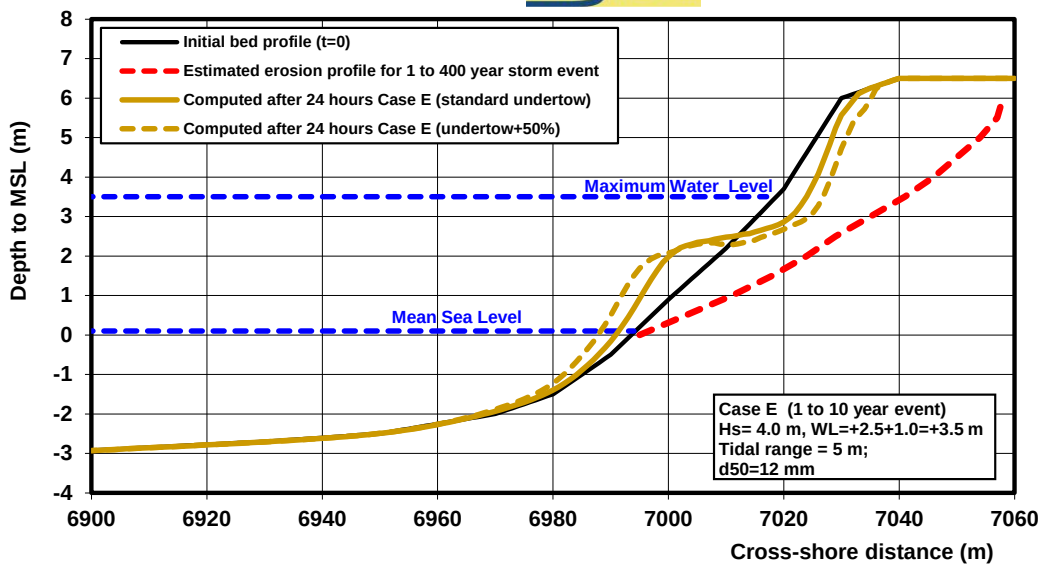

Figure 5.5.6 *Computed bed profile changes of CROSMOR for Case E, Pevensey beach (d_{50}=12 mm)*

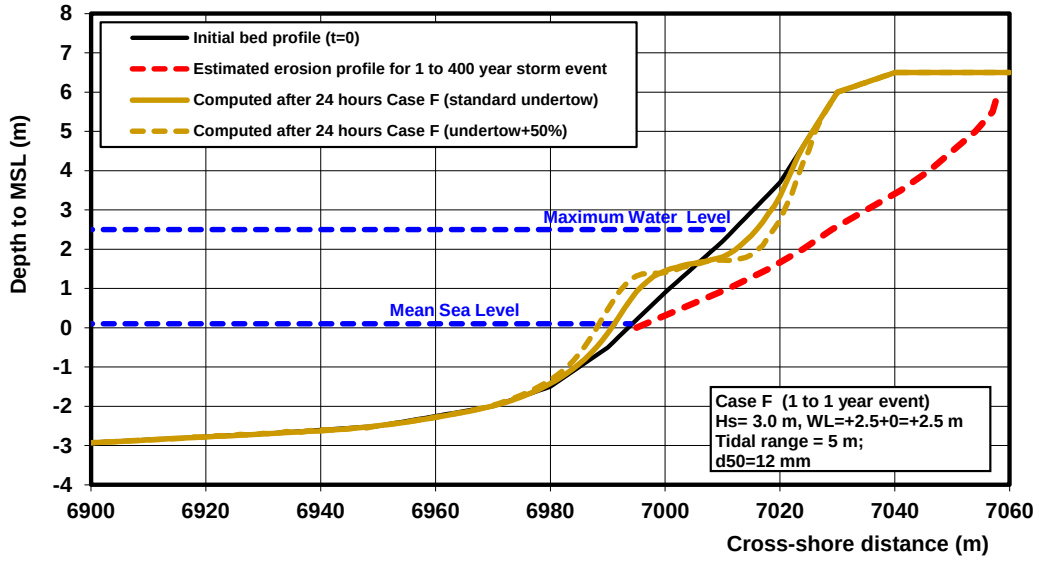

Figure 5.5.7 *Computed bed profile changes of CROSMOR for Case F, Pevensey beach (d_{50}=12 mm)*

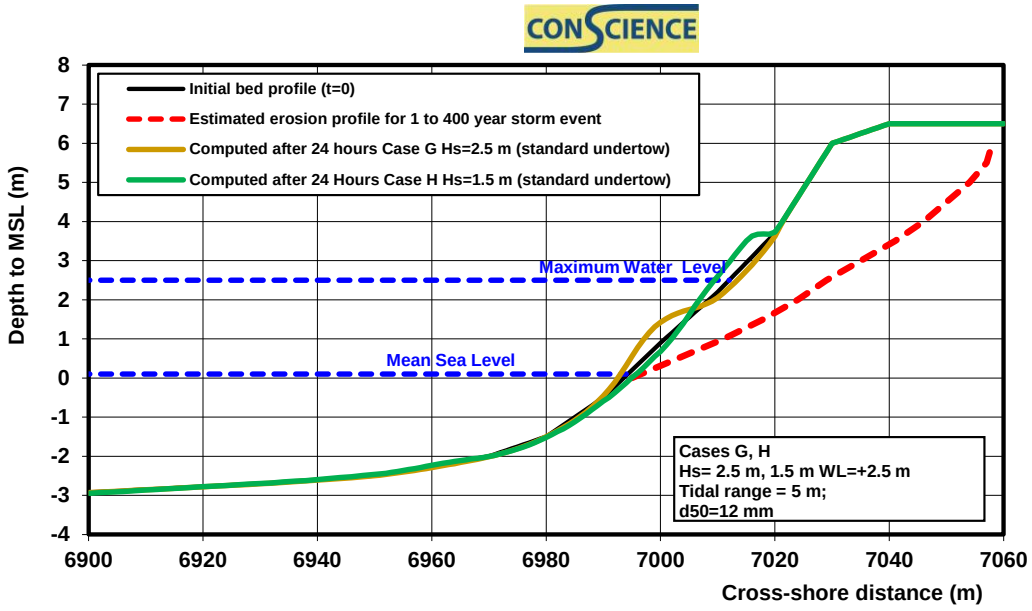

Figure 5.5.8 *Computed bed profile changes of CROSMOR for Case G, H, Pevensey beach (d_{50}=12 mm)*

Figure 5.5.9 shows the effect of the gravel size (varied in the range of 6 to 20 mm; bed roughness $k_{s,c}=k_{s,w}=2d_{50}$) on the erosion of the gravel/shingle beach for Case B. The computed total erosion area after 24 hours is about 50% higher for smaller gravel of 6 mm and 50% lower for coarser gravel of 20 mm.

Figure 5.5.10 shows the effect of the offshore wave angle between 0 and 30 degrees to the local shore normal on the erosion of the gravel/shingle beach for Case B. A lower wave angle leads to less erosion because the wave-driven longshore decreases significantly for lower wave angles, see also **Figure 3.3**. When the incoming waves are almost normal to the shore (offshore wave angle=0 degrees), the erosion is reduced by about 75% (about 4 m^3/m) compared to an offshore wave angle of 30 degrees.

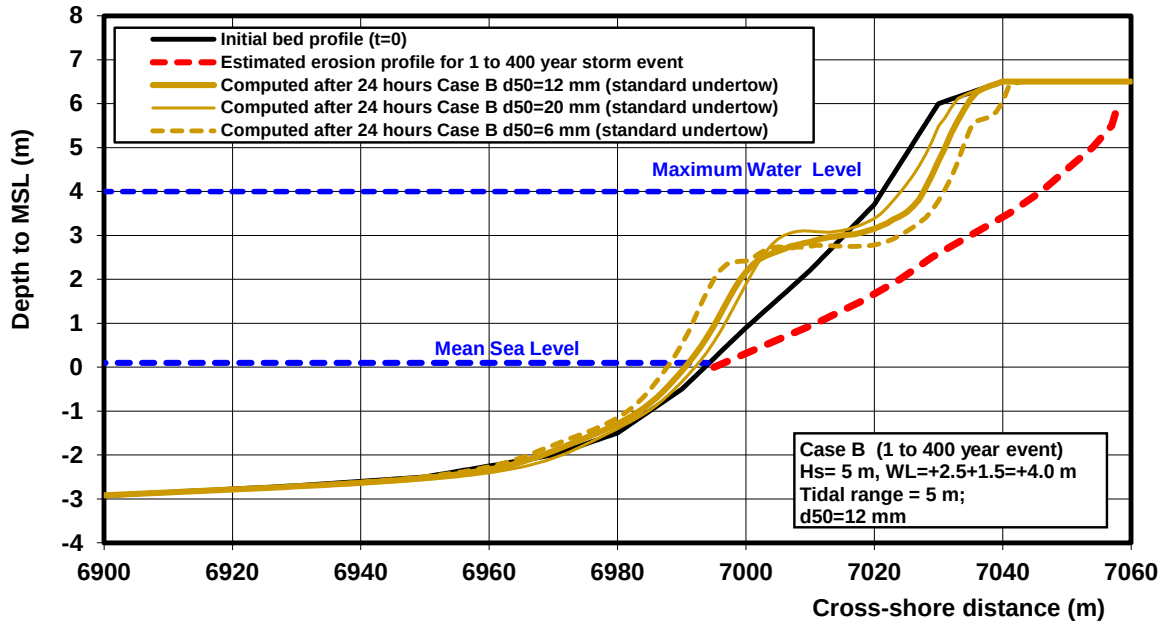

Figure 5.5.9 *Effect of shingle size on the erosion of Case B, Pevensey beach*

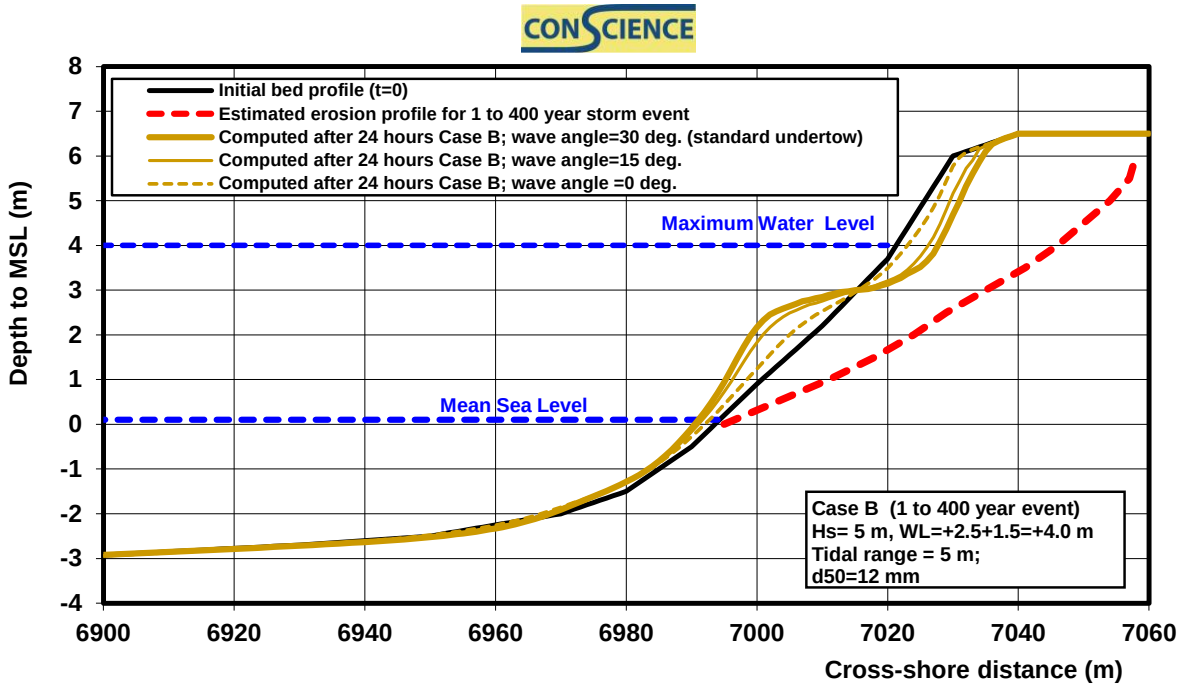

Figure 5.5.10 *Effect of offshore wave angle to shore normal on the erosion of Case B, Pevensey beach*

Figure 5.5.11 shows the accretion of the shingle barrier after 10 days of low wave conditions ($H_{s,o}$ in the range of 1 to 1.5 m). The computed total accretion area at the upper beach is about 25 m^3/m (after 10 days) for shingle of 0.02 m (sef = 1, c_{LH} = 0.3, c_{SW} = 0.3). The shingle is pushed up to the slope of the barrier by wave run-up processes which are somewhat stronger for higher waves. It will take some weeks with low waves for the shingle barrier to recover from the erosion (about 25 m^3/m) during a major storm event, assuming that sufficient shingle material is available in the foreshore zone. However, often the shingle material is carried away in longshore direction (passing around the short groynes, if present) during a major storm event. The shingle material may also be (partly) washed over the crest of the barrier during a major storm event.

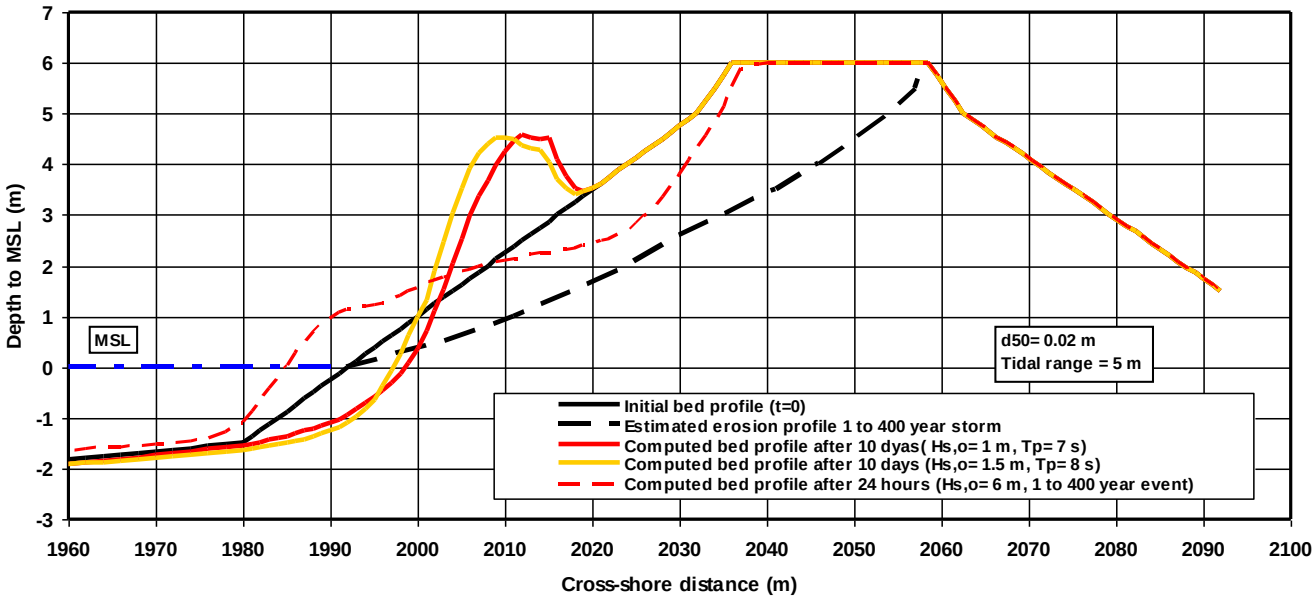

Figure 5.5.11 *Accretion of shingle barrier during low wave conditions at Pevensey Bay, UK*

5.6 Overwash of gravel/shingle barrier

Shingle barriers with a crest level at 3 to 6 m above MSL (or better HW level) are vulnerable to overwash which may easily result in landward migration (roll back) during storm conditions with surge levels of 2 to 3 m above MSL and a tidal range of 3 to 6 m (see **Figure 5.6.1**).
The CROSMOR-model has been used for exploring computations of crest erosion and landward migration of a low shingle barrier with crest level at 4 m above MSL (see **Figure 5.6.1**). The profile characteristics and boundary conditions are given in **Table 5.6.1**. Two cases are considered with a surge level at 4.5 m above MSL (water depth above crest = 0.5 m) and at 5 m above MSL (water depth above crest = 1 m). The overwash discharge has been varied in the range of 0.5 to 2 m^2/s by specifying a small velocity at the inflow boundary (x = 0) at a depth of 30 m below MSL. The fluid velocity above the crest is in the range of 0.5 to 2 m/s.

Figure 5.6.1 shows the computed significant wave height, the cross-shore and longshore velocities and the bed level changes after 1 day along the profile for a storm surge level of SSL = 4.5 m including tidal elevation (water depth above the crest = 0.5 m) and an overwash discharge of 1 m^2/s (velocity above crest = 2 m/s). The offshore wave incidence angle is set to 15°. The computed significant wave height decreases from about 6 m at the toe of the beach to about 0.3 m (for h_{crest} = 0.5 m) above the crest and remains constant at the landward side of the barrier. The cross-shore velocity is seaward-directed at the beach due to the generation of the undertow and changes to a strong landward-directed overwash flow above the crest (maximum value of 2 m/s).
The longshore velocity has its peak value (about 2.5 m/s) just seaward of the crest and decreases above the crest due to frictional effects (strong reduction of water depth). The longshore current velocity landward of the crest is strongly influenced by the wave breaking process. When the wave parameters are averaged over 1 wave length (1L; default approach) the longshore velocity first increases and then decreases when the wave breaking process decays. When the averaging process is set at 0.1L, the longshore velocity strongly decreases landward of the crest. The former approach is not realistic but the latter approach also is questionable as (breaching and) overwash is a very local process violating the longshore uniformity approach of the CROSMOR2008-model. The flow velocity landward of the crest will be three-dimensional due to spreading of the flow over the land surface.
The computed bed level changes after 1 day (24 hours) show crest erosion of the order of 1.2 m and landward barrier migration of the order of 3 m. The barrier migration reduces for a smaller overwash of 0.5 m^2/s (v_{crest} = 1 m/s). The crest lowering by erosion is not much influenced by the overwash discharge and is about 1.2 m after 1 day.

A depositional bar with a height of about 1 m and a length of about 30 m is formed at the beach, see **Figures 5.6.1** and **5.6.2**. This latter bar is mainly caused by onshore transport of shingle enhanced by relatively large longshore velocities (2.5 m/s) under oblique wave attack. When the wave incidence angle is set to 0, the bar formation is much less pronounced, as shown in **Figure 5.6.2**. The crest erosion and migration also are smaller for waves normal to the coast.

Parameter	Values
Bed profile	slope of 1 to 20 between -30 m and -3 m slope of 1 to 8 between -3 m and +4 m crest level at +4 m; crest width=3 m landward slope of 1 to 5; land surface at MSL
Sediment d_{50} **d_{90}**	0.02 m 0.04 m
Bed roughness k_s	0.04 m
Horizontal mixing	0.1 m^2/s
Peak tidal water level	0
Peak tide-induced and wind-induced velocity	1 m/s
Offshore significant wave height $H_{s,o}$	8 m (6 wave classes using Rayleigh distribution)
Peak wave period T_p	15 s
Storm surge level above MSL	4.5 and 5 m
Overwash discharge	0.5 to 2 m^2/s

Table 5.6.1 *Data of field case of shingle barrier with overwash*

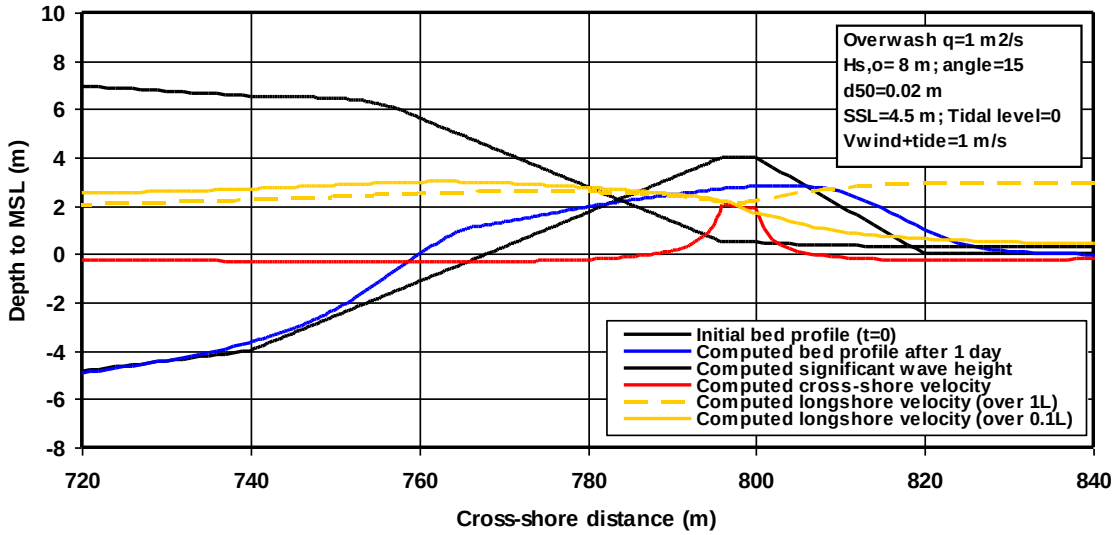

Figure 5.6.1 *Computed wave height, cross-shore and longshore velocity and bed level changes for storm surge level of 4.5 m (h_{crest}= 0.5 m) and overwash discharge 1 m^2/s (v_{crest}= 2 m/s)*

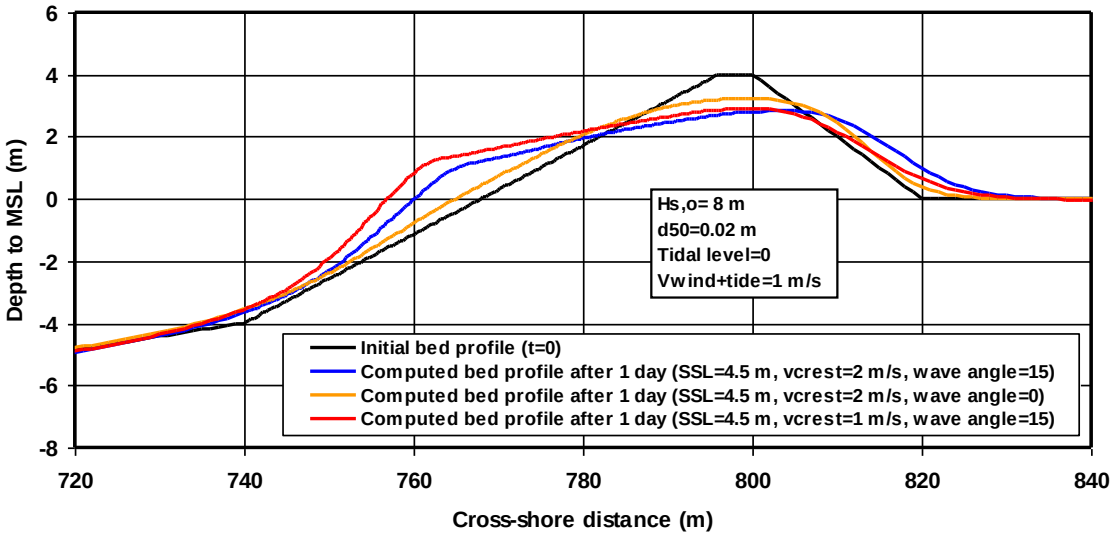

Figure 5.6.2 *Computed bed level changes for storm surge level of 4.5 m (h_{crest}= 0.5 m) and overwash discharge 0.5 and 1 m^2/s (v_{crest}= 1 to 2 m/s)*

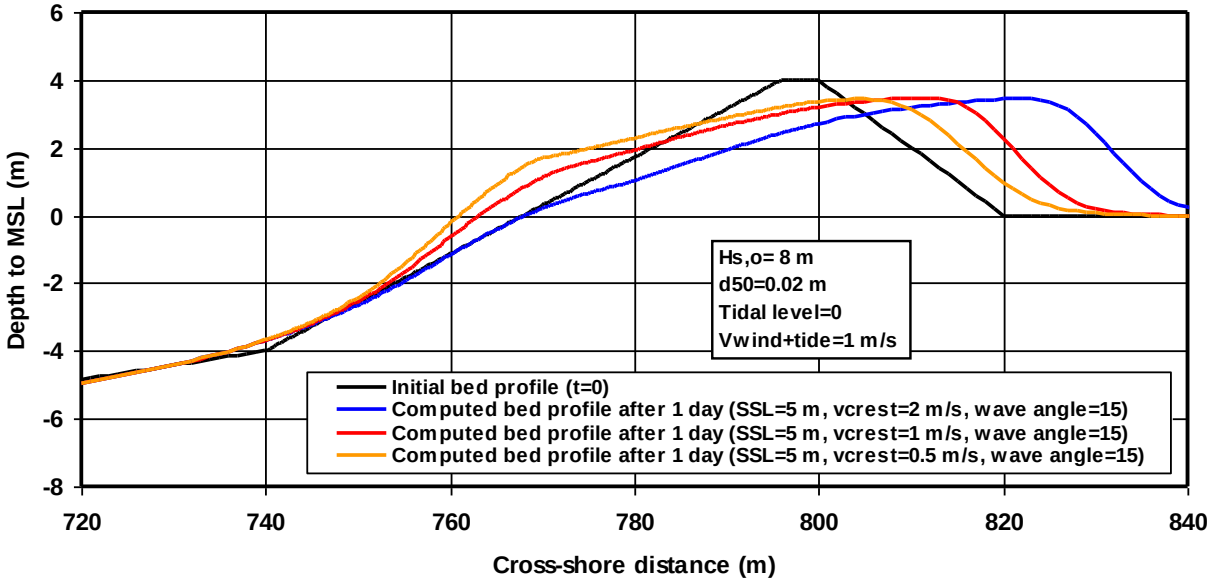

Figure 5.6.3 *Computed bed level changes for storm surge level of 5 m (h_{crest}= 1 m) and overwash discharge 0.5, 1 and 2 m^2/s (v_{crest}= 0.5 to 2 m/s)*

Figure 5.6.3 shows computed bed levels after 1 day for a storm surge level of 5 m (h_{crest} = 1 m) and overwash discharges of 0.5, 1 and 2 m^2/s (v_{crest} = 0.5 to 2 m/s). The crest erosion is about constant (about 0.6 m) for all three cases. The crest migration increases strongly with increasing flow velocity above the crest. Under extreme conditions the maximum crest migration is about 20 m/day. The probability of occurrence of a storm surge level of 5 m above mean sea level is of the order of 10^{-4} (once in 10,000 years). These high crest migration values are exceptional, but not irrealistic in comparison with the data of Hurst beach and Hurst spit where crest migration values of 20 m in one storm event and long term values of 10 m over a period of about 2 years have been observed. Measured vertical crest erosion values are in the range of 0.5 to 1.5 m at Hurst beach and spit.

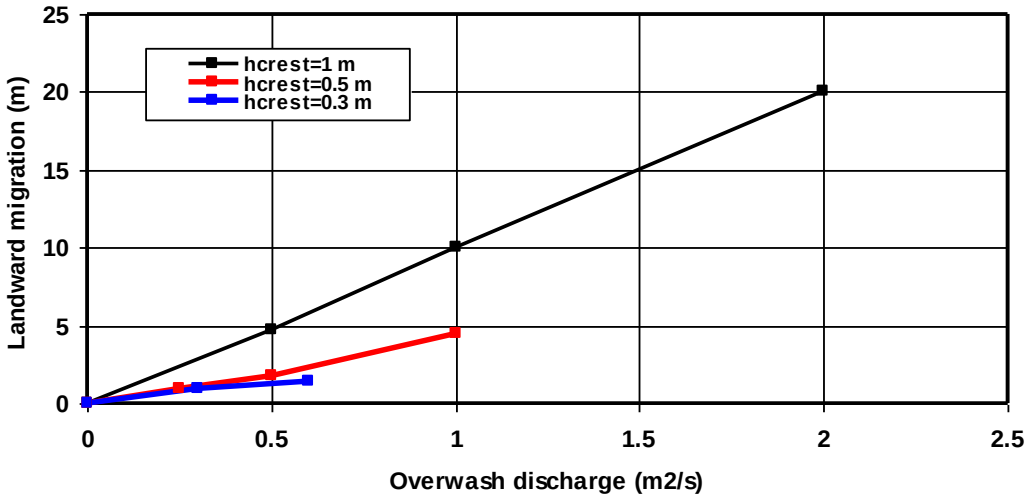

Figure 5.6.4 *Landward migration of gravel barrier as a function of overwash discharge and the initial water depth at crest during an extreme storm event (duration of 24 hours)*

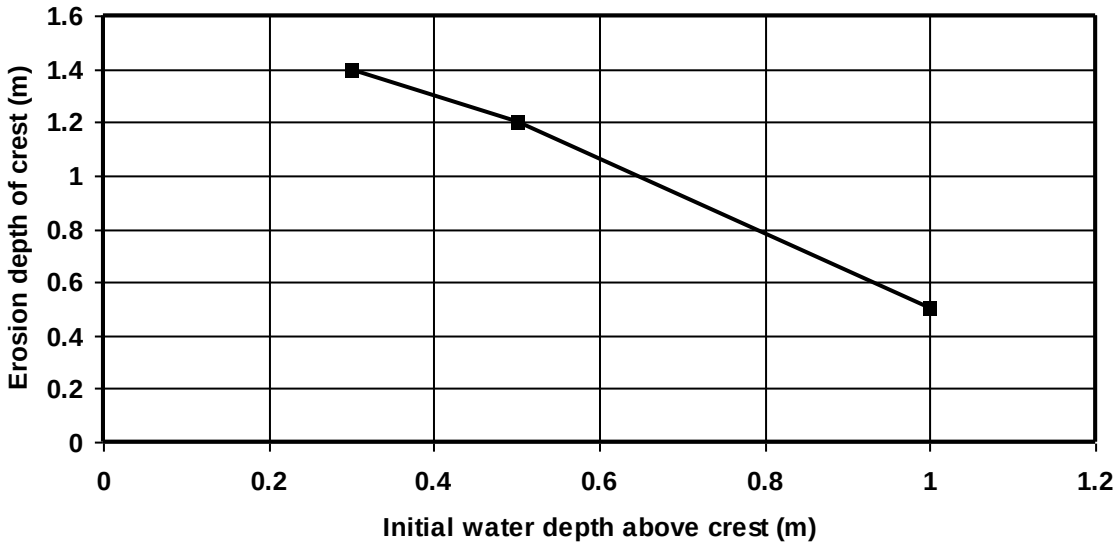

Figure 5.6.5 *Erosion of barrier crest as a function of the initial water depth at crest during an extreme storm event (duration of 24 hours)*

All computational results on crest erosion and barrier migration are summarized in **Figures 5.6.4** and **5.6.5**. **Figure 5.6.4** shows the barrier migration as a function of the overwash discharge and the initial water depth at the crest of 0.3, 0.5 and 1 m. The migration increases with increasing initial crest depth (and thus larger wave height) and with increasing overwash discharge. Extreme values are as large as 20 m/day.
Figure 5.6.5 shows the crest erosion as a function of the initial water depth at the crest. The crest erosion decreases from about 1.5 m to 0.5 m for a water depth at the crest increasing from 0.3 m to 1 m. The overwash discharge has not much effect on the erosion depth.

5.7 Coastal protection of sandy dunes using gravel/shingle material

The erosion of sandy dune coasts due to storm events is a major problem at many sites. Under extreme storm conditions the erosion volume due to a severe storm with a duration of 5 to 6 hours is of the order of 100 to 300 m^3/m (**Vellinga, 1986; Steetzel, 1993; Van Rijn, 2008**).
To show the reduction of coastal erosion using a protection layer of coarse shingle material on top of the sand surface, the CROSMOR-model has been applied to a typical cross-shore profile along the Dutch coast. The profile characteristics and boundary conditions are given in **Table 5.7.1**.

Figure 5.7.1 shows computed bed profiles after a storm duration of 5 hours for a case with a storm surge level at 5 m above MSL using sandy material (d_{50}= 0.000225 m; 0.225 mm) and shingle material (d_{50}= 0.02 m; 20 mm). The dune erosion is of the order of 170 m^3/m for the sandy case and only 15 m^3/m for the shingle case. The maximum horizontal recession for the shingle case is of the order of 2 m (corresponding to a value of about 0.7 m normal to the barrier slope of 1 to 3). The erosion values will be somewhat larger for oblique incoming waves due to the generation of longshore velocities. When cobbles ($\cong$ 0.1 m) are used, the erosion will be minimum.
Using a safety factor of 2, the minimum layer thickness of shingle to protect a sandy subsoil should be of the order of 2 to 3 m. The toe of the layer should extend to below the low water mark (-2 m below MSL) resulting in a total length of about 100 m assuming a beach slope of 1 to 8 between the -2 m and +3 m line and a barrier slope of 1 to 3. Hence, a total volume of about 200 to 300 m^3/m is required per m shoreline or 200,000 to 300,000 m^3 per km. This solution may be attractive at specific locations (near structures, harbours, inlets, etc.) where the erosion processes of the sandy dune system are excessively large resulting in relatively large maintenance costs (nourishments costs).

Parameter	**Values**
Bed profile	slope of 1 to 180 between -30 m and -3 m slope of 1 to 70 between -3 m and 0 m slope of 1 to 20 between 0 m and +3 m slope of 1 to 3 between +3 m and +15 m
Sediment **d_{50}** **d_{90}**	Sand Shingle 0.000225 m 0.02 m 0.000450 m 0.04 m
Bed roughness k_s	0.001 m 0.04 m
Horizontal mixing	0.5 m^2/s
Peak tidal water level	0 m
Peal tidal velocity	0.5 m/s (flood); -0.5 m/s (ebb)
Offshore significant wave height $H_{s,o}$	7.6 m (6 wave classes using Rayleigh distribution)
Offshore wave incidence angle	0^o
Peak wave period T_p	12 s
Storm surge level above MSL	5 m

Table 5.7.1 *Data of Dutch Reference Storm Case*

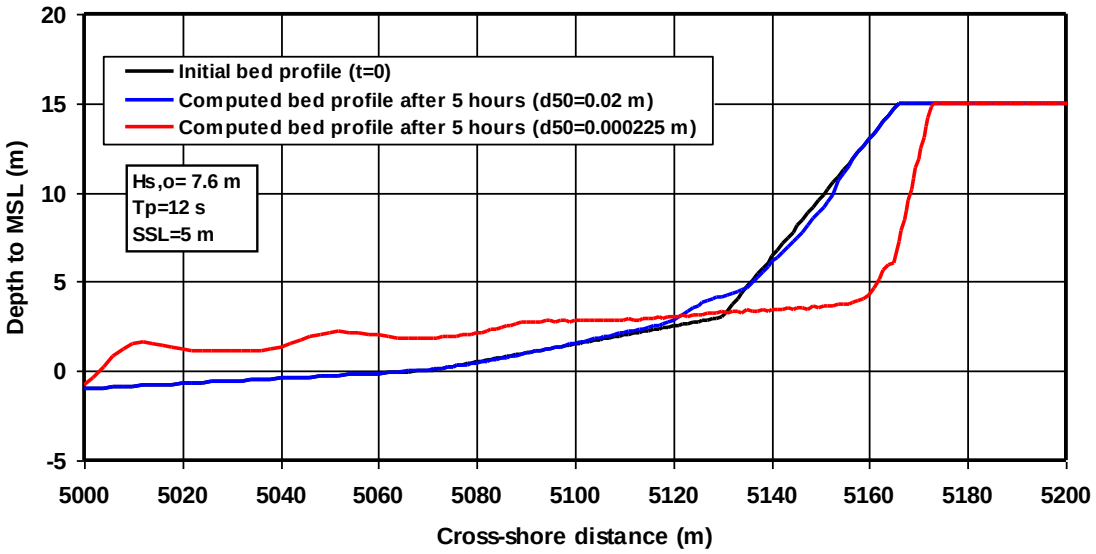

Figure 5.7.1 *Computed bed profiles after 5 hours for a storm event using d_{50}=0.000225 m and d_{50}=0.02 m for Dutch Reference Case*

5.8 Erosion graphs for gravel/shingle barrier

The CROSMOR2008-model has been used to compute the erosion volume (in m^3/m) after 24 hours due to storm events for a range of conditions. It is assumed that a high storm surge level (SSL) corresponds to a high offshore wave height. Three storm events are considered: set-up = 0.5 m with $H_{s,o}$ = 4 m (T_p = 9 s); set-up = 1 m with $H_{s,o}$ = 4.5 m (T_p = 9.5 s), set-up= 2 m with $H_{s,o}$= 5 m (T_p = 10 s) and set-up = 3 m with $H_{s,o}$ = 6 m (T_p = 11 s). The wave incidence angle is 30° to the shore normal. The shingle size is varied in the range of 0.01 to 0.1 m. The tidal range is 5 m for all events. To obtain a conservative estimate of the erosion volume, the undertow velocities near the beach are increased by 50% and the sediment pick-up in the swash zone has been increased (sef = 2). The swash velocities and the streaming velocity near the bed have not been taken into account (c_{SW} = 0, c_{LH}= 0). The results are shown in **Figure 5.8.1**. The erosion area (in m^3/m) increases with increasing set-up and decreasing sediment size. The largest erosion area above the storm surge level is about 45 m^3/m for SSL = 3 m and d_{50} = 0.01 m. The smallest erosion area (about 5 to 10 m^3/m) occurs for a cobble barrier. This plot can be used to get a first estimate of the erosion of gravel/shingle barriers.

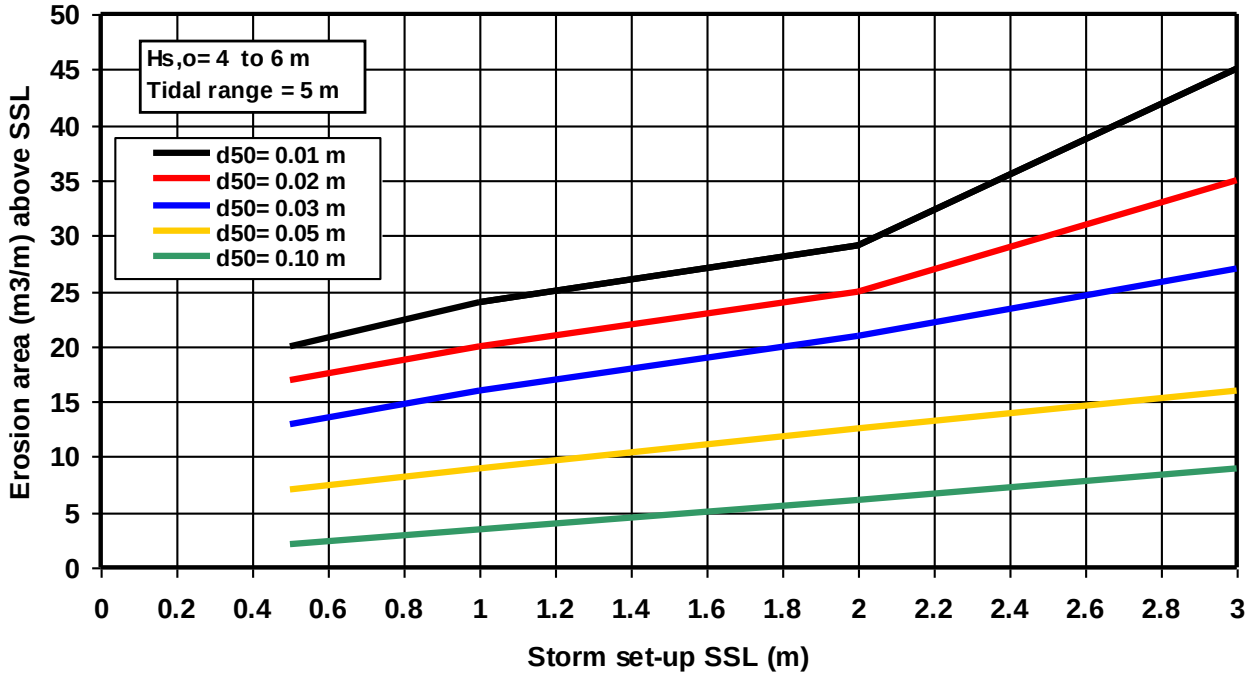

Figure 5.8.1 *Erosion area (after 24 hours) as function of storm set-up and shingle/cobble size*

5.9 Derivation and calibration of beach erosion prediction equation

Model

Erosion of the upper beach above the level of +3 m (to MSL) occurs mainly during major storm events when the tide is high.

The computed erosion volumes of the CROSMOR-model are shown as function of the sum of the nearshore breaking wave height and the maximum water level during a storm event ($Y=H_{s,br}+WL_{max}$) with duration of $\Delta t= 4$ hours in **Figure 5.9.1**. The basic input data are given in **Table 5.9.1**. The nearshore breaking wave height is about 50% of the offshore wave height based on CROSMOR-runs ($H_{s,br} \cong 0.5\ H_{s,o}$).

The computed beach erosion volumes of the CROSMOR-model can represented by:

$$E_v = 0.2\ \gamma\ (Y-Y_{critical})\ \Delta t \qquad \text{for } H_{s,br} > 2 \text{ m and } Y>3.5 \text{ m} \qquad (5.9.1)$$

with:

E_v= upper beach erosion volume per unit width per hour during storm event ($m^3/m/hour$);

Δt= duration of storm event (hours);

$Y= H_{s,br}+WL_{max}$ (m)

$H_{s,br}$= significant nearshore breaking wave height (m);

WL_{max}= maximum water level above MSL during storm event, $Y_{critical}$= 3.5 =value at which $E_v=0$;

γ=calibration coefficient (default=1; $\gamma \cong 0.6$ based on measured erosion volumes, see below).

Analysis results of large-scale flume experiments with gravel beaches shows that the onshore transport capacity is of the order of 10 m^3/m per day for offshore waves of 1 m and sufficiently high water levels. Hence, storm erosion can be restored during daily conditions with relatively low waves. However, this may take time (weeks).

It is assumed that the swash bar development occurs for $Y_{critical} < 3.5$.

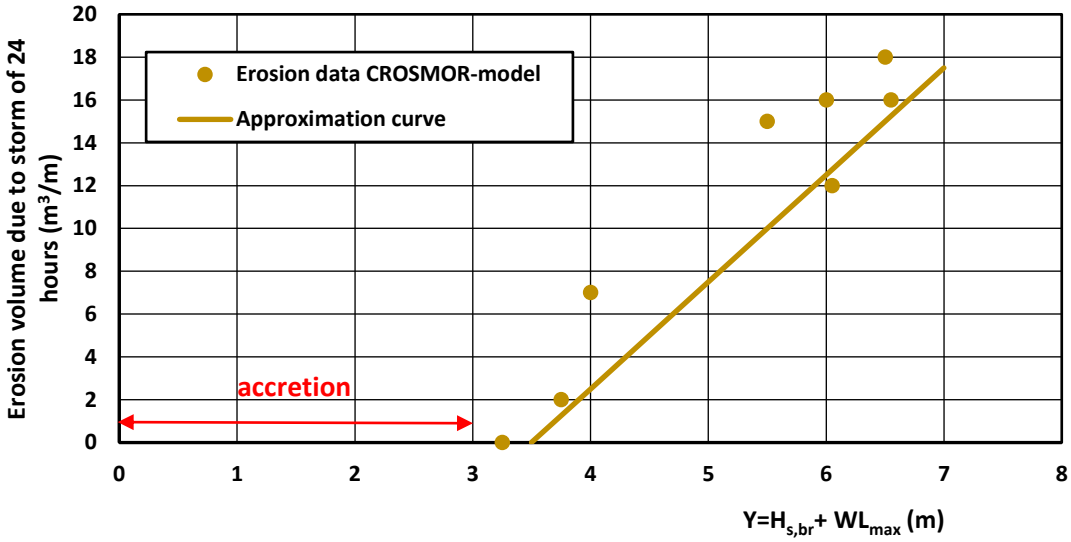

Figure 5.9.1 *Erosion volume per unit width per day as function of the sum of significant nearshore breaking wave height ($H_{s,br}$) and maximum water level (WL_{max}).*

Case A	Storm setup s (m)	Tidal amplitude η (m)	Offshore significant wave heihght $H_{s,o}$ (m)	Breaking wave height $H_{s,br}$ (m)	Sum of $H_{s,br}$ and WL_{max} (=η+s) (m)
A	2	2.5	3	2.2	6.7
B	1.5	2.5	5	2.8	6.8
C	1.3	2.5	5.5	3	6.8
D	1.3	2.5	4.5	2.8	6.6
E	1	2.5	4	2.5	6
F	0	2.5	3	2	4.5
G	0	2.5	2.5	1.75	4.25
H	0	2.5	1.5	1	3.5

Table 5.9.1 *Basic data of computed erosion values of CROSMOR-model (d_{50}=0.012 m=12 mm)*

Calibration storm events in autumn 2020

Two minor storm events were recorded in the period between the pre- and post-storm surveys, as follows:

- 18th October: $H_{s,o,max}\cong$2 m (T_p=6.7 s); $WL_{max}\cong$3.7 m (Y=4.7; $H_{s,br}\cong$0.5 $H_{s,o}$); wave direction≅ 160° to N (wave vector=340° to N); angle to shore normal=20° (waves from east of shore normal)
- 14th November: $H_{s,o,max}\cong$2.5 m (T_p=7.1 s); $WL_{max}\cong$3.8 m (Y=5.05; $H_{s,br}\cong$0.5 $H_{s,o}$); wave direction≅ 200° to N (wave vector=20° to N); angle to shore normal=60° (waves from west of shore normal).

Information of erosion losses due to storm events is given by Herrington (2022a).

Figure 5.9.2 shows pre- and post storm profiles at location 589 (about 3.5 km from Sovereign harbour; angle shore normal=320° to N). The total erosion at the upper beach (above +3 m OD) is about 10 m^3/m. The eroded sediment is accumulated at the toe of the slope. Typically, during calmer conditions, a period of restorative changes takes place where material at the toe of the slope is moved back up of the profile, but it can not reach the eroded upper part of the slope due to lower runup levels during post storm conditions.

The two autumn 2020 storms were quite similar with only little time in between them. Probably too short for the beach to restore. Most likely, the major part of observed storm erosion of about 10 m^3/m occurred in storm 1

(say 7±1 m^3/m). The erosion during storm 2 was most lekey significantly smaller as the profile was still adjusted to conditions of similar storm 1.

The computed erosion volume based on the approximation curve (CROSMOR-results) is about 8±2 m^3/m for Y=5±0.3 (storm1), which is in good agreement with the observed value of storm 1. The overprediction may be related to the relatively long storm duration of 24 hours used in the CROSMOR-runs. This effect can be taken into account by a reduction factor.

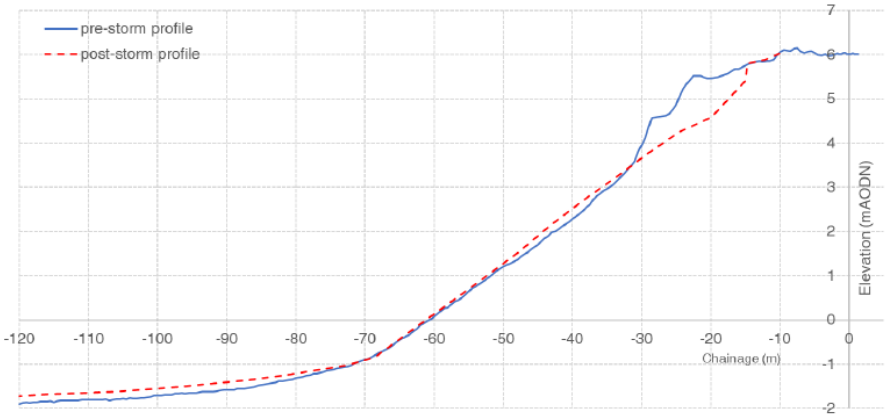

Figure 5.9.2 *Pre-storm (September 2020) and post-storm (15th November 2020) beach profiles at 589 (Herrington Consulting LTD, 2022);*
Photograph shows ridge crest of the post-storm beach profile at location 589 on the afternoon of 15th November 2020.

<u>Calibration storm event Eunice 18-19 February 2022</u>

Three storms affected the south coast of the UK within the time span of a week (12-20 February 2022), see **Figure 5.9.3**. On 18 February at 1 hour 45 minutes after high water, the Cefas (Hastings) wave buoy (only 1 km from the Pevensey wave point) recorded a significant wave height of 5.3 m (4.8 m at Pevensey buoy) when SWL is about 3.7 m OD.

The wave and water level data are, as follows:

- storm 14 February: $H_{s,o}$ + WL_{max}=2.8 + 2.3 = 5.1 m (1.6 m above critical value of 3.5, see Eq. 6.4.1);
- storm 17 February: $H_{s,o}$ + WL_{max}=3.0 + 3.1 = 6.1 m (2.6 m above critical value of 3.5, see Eq. 6.4.1);
- storm 18 February: $H_{s,o}$ + WL_{max}=3.7 + 4.8 = 8.1 m (4.6 m above critical value of 3.5, see Eq. 6.4.1).

A beach level survey had been undertaken on Monday 7th February, and given the intensity of Storm Eunice (18-19 February), and an additional survey was done on Saturday 19th February. Between these two surveys, a week of bypassing (trucks) of shingle from the southwest beach added 3,740 m^3 to the scour hole area near Sovereign harbour.

The losses of shingle along the frontage between 7 and 19 February are, as follows (Herrington 2022b; Personal Communication PCDL-LVRS, 2023):

- about 42,000 m^3 above level +3 m OD (15% in Section 0-2 km; 35% in Section 2-5 km, 30% in Section 5-7 km and 20% in Section 7-9 km);
- about 20,000 m^3 above level -2 m OD (gain of 22,000 m^3/m between -2 m and +3 m OD).

Although the total amount of sediment lost is estimated at 20,000 m^3 above -2 m OD, not all of it was due to Storm Eunice. Three methods are herein used to estimate the erosion contribution of Storm Eunice.

Method 1: The process agreed for analysing Storm Event data was to take offshore wave data, transform it to the nearshore and then extract longshore wave power (LWP) per tide.

Applying the same rationale to the 23 tides between 7th and 19th February, data captured by the CEFAS, Hastings wave buoy was processed and this shows that 22% of the total LWP was due to Storm Eunice.

When applied to the total loss of 20,000 m^3, the Estimated Shingle Loss becomes 4,400 m^3 above -2 m OD and 9200 m^3 above +3 m OD

Method 2: The erosion contribution of Storm Eunice can also be assessed by considering the longshore transport in the period of day 17 to 19.5. **Figure 5.9.3** shows the wave data at Pevensey buoy location and computed longshore transport of single at location Cooden in this period (input data: d_{50}=12 mm, beach slope 1 to 10, shore normal angle at Cooden=350°). The wave height $H_{s,o}$ is about 4 m during storm Eunice on 18 February 2022. The wave direction is mostly between 220° and 230° to N.

The computed LST values are as follows:

- day 13 to 15 (72 hours): LST=1465 m^3; (≅25%);
- day 15-18 (72 hours): LST=1730 m^3; (≅30%);
- day 18-19.5 (36 hours Eunice): LST=2310 m^3; (≅40%);
- day 7 to 19.5 (180 hours): total LST=5750 m^3; (100%).

The computed LST is highest during Storm Eunice (day 18-19.5). The LST at Cooden during storm Eunice is 40% of the total LST.

Method 3: The erosion equation (5.6.1) with γ=1 was used to computed the erosion above +3 m OD using the wave data from Pevensey buoy for the period of day 7 to day 19.5 resulting in a computed total erosion volume of 25,000 m^3 (about 2.8 m^3/m) The computed erosion volume of Storm Eunice (day 18-19.5) is 18,000 m^3 (2 m^3/m) which is about 70% of the computed total volume of 25,000 m^3.

Summarizing, the contribution of Storm Eunice to the total erosion between the two surveys of 7 and 19 February 2022 is in the range of 22% to 70%, depending on the method used (longshore wave power LWP, longshore sediment transport LST or cross-shore erosion).

The erosion volume predicted by Equation (5.6.1) is about 25,000 m^3, which is 60% of the observed value of 42,000 m^3 in the period 7-19 February 2022. This latter value also includes the (unknown) loss due to longshore transport at the terminal groyne of Cooden. The computed total LST over the period of 7-19 February is about 5,000 m^3 (see method 2). Assuming that this value is a reasonable estimate of the loss due to LST, the total computed loss is 25,000+5,000=30,000 m^3 (70% of the observed value of 42,000 m^3, which is a very reasonable result).

The loss to the east also depends on how full the terminal groyne bay is prior to a storm. If several groyne planks are visible, then only major events with 2 m or more waves are able to drive significant quantities past the groyne.

Often, a significant bank of sediment can be seen down drift of the terminal groyne at the end of a storm event. There is no way of knowing how much passed during the early part of the event and was subsequently dispersed much further east and beyond visual/survey range (Personal Communication PCDL-LVRS).

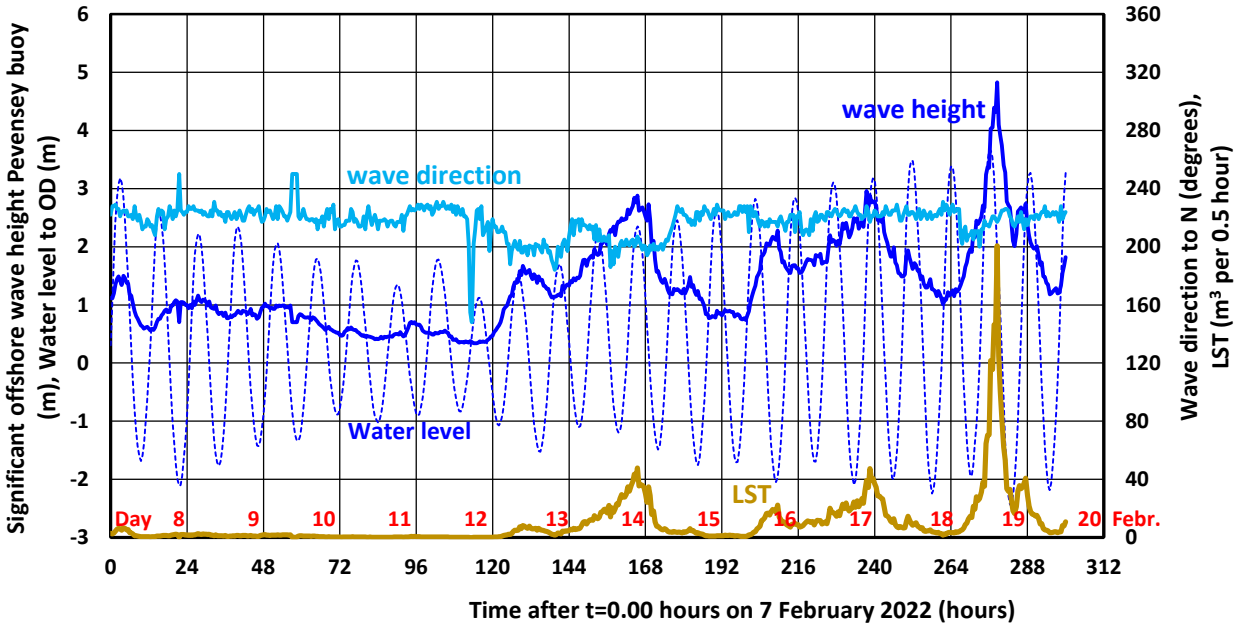

Figure 5.9.3 *Wave data at location Pevensey buoy and longshore single transport at location Cooden in period 7-19 February 2022*

Calibration storm event Ciaran 2 November 2023

Pre- and post surveys haven been done by PCDL (Personal Communication with Ian Thomas of PCDL).
The total volume (in m^3) of shingle between toe and crest along the frontage from Sovereign-harbour to Cooden is, as follows:

	1st Nov	3rd Nov	Change
Above 0 m to OD	1,970,166	1,965,332	-4,834
Above -1.5 m to OD	2,882,576	2,887,319	+4,743
Above +2.5 m to OD	841,323	798,664	-42,659

Essentially, about 43,000 m^3 is lost from the top region of the beach (about 30% more than during Storm Eunice 18-19.5 February 2022) and carried to lower beach areas (mostly between 0 m and +2.5 m OD).
The erosion volume at the upper beach per unit width of coastline is 43,000/9000 ≅ 4.8 m^3/m for Storm Ciaran.
The computed beach erosion volume above the level +3 m OD based on Equation (6.4.1) with γ=1 is 3.9 m^3/m for Storm Ciaran (input wave data from Pevensey buoy), which is somewhat too low compared to the observed value of 4.8 m^3/m.

6. Summary and conclusions

Beaches consisting of gravel (2 to 64 mm), pebbles and cobbles (64 to 256 mm) are generally known as *coarse clastic beaches* and can be found in many mid- and high-latitude parts (formerly glaciated) of the world (England, Iceland, Canada, etc.). Gravel beaches are also found along unconsolidated cliff-type coasts eroded by wave attack (Mediterranean coasts) and along tectonic coasts where steep streams deliver coarse material to the shore. Some of these beaches have a large proportion of sand intermixed with gravel, especially in the foreshore zone.
Gravel beaches are also known as shingle beaches or coarse clastic beaches. Clasts are individual grains within coarse populations. Subgroups are pebbles and cobbles (rounded clasts between 64 and 256 mm); boulders are clasts larger than 256 mm. The term shingle is most commonly identified with the coarse beaches of southern England.
Gravel on beaches is moved almost exclusively by wave action (asymmetric wave motion); tidal or other currents are not effective in moving gravel material.
The gravel particles move up the beach to the run-up limit by strong bores (uprush) and move down the beach close to the line of the steepest beach slope by the backwash (less strong due to percolation) plus gravity, resulting in a saw-tooth movement. Waves of long periods on steep beaches can produce peak swash velocities up to 3 m/s. Gravel particles in shoaling and breaking waves generally move as bed load. As the near-bed peak orbital velocity in the onshore direction is greater than the offshore-directed value, the particles will experience a net onshore-directed movement during each wave cycle. The finer grains may go into suspension as a result of the turbulence produced by the breaking waves and may be transported offshore or inshore depending on the strength of the undertow.

Gravel transport mainly takes place in the swash zone. The swash zone is the zone which is intermittently wet and dry showing relatively large velocities during the uprush and backwash phases of the saw-tooth swash wave cycle due to bore propagation and bore collapse, often in combination with low-frequency oscillations which generally grow in amplitude towards the shoreline. It is a particularly complex zone of the nearshore where short and long waves, tides, sediments and groundwater flow (infiltration/percolation) all play an important role. The swash zone is the most dynamic part of the nearshore zone of vital importance for the behaviopur of the gravel/shingle barrier.

Wave-induced run-up is caused by two different processes: set-up, which is the maximum time-averaged water level elevation at the shoreline and swash oscillations, which are the time-varying vertical fluctuations about the temporal mean value (set-up water level). Wave run-up along steep sloping gravel barriers can be estimated using the experimental data of laboratory and field experiments.
Swash velocity measurements show that the swash related to the incident waves on steep beaches is skewed and asymmetric (saw-tooth waves), i.e. the backwash is not simply the reverse of the uprush. Generally, onshore flow velocities during the uprush are larger but of shorter duration than the seaward velocities during the backwash. Maximum landward velocities occur at the start of the uprush, whereas maximum seaward velocities take place at the end of the backwash. The water depths that occur during the uprush are generally larger than those that occur during the backwash.
The dissimilarity in the hydrodynamics of the wave uprush and backwash is reflected in different modes of sediment transport. Turbulence-dominated suspended transport may be significant during the uprush phase whereas sheetflow type of bed load transport dominates during the backwash phase. During the uprush phase the sediment transport is a combination of sediments mobilised under and directly after bore collapse which are then advected landwards and of locally entrained sediments from the bed by developing boundary layer flow at the end op the uprush, whereas sediment transport during downrush mainly is related to locally entrained sediments. Measurements of sheet flow transport for half saw-tooth waves in a wave tunnel indicate that the sediment transport under steep fronts (decelerating flow) is about twice as large as under steep rears (accelerating flow).

Swash motion over a steep permeable bed of coarse grains (gravel/shingle) is complicated by the presence of infiltration under wave uprush and exfiltration under wave downrush. Vertical flow through a porous bed can influence sediment motion in two ways: 1) seepage forces changing the effective weight of the surficial sediments

and 2) the occurrence of boundary layer thinning (resulting in higher shear stresses) due to infiltration and thickening (smaller shear stresses) due to exfiltration. Generally, swash-related infiltration-exfiltration effects across a saturated beach face enhance the upslope transport of sediment transport.

Various experiments on the behaviour of gravel slopes under wave attack have been performed by Deltares/Delft Hydraulics (1989) in the large-scale Deltaflume (length of 200 m, width of 5 m and depth of 7 m). Gravel and shingle material have been used (d_{50}= 0.0048 m and d_{50}= 0.021 m). The initial beach slope was 1 to 5 (plane sloping beach) in all (nine) experiments. The most characteristic features are: the formation of a swash bar above the still water level (SWL) due to onshore transport; the formation of a small breaker bar; the generation of a scour pit below SWL and the presence of a small transition zone direct above and beneath SWL with almost no deformation. Similar tests have been performed in the GWK (Hannover, Germany). The BARDEX-experiments in the Deltaflume of Deltares (2008) include time-varying water levels to simulate tidal variations and wave overtopping/overwashing to simulate crest erosion of the barrier.

Two models (process-based CROSMOR2008-model and parametric SHINGLE-model) have been used to simulate the cross-shore swash bar formation under low wave conditions and gravel barrier erosion under high wave conditions (storm events). The SHINGLE-model is a parametric profile model based on shape functions. The process-based CROSMOR-model describes the propagation and transformation of individual waves (wave by wave approach) along the cross-shore profile using a probabilistic approach by solving the wave energy equation for each individual wave. The detailed swash processes in the swash zone are not explicitly modelled but are represented in a schematized way by introducing a time-averaged effective swash velocity in a small zone just seaward of the last grid point. The swash velocity is of the order of 1 to 1.5 m/s. The deposition (or erosion) profile in the swash zone is assumed to have a triangular shape.

Test results of the Deltaflume and GWK experiments have been used to calibrate the CROSMOR-model for gravel and shingle slopes. Qualitatively the results are in reasonable agreement with the measured values. A swash bar of the right order of magnitude is generated above the waterline in both experiments, but the computed swash bars are too smooth whereas the measured swash bars have a distinct triangular shape and are positioned at a higher level on the slope. Simular results are obtained for the other large-scale laboratory tests.

To demonstrate the applicability of the process-based CROSMOR-model for prototype shingle barriers, the model has been applied to a real field case (Pevensey Bay, UK) and a schematized field case. The SHINGLE model of HRWallingford has also been applied to the field case of Pevensey Bay. Various storm cases are considered representing events with a returrn interval of 1 to 400 years and an extreme event with a return interval of 10000 years. The CROSMOR-model results and the SHINGLE-model results show rather good agreement of computed erosion values for the storm case with the largest offshore wave height of 6 m. The SHINGLE-model predicts a relatively large build-up of the crest. The agreement of computed profiles for the other storm cases with smaller offshore wave heights is less good.

The CROSMOR-model has also been applied to a schematized field case with a relatively steep nearshore slope. Wave-induced longshore velocities are relatively large for oblique wave approach along the steep slope. The longshore current velocity has a maximum of 3 m/s for an offshore wave angle of 15^o and 4 m/s for an angle of 30^o, just landward of the toe of the beach slope. The longshore transport increases strongly in the nearshore zone and is maximum at the location where the longshore velocity is maximum (around 0 m depth line). The computed longshore transport rates vary roughly between 5 m^3/day and 9000 m^3/day (including pores) for offshore wave heights between 1 and 8 m. About 80% of the longshore transport occurs in the surf zone landward of the -6 m depth contour and about 70% landward of the -4 m depth line.

Morphological simulation results for superstorm conditions (offshore wave height of 8 m) show the generation of a small swash bar at the landward end of the beach (above +6 m line) and a breaker bar at the toe of the beach

(below the +1 m line). The total erosion volume around the water line (=around storm surge level line) is about 20 to 25 m^3/m after 1 day. The total volume of the breaker bar is about 50 m^3/m after 1 day due to erosion of the beach (seaward transport) and erosion of the shoreface (landward transport). The crest level of the gravel slope should be larger than about 10 m to prevent overwashing of the crest under superstorm conditions.

Shingle barriers with a low crest level at 3 to 4 m above MSL are vulnerable to overwash which may easily result in landward migration (roll back) during storm conditions with surge levels of 3 to 4 m above MSL. The CROSMOR-model has been used for exploring computations of crest erosion and landward migration of a gravel barrier with a low crest level at 4 m above MSL. The overwash discharge has been varied in the range of 0.5 to 2 m^2/s by specifying a small velocity at the inflow boundary (x= 0) at a depth of 30 m below MSL. The fluid velocity above the crest is in the range of 0.5 to 2 m/s.
The longshore velocity has its peak value (about 2.5 m/s) just seaward of the crest and decreases above the crest due to frictional effects (strong reduction of water depth). The computed bed level changes after 1 day (24 hours) show crest erosion of the order of 1 m and landward barrier migration of the order of 3 m. The barrier migration reduces for a smaller overwash of 0.5 m^2/s (v_{crest}= 1 m/s). The crest lowering by erosion is not much influenced by the overwash discharge and is about 1 m after 1 day. A depositional bar is formed at the beach. This latter bar is mainly caused by onshore transport of gravel enhanced by relatively large longshore velocities (2.5 m/s) under oblique wave attack. When the wave incidence angle is set to 0, the bar formation is much less pronounced. The crest erosion and migration also are smaller for waves normal to the coast.
Under superstorm conditions (water level at 5 m above MSL) the crest erosion is up to 1 m and the maximum crest migration is about 20 m/day. Data of Hurst beach and Hurst spit show crest migration values of 20 m in one storm event and long term values of 10 m over a period of about 2 years. Measured vertical crest erosion values are in the range of 0.5 to 1.5 m at Hurst beach, which are of the same order of magnitude as the computed values.

Erosion of sandy dune coasts due to storm events is a major problem at many sites. Under extreme storm conditions the erosion volume due to a severe storm with a duration of 5 to 6 hours is of the order of 100 to 300 m^3/m and shoreline recession values are of the order of 10 to 30 m. These values can be significantly reduced by using a protection layer of shingle or cobbles on the sandy dune face. The maximum horizontal recession for a dune protected by a layer of shingle is of the order of 2 m. When cobbles (of about 0.1 m) are used, the erosion will be minimum. Using a safety factor of 2, the minimum layer thickness of shingle to protect a sandy subsoil should be of the order of 2 to 3 m. The toe of the layer should extend to below the low water mark (-2 m below MSL) resulting in a total length of about 100 m assuming a beach slope of 1 to 8 between the -2 m and +3 m line and a barrier slope of 1 to 3. A total volume of about 200 to 300 m^3/m is required per m shoreline or 200,000 to 300,000 m^3 per km. This solution may be attractive at specific locations (near structures, harbours, inlets, etc.) where the erosion processes of the sandy dune system are excessively large resulting in relatively large maintenance costs (nourishments costs).

7. References

Baldock, T.E. and Holmes, P., 1999. *Simulation and prediction of swash oscillations on a steep beach. Coastal Engineering, Vol. 36, p. 219-242*

Barnes, M.P., O'Donoghue, T., Alsina, J.M. and Baldock, T.E., 2009. *Direct bed shear stress measurements in bore-driven swash. Coastal Engineering, Vol. 56, p. 853-867*

Bradbury, A.P., 2000. *Predicting breaching of shingle barrier beaches-recent advances to aid beach management, Proc. 35th, Annual MAFF Conference of River and Coastal Engineers, p. 05.3.1-05.3.13*

Bradbury, A.P. and Powell, K.A., 1990. *The short term profile response of shingle spits to storm wave action, p. 2694-2707 Proc. 22nd ICCE, Delft, The Netherlands*

Buscombe, D., Williams, J.J. and Masselink, G., 2008. *Barrier dynamics experiments (BARDEX), experimental procedure, technical information and data report. School of Geography, University of Plymouth, UK*

Butt, T. and Russell, P., 2000. *Hydrodynamics and cross-shore sediment transport in the swash zone of natural beaches: a review. Journal of Coastal Research, Vol. 16, p. 255-268*

Carter, R.W.G. and Orford, J.D., 1993. *The morphodynamics of coarse clastic beaches and barriers: a short and long term perspective. Journal of Coastal Research, SI 15, p. 158-179.*

Chadwick, A.J., 1989. *Field measurements and numerical model verification of coastal shingle transport, p. 381-402. BHRA, Fluid Engineering Centre, Bedford, England*

Conley, D.C. and Griffin, J.G., 2004. *Direct measurements of bed stress under swash in the field. Journal of Geophysical Research, Vol. 109, C03050*

Cowen, E.A., Mei Sou, I, Liu, P.L. and Raubenheimer, B., 2003. *Particle image velocimetry measurements within a laboratory generated swash zone. Journal of Engineering Mechanics, ASCE, Vol. 129, No. 10, p. 1119-1129*

Cox, D.T., Hobensack, W., Sukumaran, A, 2000. *Bottom stress in inner surf and swash zone. Proc. 27th ICCE, Sydney, Australia. p. 108-119*

Dally, W.R. and Osiecki, D.A., 1994. *The role of rollers in surf zone currents. Proc. 24th ICCE, Kobe, Japan*

Davies, A.G. and Villaret, C., 1997. *Oscillatory flow over rippled beds. In: J.N. Hunt (ed.), Gravity waves in water of finite depth: Chapter 6, p. 215-254. Advances in fluid mechanics, Computational Mechanics Publications*

Davies, A.G. and Villaret, C., 1998. *Wave-induced currents above rippled beds, p. 187-199. In: Physics of estuaries and coastal seas, edited by J. Dronkers and M. Scheffers, Balkema, Brookfield*

Davies, A.G. and Villaret, C., 1999. *Eulerian drift induced by progressive waves above rippled and very rough bed, p. 1465-1488. Journal of Geophysical Research, Vol. 104, No. C1*

Deltares/Delft Hydraulics, 1989. *Scale effects in stability of gravel and stone slopes under wave attack in Deltaflume (in Dutch). Report M1983 Part IV, Deltares/Delft Hydraulics, Delft, The Netherlands*

Elfrink, B. and Baldock, T., 2002. *Hydrodynamics and sediment transport in the swash zone: a review and perspective. Coastal Engineering, Vol. 45, p. 149-167*

Grasmeijer, B.T., 2002. *Process-based cross-shore modelling of barred beaches. Doctoral Thesis. Department of Physical Geography, University of Utrecht, Utrecht, The Netherlands*

Grasmeijer, B.T. and Van Rijn, L.C., 1998. *Breaker bar formation and migration. Proc. 26th ICCE, Copenhagen, Denmark*

Halcrow, 2006. *South Foreland to Beachy Head Shoreline Management Plan.*

Harvey, R., 2016. *Pevensey Sea Defences (case study 61). Internet publication*

Herrington Consulting Limited, 2022a. *Pevensey Bay Design Review, Canterbury, UK*

Herrington Consulting Limited, 2022b. *Storm Eunice – 18th February 2022, Canterbury, UK*

Houwman, K.T. and Ruessink, B.G., 1996. *Sediment transport in the vicinity of the shoreface nourishment of Terschelling. Dep. of Physical Geography, University of Utrecht, The Netherlands*

HR Wallingford, 1995. *Langley Point to Cooden Sea Defences, physical model studies. Report EX 3241.*

Idier, D., Dumas, F. and Muller, H., 2012. *Tide-surge interaction in the English channel. Nat. Hazards Earth Syst. Sci. Vol. 12, 3709-3718. Doi: 10.5194/nhess-12-3709-2012*

Isobe, M. and Horikawa, K., 1982. *Study on water particle velocities of shoaling and breaking waves. Coastal Engineering in Japan, Vol. 25*

King, D.B., 1991. *Studies in oscillatory flow sediment bed load transport. Doctoral Thesis, University of California, San Diego, USA*

Kobayashi, N. and Wurjanto, A., 1992. *Irregular wave set-up and run-up on beaches. Journal of Waterways, Port, Coastal and Ocean Engineering, Vol. 118, No. 4, p. 368-386*

López de San Román-Blanco, B., Coates, T., Holmes, P., Chadwick, A., Bradbury, A., Baldock, T., Pedrozo Acuña, A., Lawrence, J. and Grune, J., 2006. *Large scale experiments on gravel and mixed beaches. Coastal Engineering, 53, p. 349 -362*

Masselink, G. and Hughes, M.G., 1998. *Field investigation of sediment transport in the swash zone. Continental Shelf Research, Vol. 18, p. 1179-1199*

Masselink, G., Evans, D., Hughes, M.G. and Russell, P., 2005. *Suspended sediment transport in the swash zone of a dissipative beach. Marine Geology, Vol. 216, p. 169-189*

Masselink, G., and Russell, P., 2006. *Flow velocities, sediment transport and morphological change in the swash zone of two contrasting beaches. Marine Geology, Vol. 227, p. 227-240*

Meyer-Peter, E. and Mueller, R. 1948. *Formulas for bed load transport. IAHR 2nd meeting, Stockholm, 41-64*

New Civel Engineer, 2011. *The sea change in saving UK coastlines; sea defences Pevensey Bay. www.nce.co.uk*

Nicholls, R.J. and Wright, P., 1991. *Longshore transport of pebbles: experimental estimates of K-factor. Coastal Sediments, Seattle, USA, p. 920-933*

Nicholls, R.J. and Webber, N.B., 1988. *Characteristics of shingle beaches with reference to Christchurch Bay, South England, p. 1922-1936, Proc. 21st ICCE, Malaga, Spain*

Nielsen, P., 1992. *Coastal bottom boundary layers and sediment transport. World Scientific, Singapore*

Obhrai, C., Powell, K.A. and Bradbury, A.P., 2008. *A laboratory study of overtopping and breaching of shingle barrier beaches. Proc. 31st ICCE, Hamburg, Germany.*

Powell, K A., 1990 *Predicting short term profile response for shingle beaches. HR Wallingford Report SR 219, Wallingford, UK.*

Pritchard, D. and Hogg, A.J., 2005. *On the transport of suspended sediment by a swash event on a plane beach. Coastal Engineering, Vol. 52, p. 1-23*

Ruessink, G.B. and Van Rijn, L.C., 2010. *Skewness and asymmetry of nearshore waves (in preparation)*

Ruessink, B.G., Ramaekers, G. and Van Rijn, L.C., 2012. *On the parameterization of the free-stream non-linear wave orbital motion in nearshore morphodynamic models. Coastal Engineering 65, 56-63*

Steetzel, H., 1993. *Cross-shore transport during storm surges. Doctoral Thesis. Department of Civil Engineering, Delft University of Technology, Delft, The Netherlands*

Stockdon, H.F., Holman, R.A., Howd, P.A. and Sallenger, A.H., 2006. *Empirical parameterization of setup, swash and runup. Coasal Engineering, Vol. 53, p. 73-588*

Sutherland, J. and Obhrai, C., 2009. *Monte-Carlo simulation of barrier breaching (in preparation)*

Sutherland, J. and Thomas, I., 2009. *The management of Pevensey shingle barrier. Paper EU-Conscience Project, Deltares, Delft, The Netherlands*

Sutherland, J. and Thomas, I., 2011. *The management of Pevensey shingle barrier. Ocean ND Coastal Management. DOI: 10.1016/j.ocecoaman.2011.07.004*

Svendsen, I.A., 1984. *Mass flux and undertow in the surf zone. Coastal Engineering, Vol. 8, p. 347-365*

Van Gent, M.R.A., 2001. *Wave runup on dikes with shallow foreshores. Journal of Waterways, Port, Coastal and Ocean Engineering, Vol. 127, No. 5, p. 254-262*

Van Rijn, L.C., 1993, 2006. *Principles of sediment transport in rivers, estuaries and coastal seas, including update of 2006. Aqua Publications, The Netherlands (www.aquapublications.nl)*

Van Rijn, L.C., 1997. *Cross-shore sand transport and bed composition. Coastal Dynamics, Plymouth, England, p. 88-98*

Van Rijn, L.C., 2006. *Principles of sedimentation and erosion engineering in rivers, estuaries and coastal seas. Aqua Publications, The Netherlands (www.aquapublications.nl)*

Van Rijn, L.C., 2007a. *Unified view of sediment transport by currents and waves, I: Initiation of motion, bed roughness and bed-load transport. Journal of Hydraulic Engineering, ASCE, Vol. 133, No. 6, p. 649-667*

Van Rijn, L.C., 2007b. *Unified view of sediment transport by currents and waves, II: Suspended transport. Journal of Hydraulic Engineering, ASCE, Vol. 133, No. 6, p. 668-689*

Van Rijn, L.C., 2007c. *Unified view of sediment transport by currents and waves, III: Graded beds. Journal of Hydraulic Engineering, ASCE, Vol. 133, No. 7, p. 761-775*

Van Rijn, L.C., 2007d. *Unified view of sediment transport by currents and waves, IV: Application of morphodynamic model. Journal of Hydraulic Engineering, ASCE, Vol. 133, No. 7, p. 776-793*

Van Rijn, L.C., 2008. *Modelling of beach and dune erosion. Report Z4173/Z4230. Delft Hydraulics, Delft , The Netherlands*

Van Rijn, L.C., 2009. *The prediction of dune erosion due to storms. Coastal Engineering, Vol. 54, p. 441-457*

Van Rijn, L.C. and Wijnberg, K.M., 1994. *One-dimensional modelling of individual waves and wave-induced longshore currents in the surf zone. Report R 94-09, Department of Physical Geography, University of Utrecht, The Netherlands.*

Van Rijn, L.C. and Wijnberg, K.M., 1996. *One-dimensional modelling of individual waves and wave-induced longshore currents in the surf zone. Coastal Engineering, Vol. 28, p. 121-145*

Van Rijn, L.C., Walstra, D.J.R., Grasmeijer, B., Sutherland, J., Pan, S. and Sierra, J.P., 2003. *The predictability of cross-shore bed evolution of sandy beaches at the time scale of storms and seasons using process-based profile models. Coastal Engineering, Vol. 47, p. 295-327*

Vellinga, P., 1986. *Beach and dune erosion during storm surges. Doctoral Thesis. Department of Civil Engineering, Delft University of Technology, Delft, The Netherlands*